# Selenology Today

ISSUE # 36, 2015

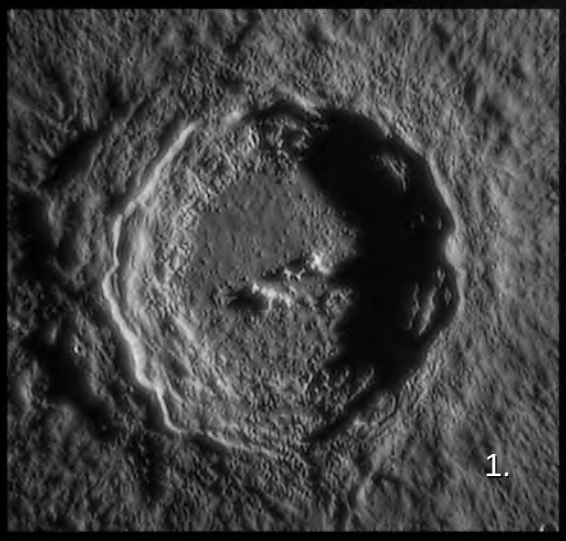
1.

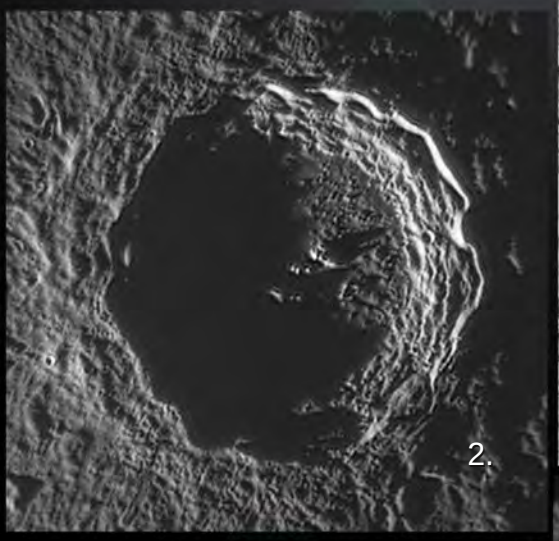
2.

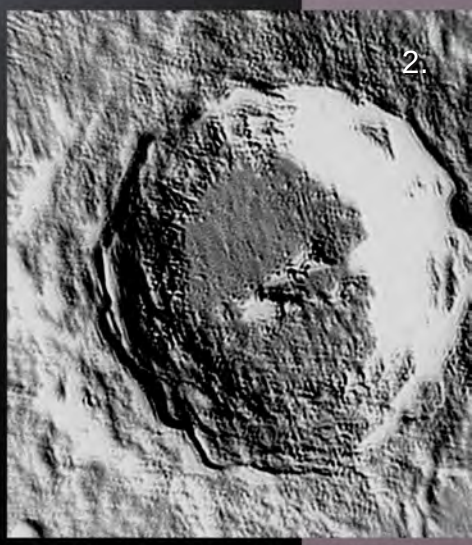
2.

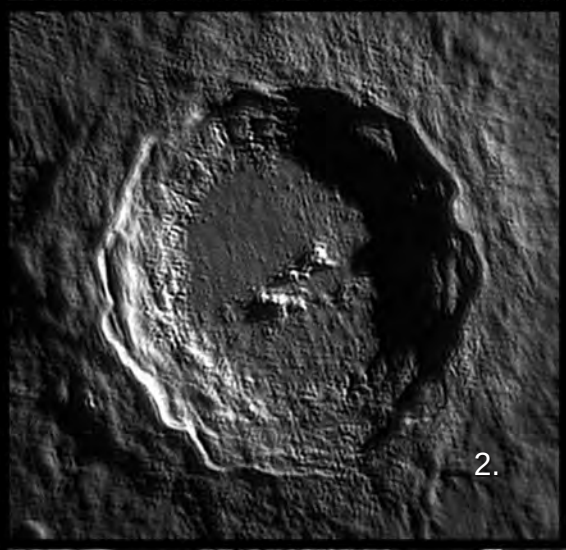
2.

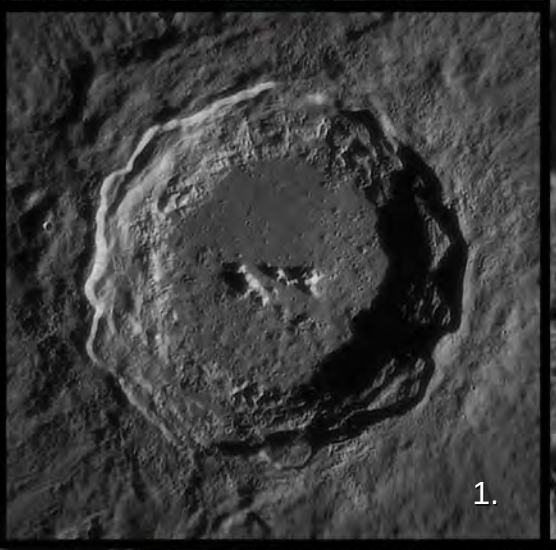
1.

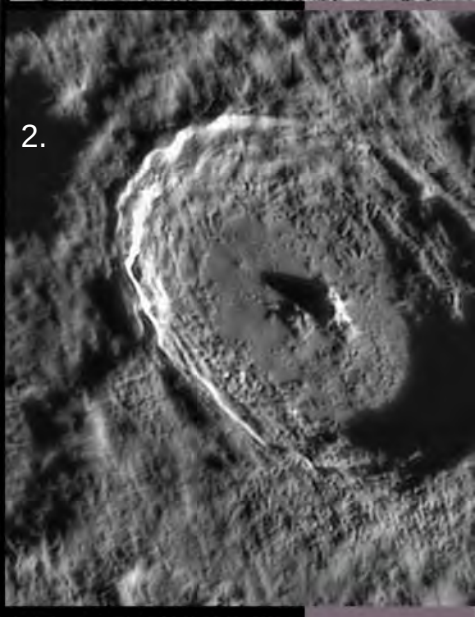
2.

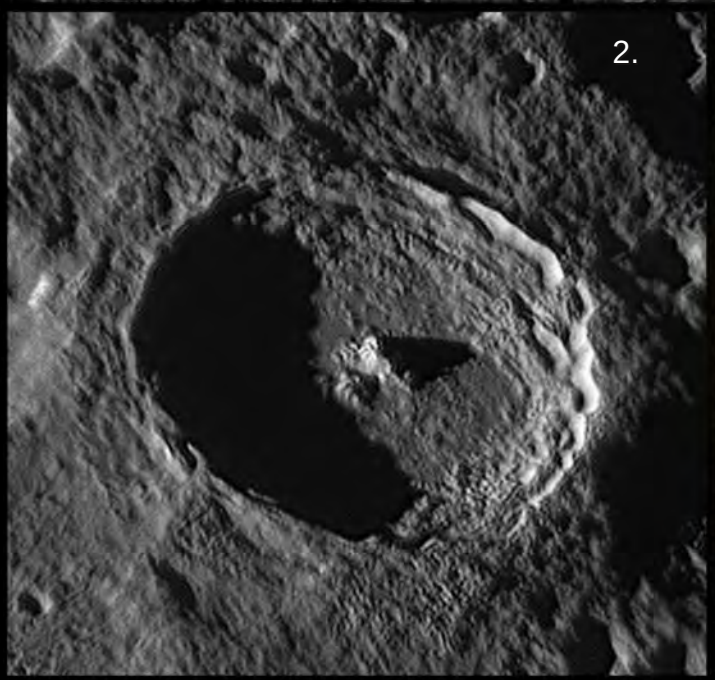
2.

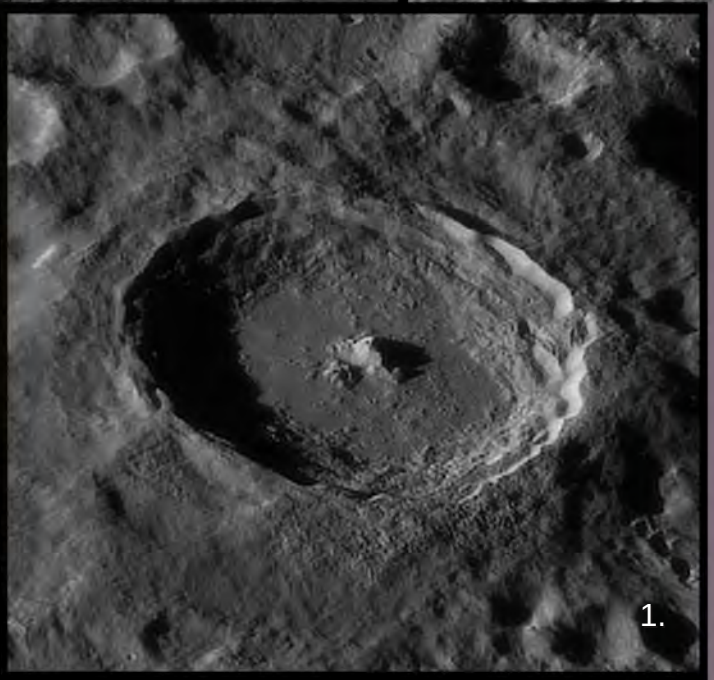
1.

ISSUE # 36, 2015

# Selenology Today

*Selenology Today is devoted to the publication of contributions in the field of lunar studies. Manuscripts reporting the results of new research concerning the astronomy, geology, physics, chemistry and other scientific aspects of Earth's Moon are welcome. Selenology Today publishes papers devoted exclusively to the Moon. Reviews, historical papers and manuscripts describing observing or spacecraft instrumentation are considered.*

Selenology Today website
http://digilander.libero.it/glrgroup/

and here you can found all older issues
http://www.lunar-captures.com/SelenologyToday.html



*Selenology Today is under a reorganization, so that further comments sent to us will help for the new structure. So please doesn't exit to contact us for any ideas and suggestion about the Journal. Comments and suggestions can be sent to Raffaello Lena editor in chief :*

gibbidomine@libero.it

Selenology Today

# Contents



COVER

craters Copernicus & Tycho


by Mike Wirths (1) & George Tarsoudis (2)

ISSUE # 36, 2015

Selenology Today

# Early Central Peak visibility in Tycho and Copernicus craters

by Maurice Collins

I have been intrigued by spacecraft images showing the interiors of craters lit only by the light reflected of their lit crater rims and Earthshine. I wondered if it would be possible to see this effect from Earth using only an average sized (20cm/8 inch) SCT telescope, the largest aperture I possess, and a Zwo Optical ASI120MC colour imager camera.

There had been Transient Lunar Phenomena (TLP) reports by amateurs of central peaks of craters being visible before they should be lit by direct sunlight. These TLP reports describe observations of faintly lit interiors of craters with misty glows, so it seemed a realistic exercise to try to capture an image of this effect to see if it were real and explainable.

On 2014 August 4 as I was imaging the 8 day Moon for a full disk mosaic, where the sun was just rising on the rim of the great rayed crater Tycho in the southern lunar highlands. Even though I did not set out planning to do this experiment that night, as I didn't know Tycho was just at sunrise, when I saw Tycho's lighting I thought this would be an ideal time to try and see if the central peak was able to be seen inside the darkened shadow of the crater interior, so I attempted to try (Fig. 1).

I had taken normally exposed images moments before at 09:15 UT at 0.006506 seconds exposure, where I could not see any central peak being lit by the sun at this stage on the live image in the SharpCap software displayed on the screen of my laptop connected to the C8 telescope. At 09:15 UT I took two exposures at 0.037511 seconds, then at 09:16 UT a longer one at 0.120403 seconds exposure.

At 09:17 UT I took another exposure of 0.120403 seconds. All were taken using the same camera, and I was able to see the central peak illuminated in the shadows by rim light, on screen, with each frame that downloaded!

I took a further exposure at 09:17 UT of 0.16136 seconds, I also took another "after" shot at 09:18 UT to show that it was not suddenly lit normally by a rising sun just at that moment using 0.008705 seconds, and neither the "before" or "after" images show the central peak being lit yet. Later when visual observing at around 09:34UT I could visually see the peak very faintly glowing inside the shadows of Tycho, lit only by the light of the brilliantly lit western rim reflecting light into the interior, that sun had not yet risen on its peak. Tony Cook did a calculation to show that the sun was at an angle of 1.6 degrees at the time of my image, which is confirmed by the Lunar Terminator Visualization Tool. LTVT also confirmed that there was no light reaching the central peak in the Digital Elevation Model (DEM) option used to draw the lunar surface at those lighting conditions (at solar angle from 1.6 degree to 1.9 degree) to confirm my observations that the peak was only lit by rim light not direct light.

The following night, 2014 August 5, the sun was just rising on the crater Copernicus, with its interior still in shadow. So I thought I would try to see if the central peaks of Copernicus were visible under similar conditions as well (Fig. 2).

At 06:00UT after taking a full mosaic of the Moon, I trained the telescope (again my Celestron 8"/20cm Schmitt-Cassegrain) on the crater and took a long exposure. I exposed for 0.037511 seconds for two images, one after the other. I really was not expecting to see anything, but in later

processing the next morning several of the central peaks were visible! I made a montage of images take at 06:00 UT long exposure 0.037511, 06:01 UT at normal exposure of 0.006506 seconds, and one taken later after the sun had risen more and was lighting the central peaks at 08:34 UT at normal exposure of 0.006506 seconds. I sent it off to Chuck Wood at Lunar Photo of the Day, and he posted it that afternoon Aug 6.

Dr. Wood was able to enhance the image further and bring out the peaks much more clearly and was able to describe three peaks being visible by the light of the reflected crater rimshine. By comparing the long exposure with the later image taken at 08:34 UT where the peaks are illuminated, it is possible to match up the same peaks lit in the long exposure image.

Several days later I was reading in H.P. Wilkins "Our Moon" [1] and noted that Percy Wilkins had also observed Copernicus's peaks and had this to report :

"On March 29, 1939, the great crater of Copernicus was finely displayed. The sun was rising there and the shadows of the western wall were just beginning to creep down the slope of the opposite or eastern wall. The whole of the interior was in shadow. Suddenly a faint glow appeared inside Copernicus and the group of little hills near the centre were seen to be not sharply defined but rather as though they were being viewed through fog. This lasted about fifteen minutes then vanished. It was not until four hours later that the first ray of direct sunshine touched the tops of the hills near the centre. Surprisingly, however, not only the tops but the whole of the hills were seen at a time when it was not sunshine which revealed them. Where, then, did the light come from?"

Though H.P. Wilkins did not figure it out, it appears to be sunlight reflected from the lit rim that has lit up the interior and central peaks, however, why it would be visible for only 15 minutes then vanish is slightly puzzling. My explanation for this would be that the light of the rim overwhelms the eye in detecting the peak after a certain level, so it vanishes until it is lit directly by sunlight at local sunrise. However, TLP researchers have possible other explanations, such as dust levitating or gaseous emission of some sort, making it temporarily visible. Further research and observations are needed to finally explain why it the central peaks are sometimes visible, and sometimes not under similar lighting conditions. Perhaps I lucked out that night in capturing it at just the right time? For more detailed information on the TLP's of central peaks, I refer you to the article in recent October 2014 BAA lunar section Circular [2], and the ALPO October 2014 "The Lunar Observer Newsletter" [3] by Dr. Tony Cook, who has analysed my observation in relation to TLPs of the past, especially the excellent observation of Tycho's central peak by Brendan Shaw observed even earlier than I detected it. Tony Cook's article also lists future watch times for similar lighting conditions at Tycho.

Please send any further observation to Dr. Tony Cook at email: atc@aber.ac.uk or to the author at mauricejscollins@hotmail.com

**Editor note:** We invite all readers of Selenology Today to send possible observations or own articles on the visibility of these central peaks also to the editorial board: gibbidomine@libero.it

Selenology Today


Fig. 1

Selenology Today

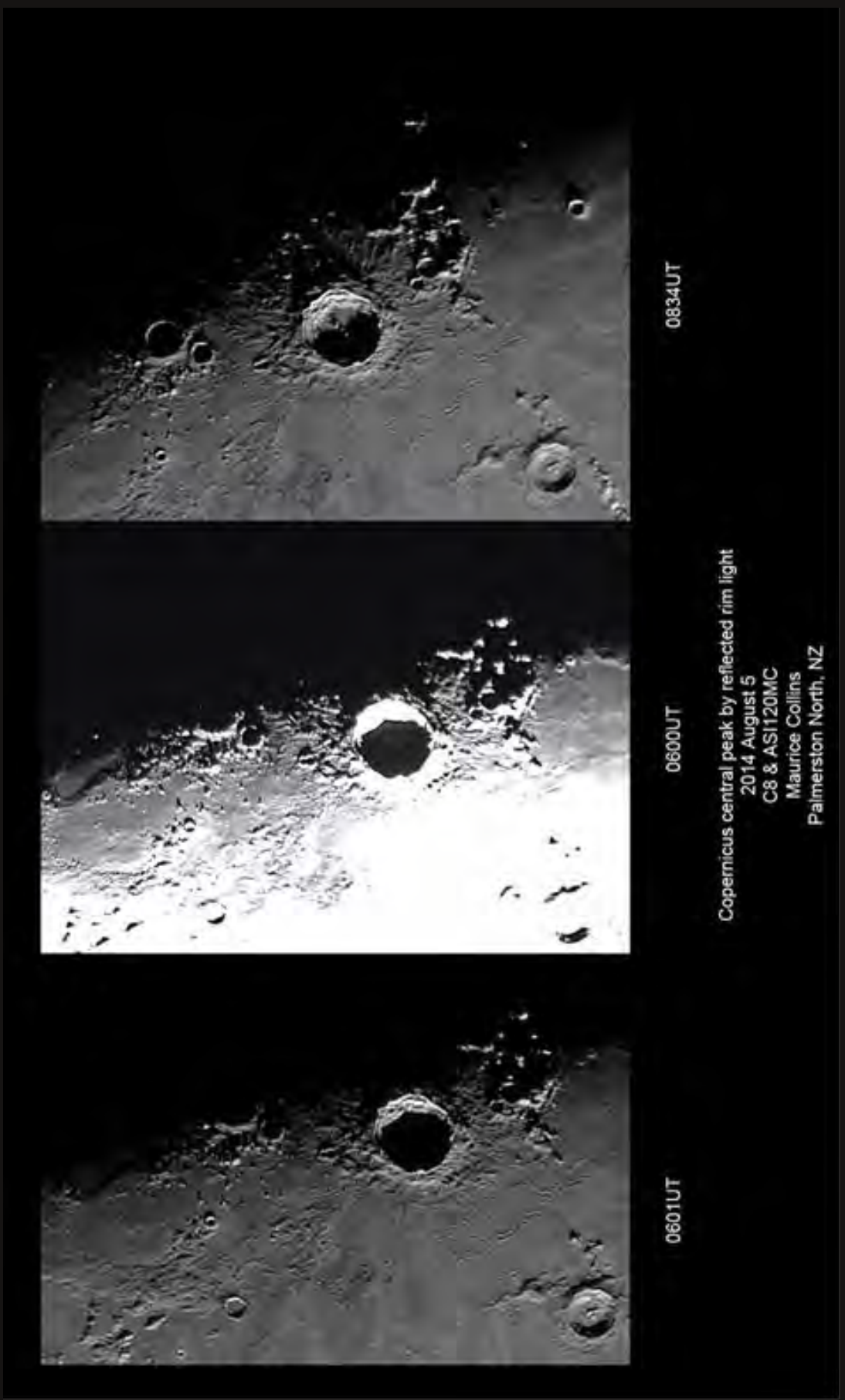


Fig. 2

Selenology Today

References:
1. Wilkins, H. Percy (1954) Our Moon. Frederick Muller Ltd, London. page 132
2. BAA LSC Oct 2014: http://www.baalunarsection.org.uk/2014-10-lsc.pdf (available soon)
3. ALPO TLO Oct 2014: http://moon.scopesandscapes.com/tlo_back/tlo201410.pdf

| Date | UT | Date | UT | Date | UT |
|---|---|---|---|---|---|
| 2014 Oct 02 | 09:50 | 2015 May 26 | 21:42 | 2016 Jan 18 | 02:14 |
| 2014 Oct 31 | 22:56 | 2015 Jun 25 | 08:47 | 2016 Feb 16 | 16:39 |
| 2014 Nov 30 | 12:54 | 2015 Jul 24 | 19:43 | 2016 Mar 17 | 06:21 |
| 2014 Dec 30 | 03:27 | 2015 Aug 23 | 06:55 | 2016 Apr 15 | 19:08 |
| 2015 Jan 28 | 18:06 | 2015 Sep 21 | 18:45 | 2016 May 15 | 07:02 |
| 2015 Feb 27 | 08:17 | 2015 Oct 21 | 07:29 | 2016 Jun 13 | 18:17 |
| 2015 Mar 28 | 21:39 | 2015 Nov 19 | 21:09 | 2016 Jul 13 | 05:12 |
| 2015 Apr 27 | 10:05 | 2015 Dec 19 | 11:34 | 2016 Aug 11 | 16:14 |

Table 1: the table displays the repeat illuminations of Tycho.

Selenology Today

# Lunar domes Atlas on line (GLR group)

*Lunar Domes Atlas*
*by Raffaello Lena, Maria Teresa Chiocchetta, Mike Wirths, Paolo Lazzarotti, Jim Phillips, Carmelo Zannelli, Stefan Buda and George Tarsoudis*

*Biographic notes*

Lunar domes are structures of volcanic origin which are usually difficult to observe due to their low heights.
Different methods for determining the morphometric properties of lunar domes (diameter, height, flank slope, edifice volume) from image data or orbital topographic data, and for determining multispectral images data providing insights into the composition of the dome material, have been examined and discussed in the book published by Springer Lunar Domes: Properties and Formation Processes. Furthermore, the book we have published provides a description of geophysical models of lunar domes, which yield information about the properties of the lava from which they formed and the depth of the magma source regions below the lunar surface.

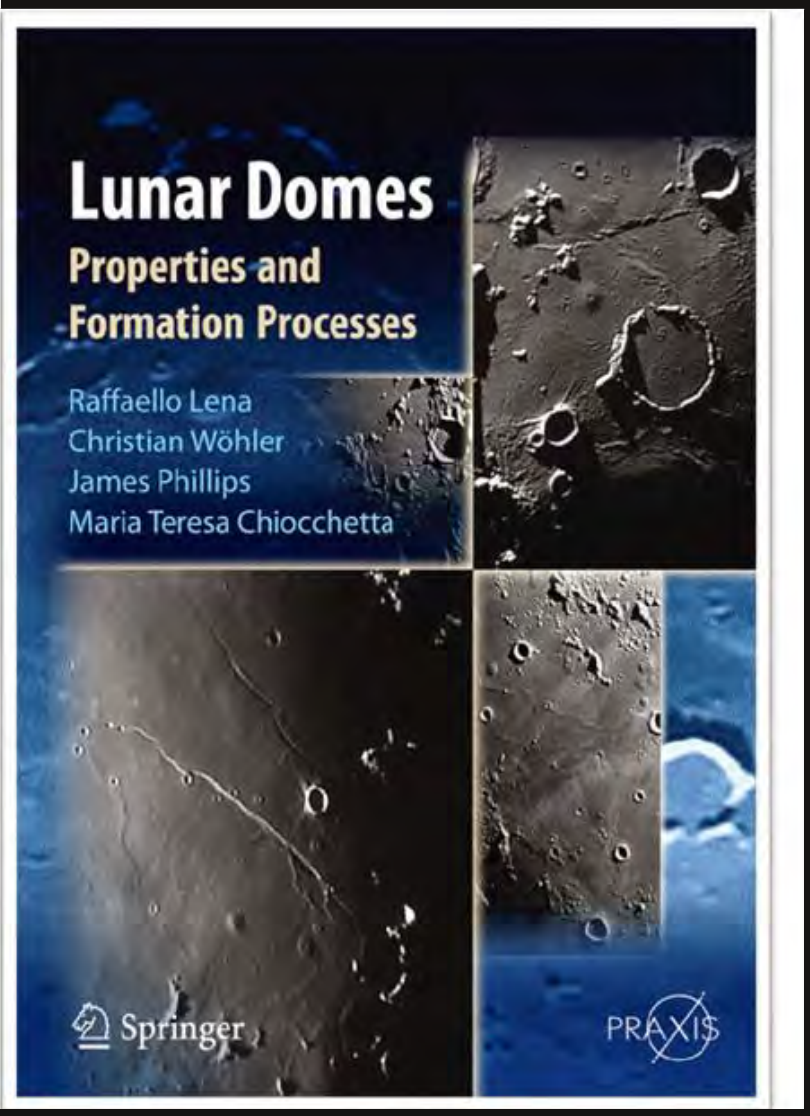


Lunar domes represent a clear testimony of the volcanic processes occurred in our Moon. In fact, the differences in dome shapes and rheologic parameters raise broad questions concerning the source regions of the various dome types allowing the knowledge of which differences in the lunar interior are responsible for the different lunar dome properties observed on the surface.

The book Lunar Domes: Properties and Formation Processes is a reference work on these elusive features, providing the methods used to study quantitatively these volcanic constructs.

The purpose of the present Lunar dome Atlas, complementary to the book, is an uniform collection of CCD terrestrial images for each dome including really high resolution imagery with the scope of a presentation of all the dome fields information, including tables describing their properties in terms of morphological measurements and rheologic properties.

Lunar domes with their typically low flank slopes display a significant contrast with respect to the surrounding surface only when the solar elevation angle is lower than 4–5°. For this reason, as illustrated in the Lunar dome Atlas, it is necessary to image these volcanic edifices under strongly oblique illumination condition. Only slightly different solar elevation angles may result in strong differences in the appearance and visibility of the lunar domes and their shadow. High resolution CCD imagery of the elusive lunar domes is the most difficult branch of the astrophotography of the Moon. Notably, the detailed study of lunar domes is only possible based on images of the lunar surface acquired under strongly oblique illumination conditions, for their measurements and for the maximum detail. The recording of finer details will be obtained with telescopes optically of high quality, large diameter, and favorable observing sites in order to reduce the effect of the atmospheric turbulence.

The domes atlas is on line at
http://lunardomeatlas.blogspot.it/

Selenology Today

Raffaello Lena was born on 2 September 1959. He has published lunar articles in Icarus, Planetary Space Science, LPSC conferences, JALPO, Selenology, JBAA other than in American and Italian magazines. Over the last decade the Geologic Lunar Research Group that he founded has produced dozens of published studies of lunar domes, faults and transient phenomena. He has been interested in the Moon since he was 10 years old and has progressed from a small Newtonian telescope to high quality scopes (6" Maksutov Cassegrain and a 5" refractor). His first interest in lunar studies is represented by the lunar domes analysis and their classification. He is the coauthor of the book Lunar domes properties and mode of formation published by Springer. He works also on interpretation of TLP and has developed procedures for interpretation of a lunar flash in order to identify if it is of real impact nature. He has been the first Italian to document a lunar impact because it was simultaneously recorded also in Switzerland from other two observing sites (independent and simultaneous observation with a distance of the observatories > 500 km). Whenever possible he listens to jazz and explores Italy's volcanoes and mountainous geology.

He has a doctorate in pharmaceutical sciences from the University of Rome and currently works on food safety.

Selenology Today

Maria Teresa Chiocchetta She has published articles in the field of lunar studies and participates in the activity of the Geologic Lunar Research Group. She is the coauthor of the book Lunar domes properties and mode of formation published by Springer. She is interested in the Moon since she was 10 years old and has progressed from a 8” Schmidt Cassegrain to a 10” Maksutov Cassegrain. She lives in Sestri Levante Genova Italy and work in the field of construction engineering.

Selenology Today

Michael Wirths My interest in Astronomy started in my early teens when I saved up enough money from mowing my Parents and neigbors lawns to buy a cheap $25 Tasco refractor. Subsequent ownership of other scopes such as driven C-8's and 6" Newts on heavy German equatorial mounts created a sense of frustration in me as I had nobody to guide me in my hobby, but that all changed when I joined the Ottawa Royal Astronomical Society of Canada. Through that club and its activities I was able to realize that the relatively low tech driven dobsonian was the path for me. My later to be observing partner and friend Attilla Danko gave me my first ever view through a large dobsonian telescope and I was amazed how much detail and colour could be seen when the seeing allowed, even better than the F-12 superplanetary 5" Astrophysics refractor that I was fortunate to own for a year. Later my experience at the famed Texas Star Party led me to the goto driven Starmasters and the sublime efforts of the master optician Carl Zambuto, these scopes are what I currently observe and image with, specifically a 45 cm (18") Starmaster. Of course during all that time my Wife Pamela Weston and I had been running an equestrian centre for well over a decade but both of us were tiring of the harsh cold Ontario winters but a lucky series of small vacations in northern Baja California Mexico gave us the opportunity to purchase a 500 hectare (1200 acre) piece of land on the periphery of the Sierra San Pedro Martir national park. This area is highly desirable for astronomy due to its clear weather and above average seeing conditions. So it came to pass that we sold everything we had in Canada to start a new adventure with an astro B&B and we are going into our 6th year here in the high Sierra. The last 8 years of my life I have surprisingly been drawn to high resolution lunar/planetary imaging, even though I never had any desire to do so before since I was stricly a visual observer. My involvment with the GLR and LPOD was of course a natural progression since like minded individuals seem to find each other no matter what geographic distance seperates them! Together we are trying to push the boundaries of what is possible for amatuers to achieve, who knows where this path will take us!

Selenology Today

Paolo Lazzarotti I was born in 1973 in Massa, Tuscany, and I started my passion with Astronomy in 1995 when the beatiful Hale-Bopp comet appeared in the sky and caught my attention. Hence, I observed and imaged anything crossing the sky but the light pollution here narrowed my interest in the planetary field only. My interest with Planets and the Moon grown up quickly over years and now I even built by myself a dedicated instrument for the hires study of the Solar System, including the Moon. I'm contributor with GLR group since many years and co-author with lots of their lunar researches and lunar articles.

# Selenology Today

James Phillips has been interested in Astronomy for most of his life. He lives in South Carolina, USA. He was lucky enough to have a Mom who knew of his interest in astronomy and his desire to have his own telescope. That was enough for Jim. While wanting to observe as many things as possible with my telescopes, the Moon, planets and double stars became my primary objects of interest. His telescopes grew as did his interest in amateur astronomy. In next years he was able to buy an R.E. Brandt achromatic doublet which was made into a telescope using irrigation pipe by Tom Dobbins. He had read about Lunar Domes by Patrick Moore (of course). Jim tried to join the ALPO lunar Dome program but found it no longer existed. At the suggestion of John Westfall the head of ALPO at the time, he started the New Lunar Dome Survey of the ALPO. This lasted for several years ending up with a catalog of lunar domes. It was not a complete list nor nearly as accurate as he had hoped but it was a start. About this time Jim started corresponding with Raffaello Lena the founder of the GLR (Geologic Lunar Research group), which wanted to continue the work on Lunar Domes to complete an accurate catalog, establishing a lasting friendship. He is interested in the GLR because the observers are so friendly and there is real work going on that I can contribute to. He is the coauthor of the book Lunar domes properties and mode of formation published by Springer. Today He observe and image with an AP 10" F/14.6 Maksutov-Cassegrain and an APM/TMB 10" F/9 apochromatic refractor with LZOS triplet lens, and uses Skynyx cameras plus Registax and Photoshop for processing.

Selenology Today

Carmelo Zannelli I was born on 29 April 1967 in Palermo, Sicily and I started my passion with Astronomy in 1977 when I was 10 years old. My first telescope was a small telescope of diameter 50 mm followed by a Newtonian 114 mm. Subsequent ownership of other scopes such as a Newtonian 130 mm, a Maksutov Newton 180 mm, a Celestron C-9,1/4, a Celestron C-11. Actually my telescope is a Celestron C-14 starbright. Between the years 1980 and 1990, with my friend Giorgio Puglia, I started with to image the deep-sky obtaining several awards in national competitions. I am graduated in Political Sciences at the University of Palermo. I am a founding member of the O.R.S.A. (Organizzazione Ricerche e Studi di Astronomia) in Palermo, association founded in 1984, and work for GLR group since many years. Today I use a camera Point Grey Flea3 for planetary imagery and a camera Basler ACE1300gm to image the Moon, both monochrome. The filters used are the Baader LRGB, placed in a motorized filter wheel.

Stefan Buda I was born in 1958 in the Eastern Bloc and I had a fascination with technology from the earliest age. When Apollo 8 flew around the Moon I was captivated by the news on the radio and never stopped following space news ever since. In my early teens I found an old booklet, in a dusty attic, that started with a vivid description of Schiaparelli observing the planet Mars and discovering "canali", then the story moved on to Lowell and all the speculation about life on Mars. I was enthralled! It did not take long before I was able to see craters on the Moon with a telescope I made from an uncut ophthalmic lens, a cardboard tube and a small magnifier. After finishing my formal education in mechanical engineering and completing my compulsory military service, at the age of 23, I put my life on the line and escaped across the Iron Curtain to the West. A few months later I found freedom in Melbourne, Australia where I've been living since. I ground my first telescope mirror in 1985, in time to observe Halley's comet with it. That was followed by many other telescopes and astrographs of increasing complexity. In the late 1990s I started experimenting with electronic imaging of the planets, first with video and then with home made CCD cameras and finally moving onto webcams. My targets were mainly the planets Mars, Jupiter and Saturn.

The Moon became interesting again for me more recently when I realized that the latest generation of frame stacking software can do an amazingly good job of unscrambling atmospheric distortions.

Selenology Today


George Tarsoudis He was born on 7 November 1970 at the Basel (Switzerland). Since 1978 he lives in Alexandroupolis (Greece).
He started passion with Astronomy in 2004 and he was one of the founding members of the Thrace Amateur Astronomy Club (TAAC).
He is a Lunar and Planetary observer and now he has a Skywatcher Telescope BK DOB14" Collapsible 355mm @f/4.5. His recent images are at the link of his website:

http://www.lunar-captures.com//Skywatcher_14inch.html

He has 69 Lunar Photo of the day (LPOD) and some publications at Magazines & Books. Moreover some his images are included in "The Astronomy Photographer of the Year book" from the Royal Observatory Greenwich. He works for Selenology Today Journal of GLR group (as publisher and editor) and has done some lectures for dissemination of astronomy to the general public.

Selenology Today

# Putative caldera being the source for at least some of the Bode pyroclastics: spectral studies

By Raffaello Lena Geologic Lunar Research (GLR) group

## Introduction

In the LPOD dated July 25, 2014, C. Wood speculates the presence a volcanic caldera, one of the largest on the Moon. In fact dark deposits extend away from the rim of a crater, consistent with the putative caldera being the source for at least some of the Bode pyroclastics. A spectral study of the mentioned deposits, according to the methods used by GLR group, was performed. In this work are described the results obtained using the Clementine and $M^3$ multispectral data. The lunar pyroclastic deposit (LPD) described in this work belongs to the black beads.

## Methods

Spectral analyses are released on the calibrated and normalized Clementine UVVIS and NIR reflectance data as provided by Eliason et al. (1999). The dark material extends beyond the crater rim suggesting an ash type deposit (Fig. 1) and displays a blue color with a compositional contrast between the LPD and the mare based on the UVVIS ratios imagery (Fig. 2). To estimate the abundances of six key elements, Wöhler et al. (2011) rely on the regression-based approach which involves the analysis of the mafic absorption trough around 1000nm present in nearly all lunar spectra. The continuum slope, the trough width, and the centre wavelengths and relative depths of the individual absorption minima occurring in it are extracted from Clementine UVVIS–NIR multispectral image mosaics. These spectral features allow on estimate of the abundances of the elements Ca, Al, Fe, Mg, Ti, and O based on a second-order polynomial regression approach, using the directly measured LP GRS abundance data as “ground truth” (Wöhler et al., 2011). The Titanium content computed with the regression method based on Clementine data is inaccurate for “blue mare” soils, so that the $TiO_2$ and FeO estimation equations by Lucey et al. (2000) may be applied (shown in Figs. 7-8).

Chandryann-1’s Moon Mineralogy Mapper ($M^3$) is an imaging reflectance spectrometer that can detect 85 channels between 460 nm and 3000 nm, and has a spatial resolution of 140 m and 280 m per pixel. For this work $M^3$ data, at a resolution of 140 mpp, were calibrated and photometrically corrected and converted to apparent reflectance. Data have been obtained through the $M^3$ calibration pipeline to produce reflectance with photometric and geometric corrections. For deriving the spectral parameters the photometrically corrected Level 2 data of the PDS imaging node have been used (Isaacson et al., 2011). The calibration of $M^3$ data is presented in detail by Green et al. (2011).

These spectra are not thermally corrected, so we do not analyze wavelengths longer than 2500 nm as these have a significant thermal emission component. This does not diminish the efficacy of the analysis because the relevant spectral features are located below 2300 nm. In order to characterize the 1000 nm band, it was used a continuum removal method that enhances the characteristic of the 1000 nm absorption band and more accurately shows the position of the band center. So a straight line between 750 nm and 1500 nm to remove the continuum was used.

The Christiansen Feature (CF) fromGridded data record (GDR) level 3 data product of Diviner Lunar Radiometer Experiment / Lunar Reconnaissance Orbiter (DLRE/LRO) data were used for further analysis. The Lunar Reconnaissance Orbiter’s (LRO) Diviner Lunar Radiometer Experiment has a spatial resolution of 950m/pixel. Diviner produces thermal emissivity data, and can provide compositional information from 3 wavelengths centered around 8µm that are used to characterize the

Christiansen Feature (CF), which is directly sensitive to silicate mineralogy and the bulk $SiO_2$ content (Greenhagen et al., 2010).

## Results and discussion

The pyroclastic deposit has a $R_{415}/R_{750}$ ratio of 0.6445 and a $R_{950}/R_{750}$ ratio of 1.0787 (Figs. 2-3). Albedo at 750 nm is an indicator of variations in soil composition, maturity, particle size, and viewing geometry. The $R_{415}/R_{750}$ colour ratio essentially is a measure for the $TiO_2$ content of mature basaltic soils, where high $R_{415}/R_{750}$ ratios correspond to high $TiO_2$ content and viceversa. The $R_{950}/R_{750}$ colour ratio is related to the strength of the mafic absorption band, representing a measure for the FeO content of the soil, and is also sensitive to the optical maturity of mare and highland materials

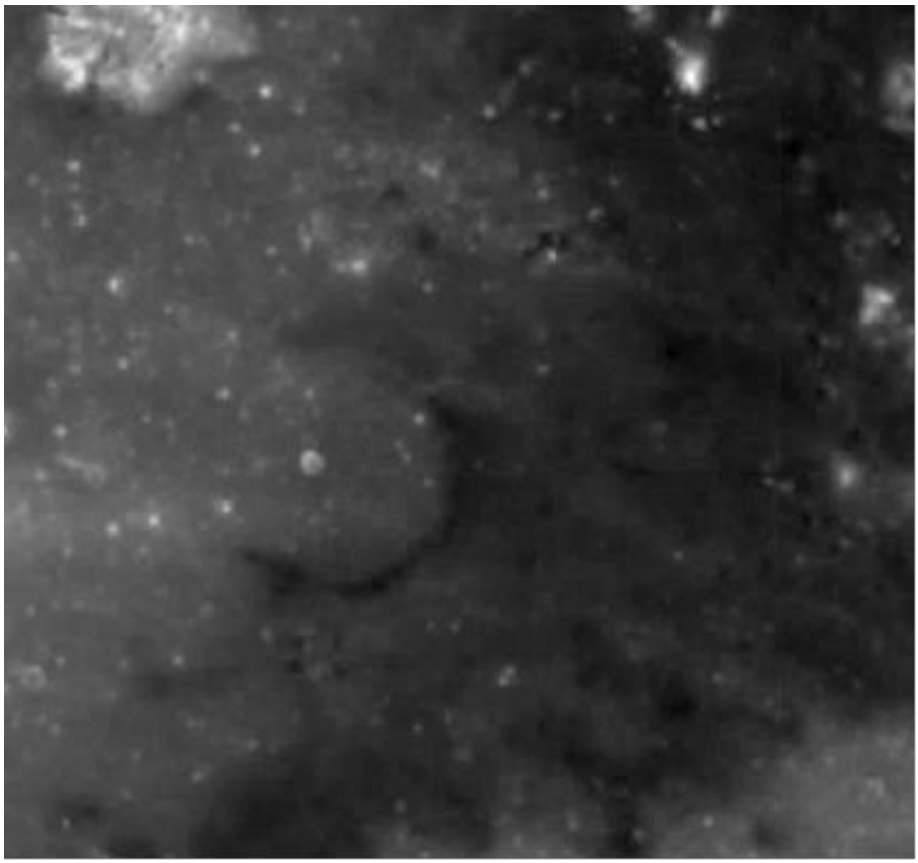

Figure 1

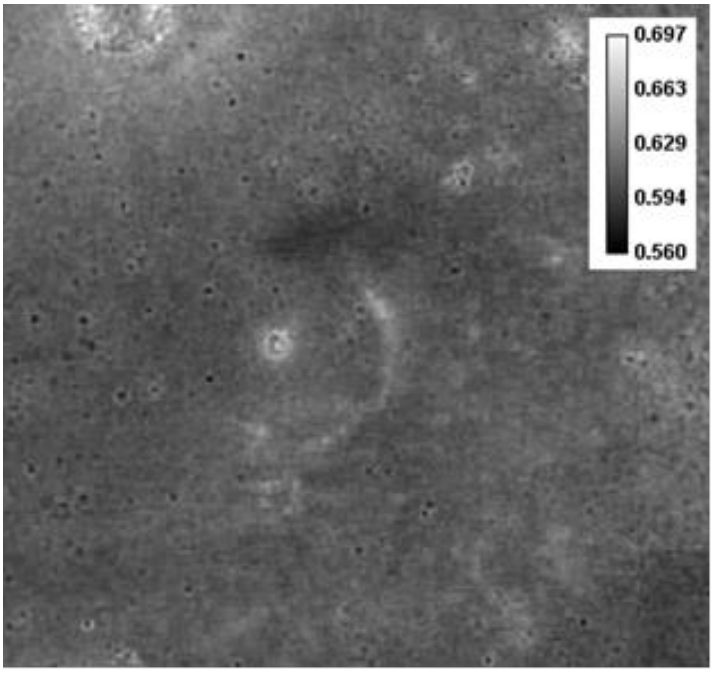


Figure 2. $R_{415}/R_{750}$ ratio

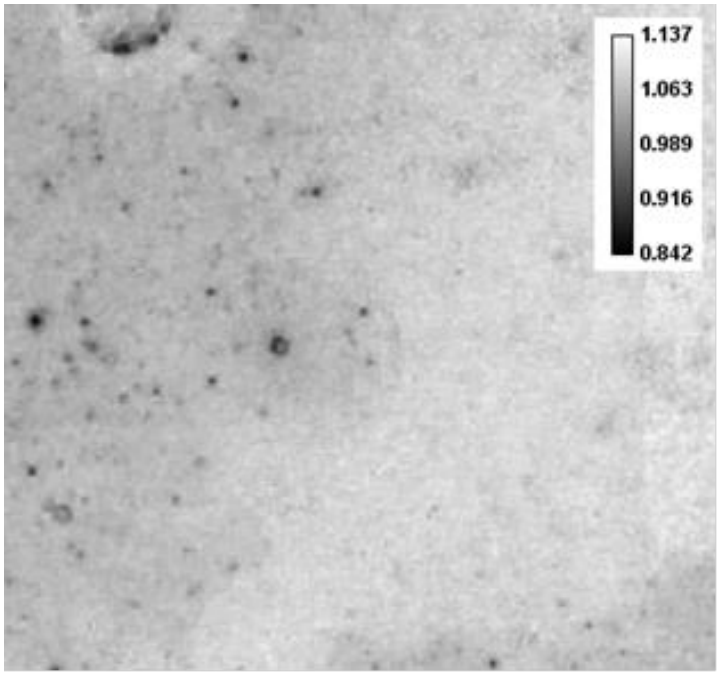


Figure 3. $R_{950}/R_{750}$ ratio

The color ratio image is obtained assigning the $R_{750}/R_{415}$, $R_{750}/R_{950}$ and $R_{415}/R_{750}$ into the red, green, and blue channels of a color image, respectively. The lunar highlands are depicted in red (old) and blue (younger). In the color ratio image the maria are depicted in yellow/orange (iron-rich, lower titanium) or blue (iron-rich, higher titanium). The pyroclastic deposit is characterized by a different color respect to the nearby soil and appears blue indicating an increased $TiO_2$ content (Fig. 4).

The petrographic map is constructed in terms of three different mare basalt end-members, where the relative content of mare basalt, Mg-rich rock, and FAN is denoted by the red, green, and blue channel, respectively (Fig. 5). The highland soils stand out clearly as anorthositic highland material (blue). Basaltic mare plains and lava-filled craters appear red orange while in the green are showed Mg-rich rock, e.g. with high olivine component.

Another petrographic map, termed petrographic basalt map (Fig. 6), was then represented as relative fractions of the three end-members: red for mare basalt with low Titanium amounts (Al 9 wt%, Ti 1.5 wt%), green for highland-like material (Al 14 wt%, Ti 0.5 wt%) and blue for titanium rich basalt (Al 6.3 wt%, Ti 3.6 wt%).

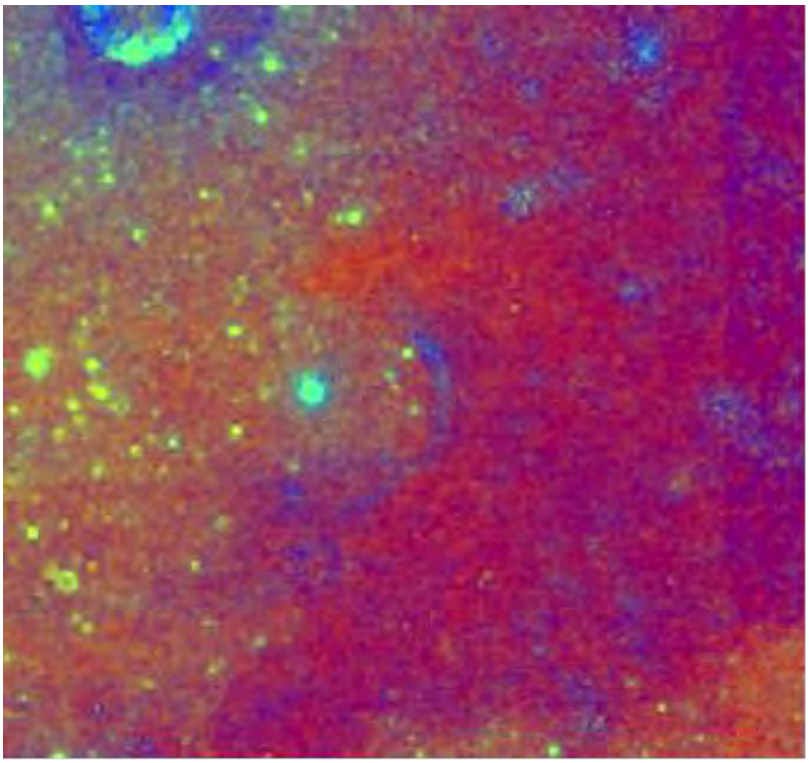

**Figure 4. Clementine color ratio image**

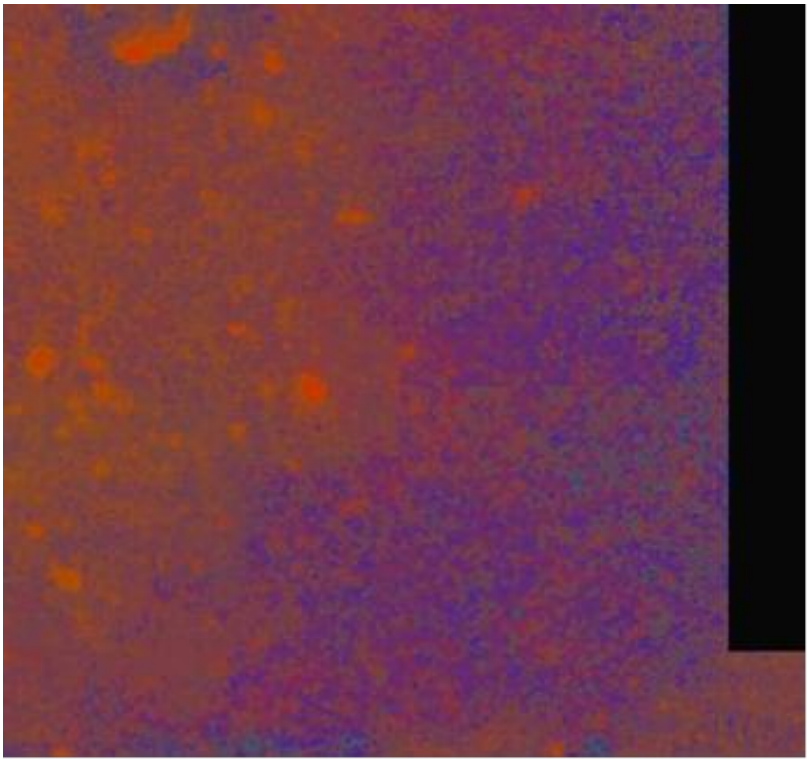

**Figure 5. Petrographic map constructed in terms of three different mare basalt end-members**

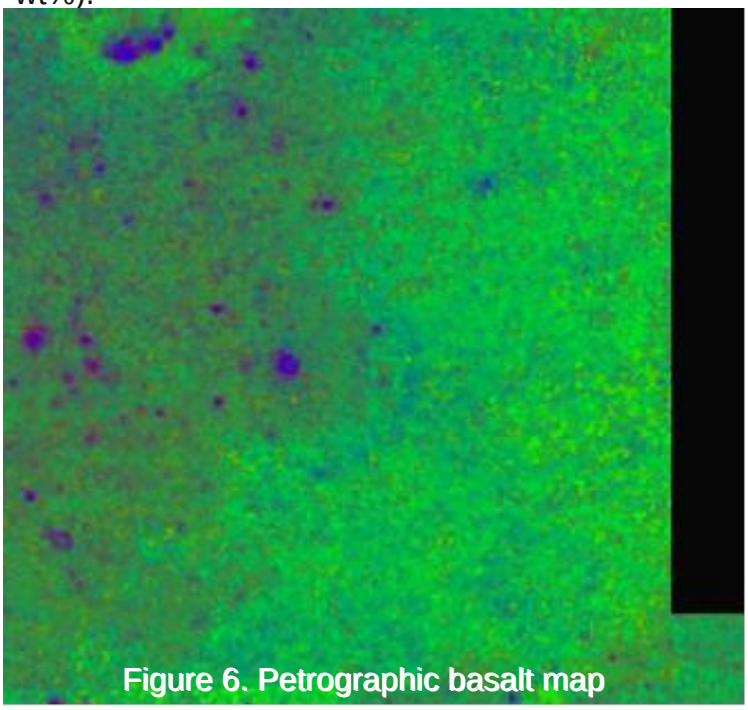

**Figure 6. Petrographic basalt map**

In this map regions appearing in green are composed of highland material (or sometime mare basalt contaminated with highland material by lateral mixing effects). The LPD displays a titanium rich composition, according to the Clementine color ratio map (Fig. 2), while the eastern soils are of highland composition. It is important to note that the derived amounts of Ti and Fe might not be appropriate for some deposits due to the possible presence of high amounts of glasses and other unknown factors. However the analysis, according to the Clementine color ratio images displaying a blue color with a compositional contrast, indicate that the "relatively" higher $TiO_2$ and FeO values (Figs. 7-8) are associated with the pyroclastic deposit if compared to nearby mare soil, which is reddish in the color ratio.

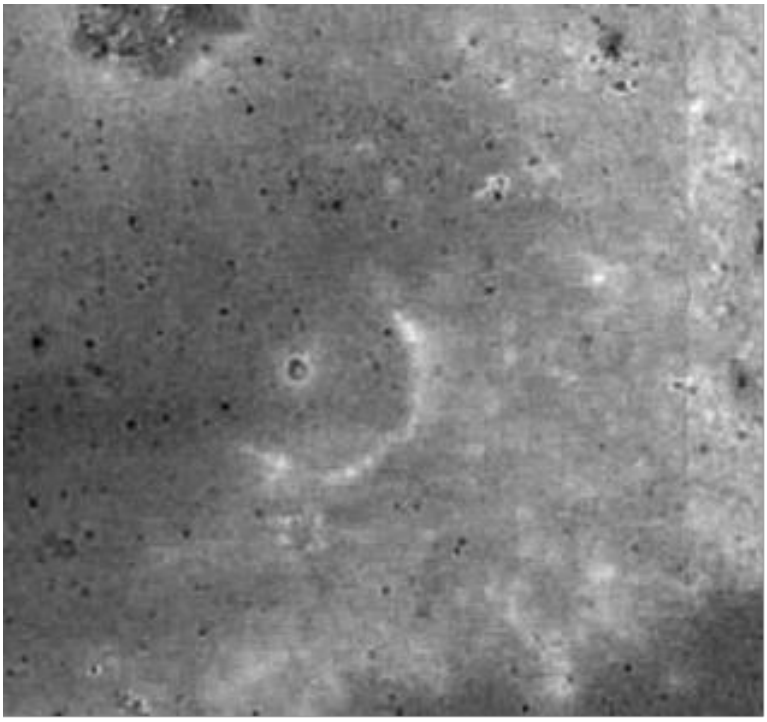

**Figure 7. $TiO_2$ content (% wt)**

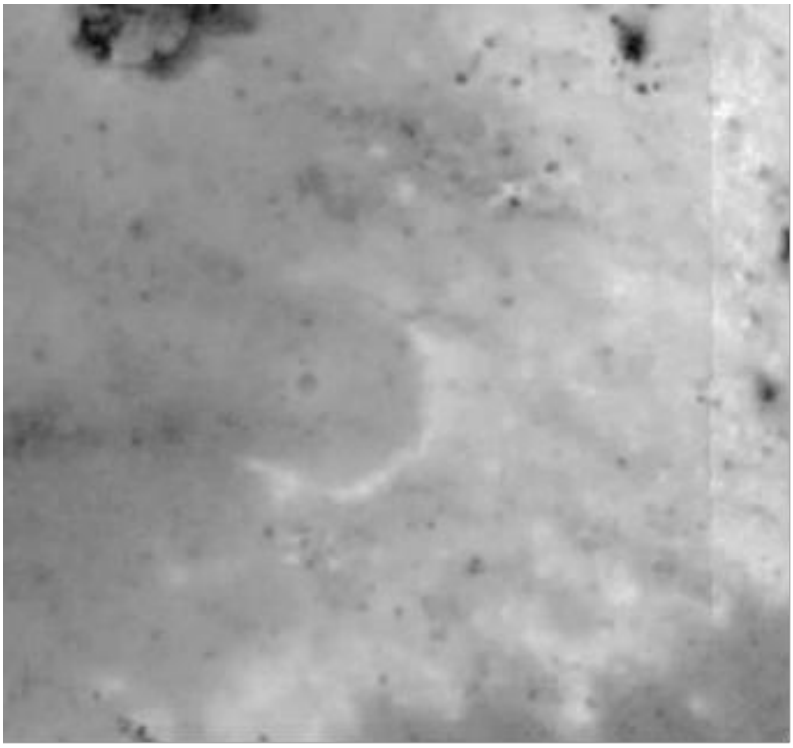

**Figure 8. FeO content (% wt)**

Spectral diagrams of the examined deposit (Fig. 9) indicate a composition similar to the black beads: mare soils are represented by the dark grey regions and highland soils by the light grey regions, according to Gaddis et al. (2003). Taurus–Littrow, Sinus Aestuum, Vaporum, and Rima Bode LPDs are all "blue" in Clementine color ratios and are known or inferred to have a significant component of high-titanium materials (in the form of ilmenite-rich black beads).

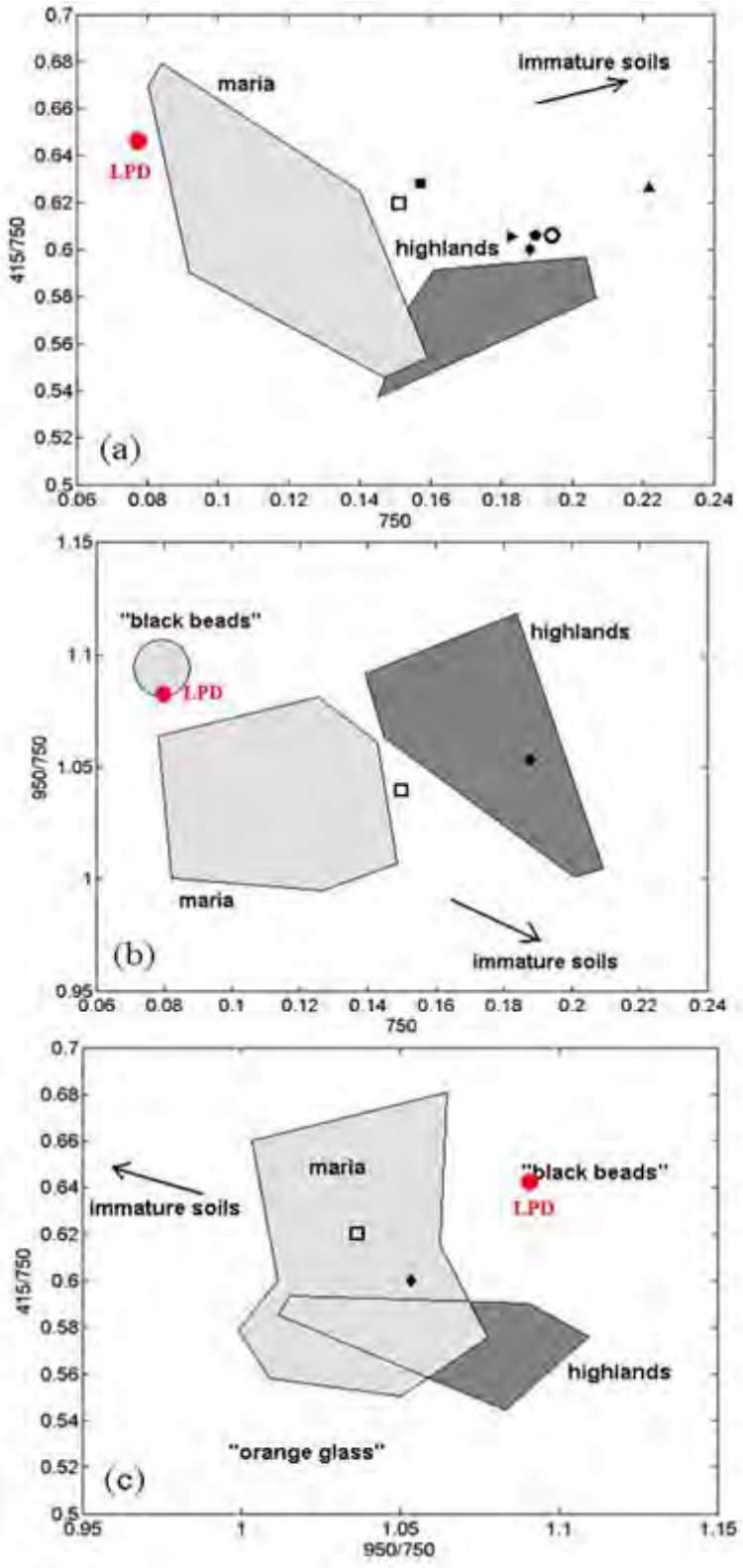


Figure 9

The spectral signature of olivine has a wide band centered beyond 1000 nm, while the pyroxenes displays a narrow trough around 1000 nm, with a minimum wavelength below 1000 nm, and a wide absorption band around 2000 nm. Chandryann-1's Moon Mineralogy Mapper ($M^3$) and Clementine data the spectra of the deposits would indicate a mixture of some olivine content and pyroxene (see Figs 10-12).

Mapped observation: **M3G20090206T010833_V01_L2_MAP.IMG.vrt**
Center point: ( lon, lat ) = ( **-4.18001, 11.53659** )
Projection: **Orthographic**
Resolution: **125 mpp**
ROI extent: **40km x 40km**

Probes (2) | Add | Drag | Delete | Spectra | Get | L2(PDS v1) Apparent Reflectance | 3 x 3

Showing L2 reflectance at: **660.61 nm**

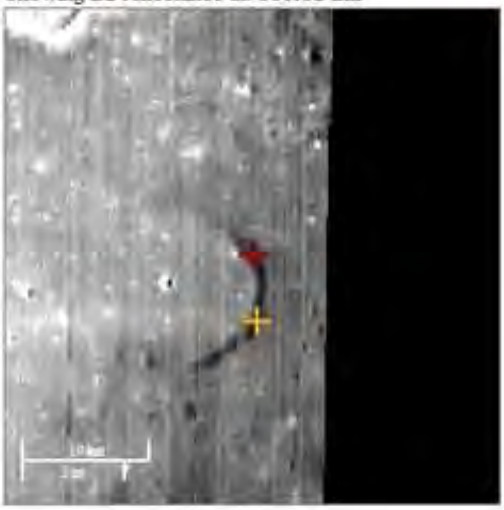

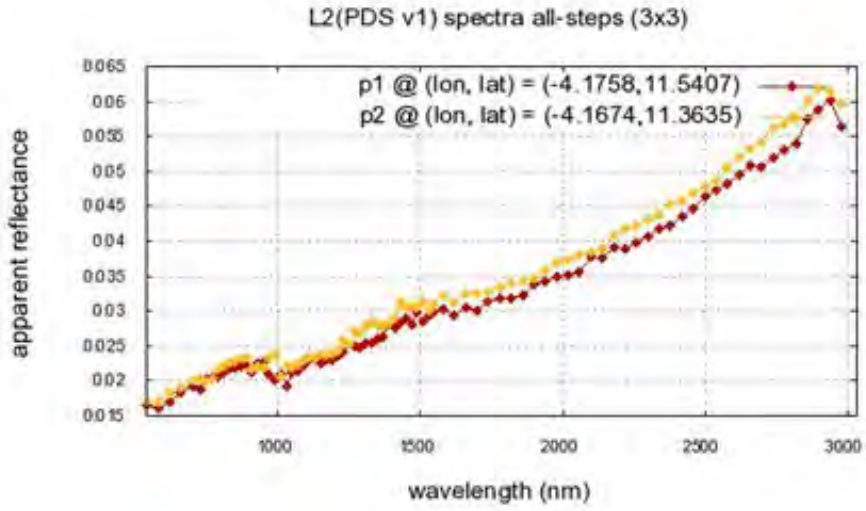


**Figure 10**

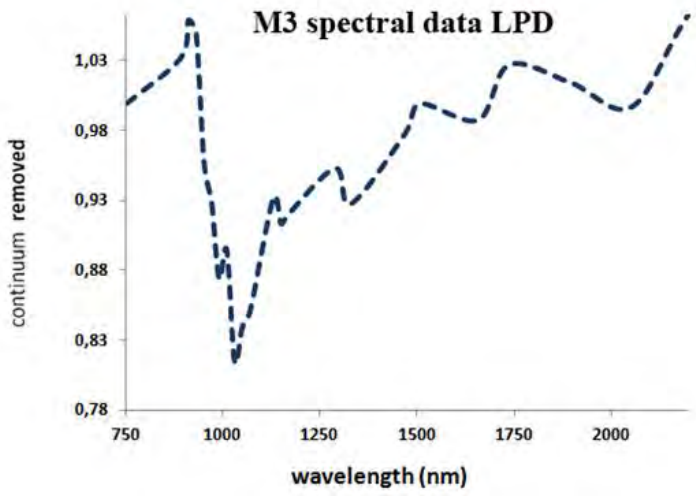


**Figure 11**

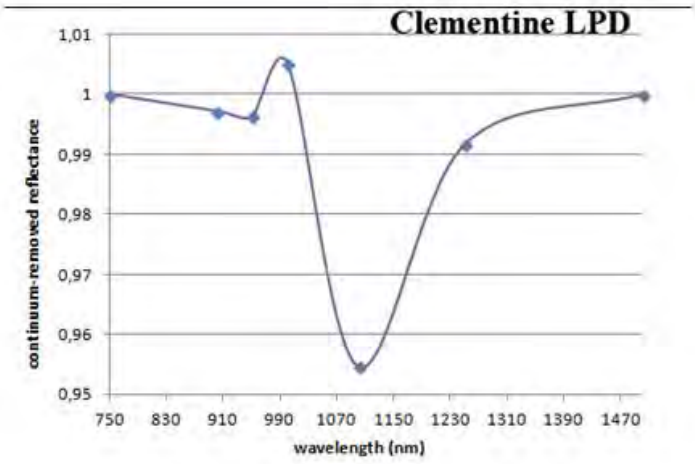


**Figure 12**

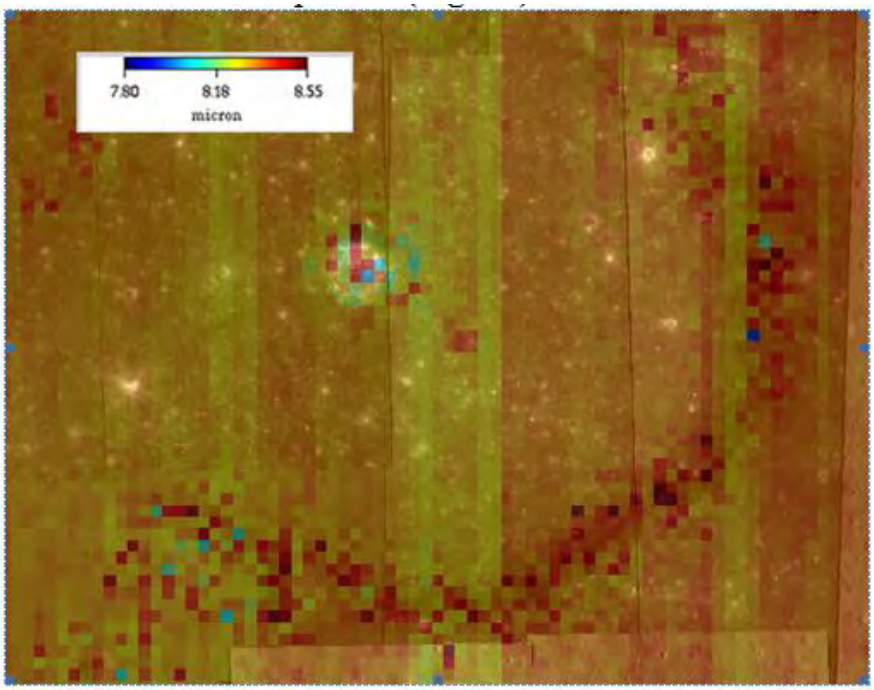


**Figure 13**

The Christiansen Feature (CF) from Gridded data record (GDR) level 3 data product of Diviner Lunar Radiometer Experiment/Lunar Reconnaissance Orbiter (DLRE/LRO) indicate values towards longer wavelength (CF ~8.55 micron) indicating less silicic composition and at least in some parts with an olivine component (Fig. 13).

In conclusion the spectral studies indicate that the dark deposit has a composition corresponding to the LPDs termed as black beads.

**References**

1) Eliason, E., Isbell, C., Lee, E., Becker, T., Gaddis, L., McEwen, A., Robinson, M.: Mission to the Moon: the Clementine UVVIS Global Mosaic. PDS Volumes USANASA PDS CL 4001 4078. http://pdsmaps.wr.usgs.gov (1999).

2) Gaddis, L.R., Staid, M.I., Tyburczy, J.A., Hawke, B.R., Petro, N.E., 2003. Compositional analyses of lunar pyroclastic deposits. Icarus 161, 262–280.

3) Green, R.O., Pieters, C.M.,Mouroulis, P., Eastwood,M., Boardman, J., Glavich, T., Isaacson, P.J., Annadurai, M., Besse, S., Barr, D., Buratti, B.J., Cate, D., Chatterjee, A., Clark, R., Cheek, L., Combe, J.P., Dhingra, D., Essandoh, V., Geier, S., Goswami, J.N., Green, R., Haemmerle, V., Head J.W., Hovland, L., Hyman, S., Klima, R.L., Koch, T., Kramer, G.Y., Kumar, A.S.K., Lee, K., Lundeen, S., Malaret, E.,McCord, T.B.,McLaughlin, S.,Mustard, J.F., Nettles, J.W., Petro,N.E., Plourde, K., Racho, C., Rodriquez, J., Runyon, C., Sellar, G., Smith, C., Sobel, H., Staid, M.I., Sunshine, J.M., Taylor, L.A., Thaisen, K., Tompkins, S., Tseng, H., Vane, G., Varanasi, P., White, M.,Wilson, D., 2011. TheMoonMineralogy Mapper (M3) imaging spectrometer for lunar science: instrument description, calibration, on-orbit measurements, science data calibration and on-orbit validation. J. Geophys. Res. 116, E00G19, http://dx.doi.org/10.1029/2011JE003797.

4) Greenhagen, B.T., Lucey, P.G., Wyatt, M.B., Glotch, T.D., Allen, C.C., Arnold, J.A., Bandfield, J.L., Bowles, N.E., Donaldson Hanna, K.L., Hayne, P.O., Song, E., Thomas, I.R., Paige, D.A., 2010.

Global silicate mineralogy of the Moon from the Diviner Lunar Radiometer. Science 329, 1507–1509, http://dx.doi.org/10.1126/science.1192196.

5) Isaacson, P., Besse, S., Petro, N., Nettles, J., and the M3 Team: M3 Data Tutorial November 2011 http://pds-imaging.jpl.nasa.gov/documentation/Isaacson_M3_Workshop_Final.pdf .

6) Lena, R., Wöhler, C., Phillips, J., Chiocchetta, M.T., 2013. Lunar domes: Properties and Formation Processes, Springer Praxis Books.

7) Lucey, P.G., Blewett, D.T., Jolliff, B.L., 2000. Lunar iron and titanium abundance algorithms based on final processing of Clementine ultraviolet-visible images. J. Geophys. Res. 105 (E8), 305 (20,297–20).

8) Wöhler, C., Berezhnoy, A., Evans, R., 2011. Estimation of elemental abundances of the lunar Regolith using clementine UVVIS-NIR data. Planet. Space Sci. 59 (1), 92–110.

9) Wood, C. http://lpod.wikispaces.com/July+25%2C+2014

Selenology Today

## Lunar South Pole

By Rik Hill

On October 4-5 the libration of the moon was favorable for observation of the lunar south pole. I enjoy peeking over the edge, so to speak, and seeing features that are only occasionally visible. I've marked some of these transient features. Note on the far left the position of the Lunar Prospector Crash on July 31, 1999. I observed that event with Dr. Ann Sprague on the 61" Kuiper Telescope (Catalina Telescope) on Mt. Bigelow in the Catalina Mountains north of Tucson. We had a large echelle spectrograph on the telescope with the slit oriented perpendicular to the limb in hopes of seeing dust, enhanced continuum or maybe even emission lines from vaporization, though this latter was very unlikely since the velocity of the impact was too slow. In the end we saw nothing that we could attribute to the impact, but the set up and anticipation was great fun.

North of Scott you can see two large craters, Schomberger and Simpelius and further on near the top of the image is Curtius. Above Demonax are also two large craters, Boguslawsky and Manzinus. Over near the right edge of the image is the great 134km diameter crater Boussingault and above it is Mutus with the two smaller (17 and 24 km) craters on opposite walls. Over on the left edge just barely seen is the landmark 117km diameter crater Moretus.

The 2 images that made this montage, each made from 500/3000 AVI frames, were stacked using Registax 6, knit together with AutoStitch and final processing done with GIMP and IrfanView.

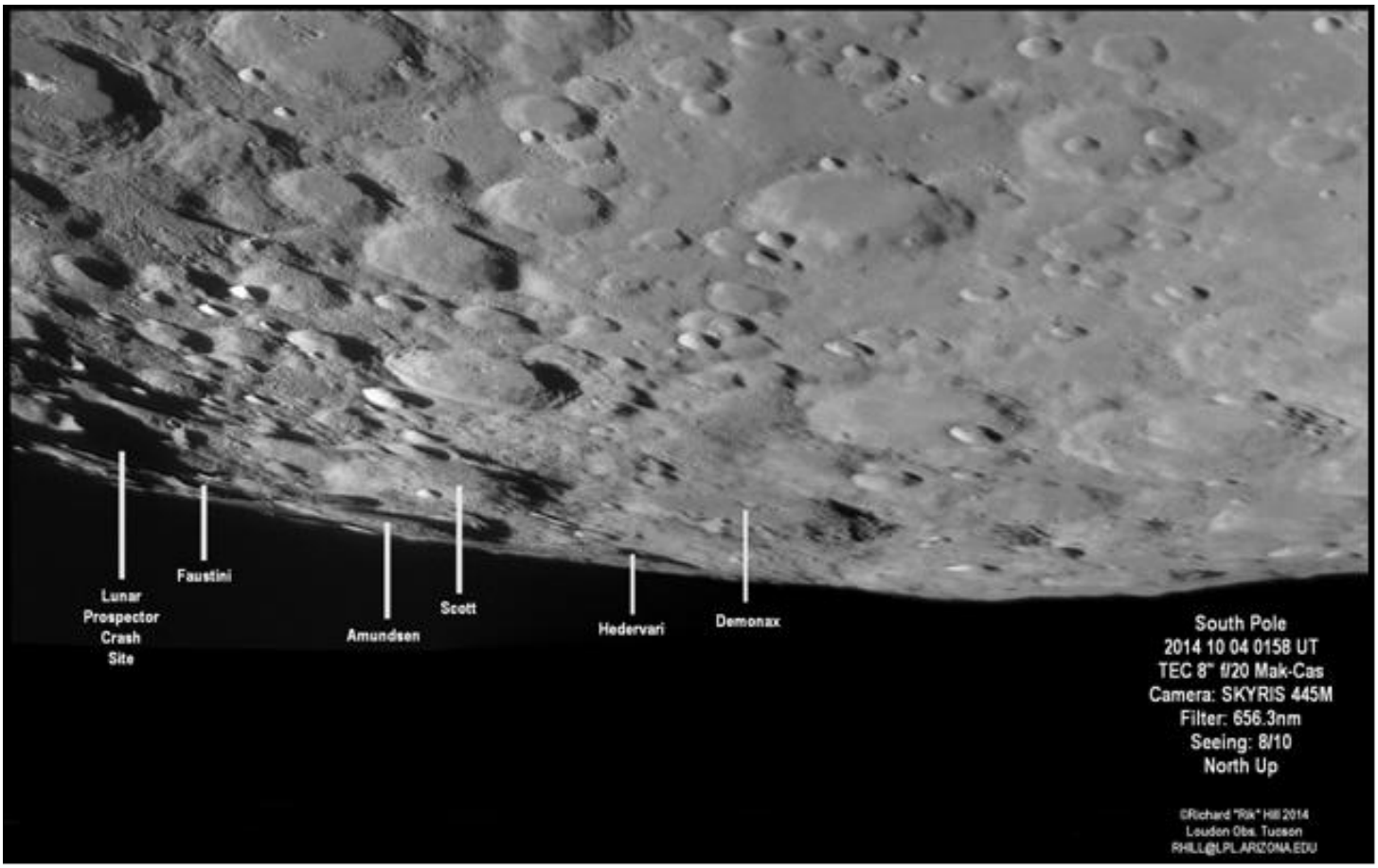

# Lunar eclipse October 8 2014

I wish I had my small telescope (80mm LOMO F/6) with me but I did what I could using a Nikkor 70-200 F/2.8 lens with my Nikon D810.

NIKON D810
NIKKOR LENS 200MM @ F/2.8
ISO Various

Here are a few images from the start of the eclipse and at/near totality with the Blood Moon appearance or, if squeamish a copper penny color.

By Jim Phillips

Selenology Today

# Selenology Today


By Maurice Collins

The view through binoculars was nice, not so nice through my little ETX which couldn't grab much feeble light. I tried some afocal shots through it with a 32mm eyepiece at 11:53pm which I have made into a montage (they are a bit blurred). It was quite dark, and not easily seen in the ETX but there was thin clouds most of the time, but it looked ok in binoculars and naked eye. Not sure what Danjon I would rate it, I agree with the estimates I've seen so far of 2 or 3.

Not as good as the last eclipse from here where it was nice and clear until after mid-eclipse. This time round I kept taking the ETX back inside when it clouded over as couldn't tell if it was going to rain or not. I gave up around 12:30pm where it looked pretty solid cloud.

Anyway, least we saw it and it was nice!

ISSUE # 36, 2015

Selenology Today

# The Strombolian eruption style and the volcanic eruptions from Stromboli

By Raffaello Lena Geologic Lunar Research (GLR) group

## Abstract

In this paper is described the Strombolian activity, including an overview of the Italian volcano Stromboli. The images of the volcano, and its eruptions, are taken by the Author. Some samples of volcanic rocks, from the private collection of the Author, are presented and described. A comparison with lunar strombolian eruption is given.

## Introduction

Volcanic eruptions created lava flows, pyroclastic deposits, pits, and domes on the Moon. The same process continues to operate on Earth, most reliably visible at Stromboli volcano which has erupted for more than a millennium (Wood, 2008; see also Alean and Fulle, stromboli online). Some of the lunar pyroclastic deposits on the moon have been described and modelled as compatible with a Strombolian or Vulcanian style of eruption.

## General overview

More than 100 lunar pyroclastic deposits have been recognized and classified as small and regional deposits on the basis of size and morphology (Gaddis et al, 2003 and references therein). Characterization of the nature of the lunar pyroclastic deposits (LPDs) is essential for models of formation, segregation and emplacement of lunar magmas. There are two styles of volcanism that might leave dark mantling units on the moon. Regional deposits are thought to have been emplaced as products of continuous or Strombolian-style eruptions, with wide dispersion of well-sorted pyroclasts (Gaddis et al, 2003; ). Intermittent or Vulcanian-style eruptions likely have produced the small pyroclastic deposits, with explosive removal of a plug of lava within a conduit and forming an endogenic vent (Head and Wilson, 1979; Weitz et al, 1998).

Thus the Strombolian eruptions may have formed the largest dark mantle deposits on the moon while the Vulcanian eruptions feature short explosions of gas and rocks and tend to be smaller than Strombolian eruptions. Because gases need to build up near the vent, they do not involve large volumes of magma. Hence, Vulcanian eruptions likely form the smaller patches of dark materials on the moon, with a recognizable central pit or vent structure (Head and Wilson, 1979).

Among the largest of the dark mantle deposits are Aristarchus plateau, Mare Humorum, South Mare Vaporum and Sulpicius Gallus deposits.

On the Earth continuous Strombolian explosions, sometimes accompanied by lava flows, have been recorded at Stromboli (Italy) for more than a millennium.

Stromboli, the North East of the Aeolian Islands, is the emergent summit of a volcano that grew in several eruptive periods, the last of which formed the western portion of the island (Fig.1a). Ginostra, located to the West, is likely the smallest port in the world (Fig 1b). About 200000 years ago, Stromboli had not yet reached sea level but another volcano, called Strombolicchio, was active. Today Strombolicchio is an eroded volcanic neck of basaltic andesitic composition (Fig.2).

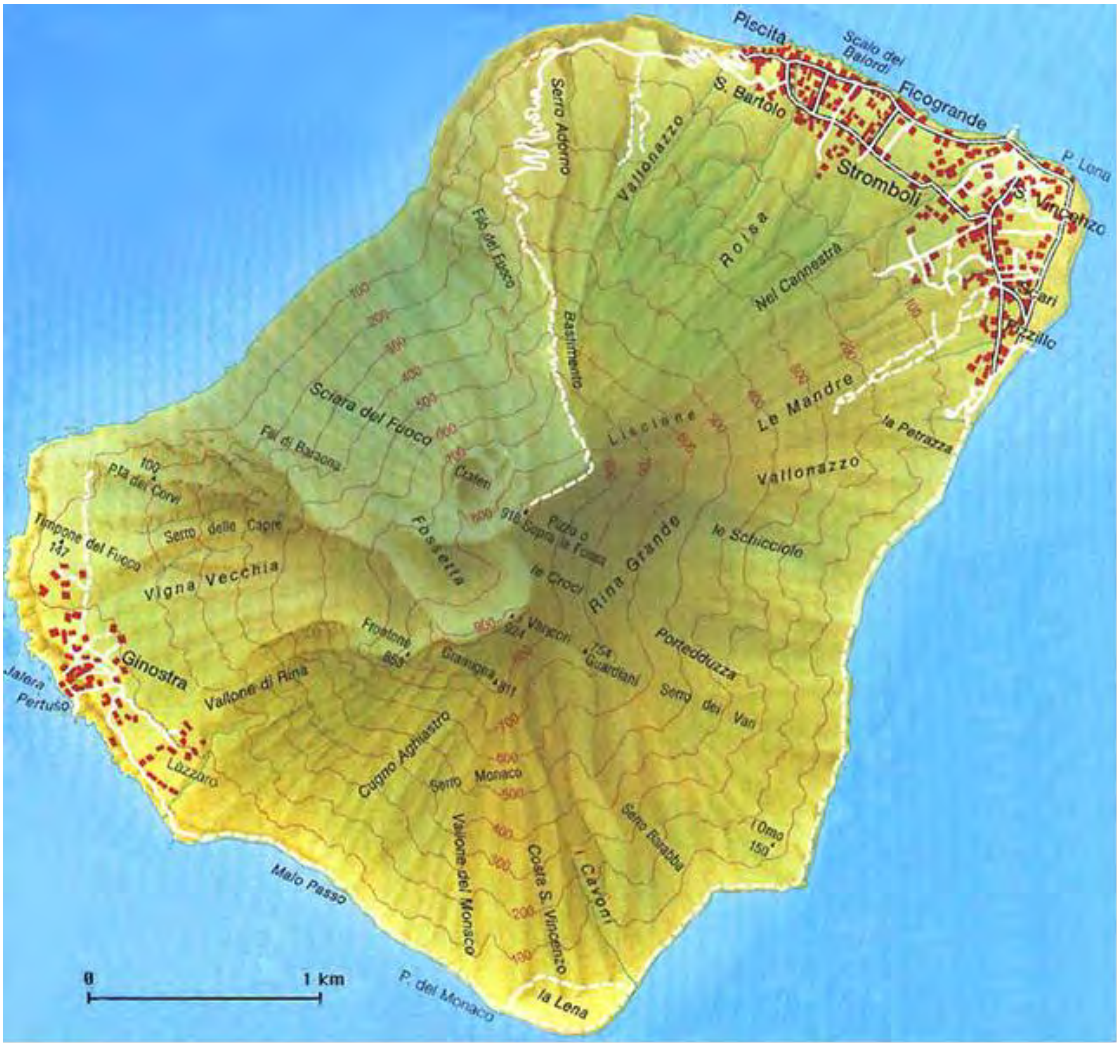


**Figure 1a**:
map of Stromboli

**Figure 1b**:
Ginostra village (image by the author)

Figure 2:
Strombolicchio an eroded volcanic neck (image by the author)

The geologic evolution of Stromboli volcano is recorded in its subaerial part and four major periods (Paleostromboli, Vancori cicles, Neostromboli, Recent Stromboli) have been recognized and further subdivided in 30 volcanostratigraphic units (Fig.3). These main divisions are defined largely by collapse episodes of the volcanic edifice (Fig. 3). The Vancori products filled the remnants of the Paleostromboli edifice, a caldera formed at the end of the Paleostromboli period (Hornig-Kjarsgaard et al., 1993). A lateral collapse defines the end of the Vancori period and the Neostromboli collapse, which occurred in the same direction, defines the end of the Neostromboli period (Hornig-Kjarsgaard et al., 1993; Tibaldi et al., 1994; International Geoscience program and references therein). Subsequently, a new vent became active in the area of Pizzo sopra la Fossa (Fig. 1), marking the onset of the recent activity of the volcano. Several smaller collapses have occurred in the same area, forming the Sciara del Fuoco in its present shape and resulting in a highly faulted volcanic edifice. The Sciara del Fuoco formed about 5000 years ago (cf. Fig.4). During the first two periods pyroclastites (ignimbrites, surge and lahar deposits) predominate over lavas. The more recent products are generally basalts and andesites spanning the complete range of subduction-related magma series from calc-alkaline to shoshonitic. The activity of the Vancori and Recent periods is shoshonitic, whereas the Neostromboli period products are richer in potassium (Francalanci et al., 1989).

In locality Piscità (Fig.1) a lava tube is visible, which formed after the surface of a lava flow cooled and solidified, developing a continous crust beneath which the still molten interior lava continued to flow toward the sea. The active vents are well visible from the Sciara del Fuoco or from the highest peak of the volcano Pizzo sopra la fossa (cfr. Figs 1 and 3). The slope below the vents is covered with debris from the October 1993 explosions. Interestingly some small yellowish patches between dark ash located near the crater 1 are apparent. They are remains of Neostromboli volcano, which have been chemically altered by corrosive action of the fumaroles, still visible in the upper portion of the cone. Figs. 1-10 provide the stratigraphic relationship and the different volcanic products that can be observed today in Stromboli. All the images were taken by the Author.

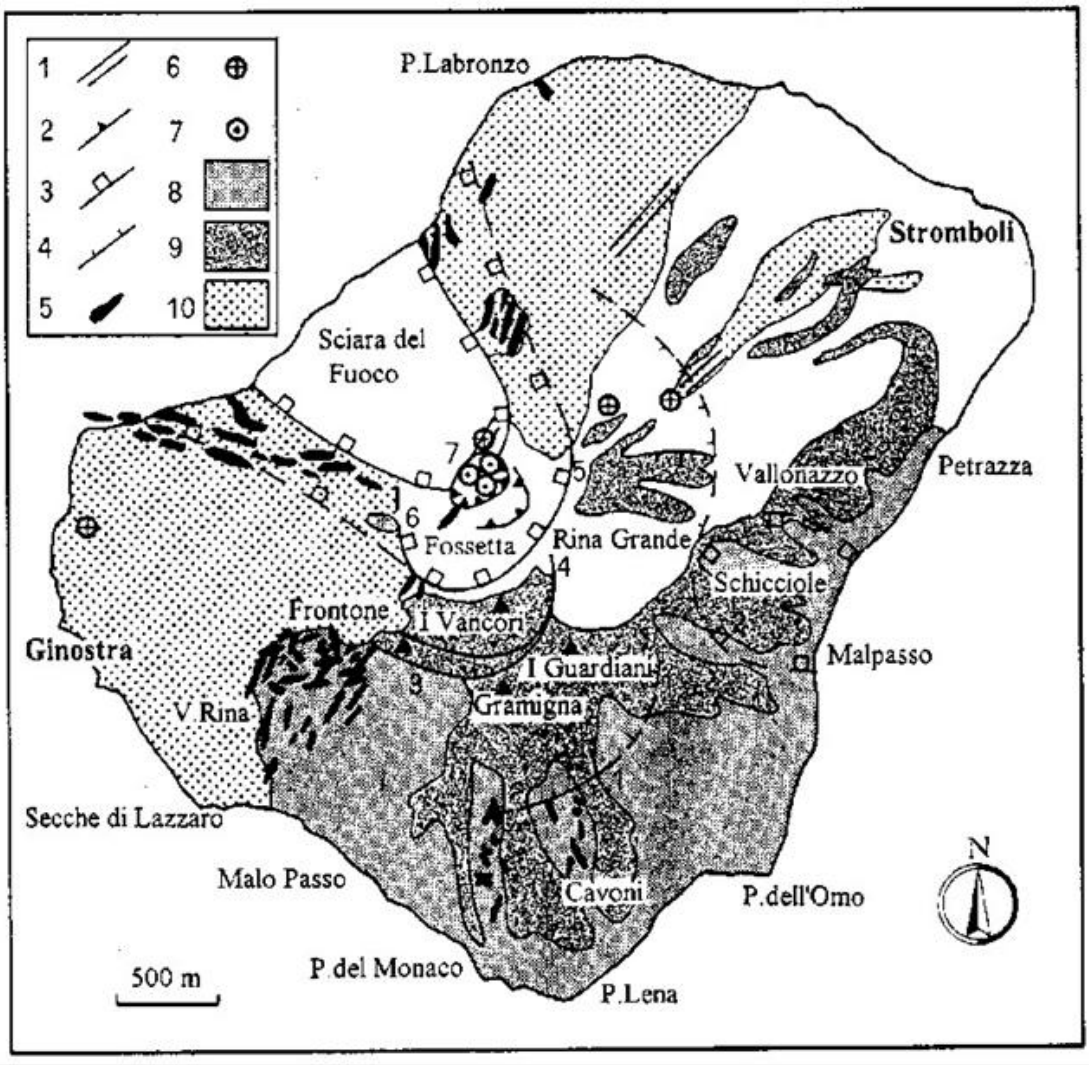


**Figure 3:**

Geologic map of Stromboli; 1, eruptive fissure; 2, crater rim; 3, flank and sector collapses; 4, summit caldera; 5, dike; 6, young parasitic vent; 7, active vent; 8, oldest rock units comprising Paleostromboli I, II e III; 9, Vancori series; 10, Neostromboli rocks; in white are the Recent Period deposits (from Pasquarè et al, 1993).

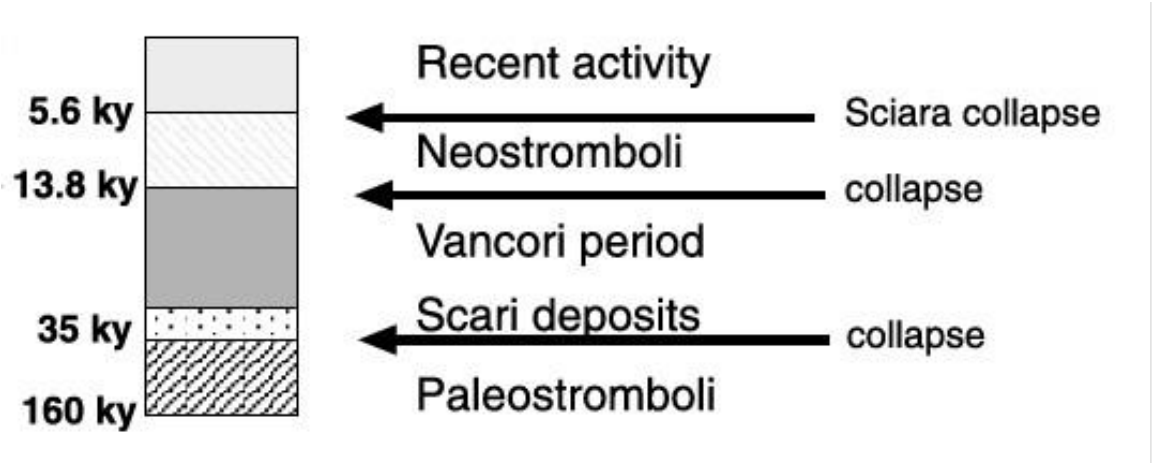


**Figure 4** : periods of volcanism and collapse in Stromboli

**Figure 5 a.**

Basalts and scoria from the Paleostromboli volcano (image by the author)

## Eruption style and Mineralogic characteristics

The magmas of the Aeolian islands are similar to those of volcanoes that make up the "belt of fire" in Pacific ocean. They show, over time, the trend towards ever more basic compositions (lower content of silica) and more rich in potassium. The sample shown in Fig. 11 is an andesite with reddish hue and vescicular texture. The main phenocrysts are plagioclase feldspar and with the presence of pyroxene (clinopyroxene) and olivine. For a detailed account of the mineral chemistry of Strombolian basalts refer to Francalanci et al (1989) and Wilson et al (2006). However Strombolian eruptions normally occur several times per hour from one or more of the active vents sited 150 m below the Pizzo Sopra la Fossa (Fig. 1). These explosions led to fallout of fresh lapilli or scoria. Samples of lapilli and scoria (see Fig. 12) collected on Stromboli belong to the black scoriaceous volcanic material normally erupted during Strombolian activity.Figure 12 shows a vesicular, black in color, glassy rock formed during eruptions, when decreasing pressure causes gas to «bubble out» of andesitic and basaltic magma. The black color is mostly due to its iron content. As shown from volcanic material and petrologic analysis, the activity in Stromboli and nearby Vulcano island, is different from the material produced during the volcanic activity in the Lipari island, another Aeolian island, which contains craters and lava domes on a basement of submarine volcanic deposits. The latest eruption in historic times, probably in 729 AD, at Monte Pilatus at the NE tip of the Lipari island, formed obsidian lava flow and deposit of pumice (cfr. Figs. 13 and 14).

Stromboli has an activity characterized by the intermittent explosion or fountaining of lava from the vents, especially from crater 1 (the NE-crater) and crater 3 (the SW-crater), with scoria, lapilli and ash ejected within a very restricted area close to the vents (Fig. 15). Occasionally the volcano enters a period of more activity called a ‘paroxysm’. This is characterized by the ejection of the volcanic products outside the caldera rim and bombs can even land on the villages on the island. Bertagnini et al.(1999) reported emission of “golden pumice” when associated with paroxysmal explosive events.

The magma in a Strombolian eruption rises slowly in the vent, allowing bubbles to coalesce and separate from the melt, as they rise to the top of the magma column. Upon reaching the surface, the gas pocket disrupts the magma, throwing it out ballistically. The whole cycle repeats, with individual blasts separated by anything from a fraction of a second to hours (Fig. 16).
Two main possibilities have been proposed to explain the paroxysmal explosive events: changes in the volatile flux, or changes in the groundwater level. Recently it has been demonstrated that paroxysm is heralded by anomalous increases in sulphur degassing (Aiuppa & Federico, 2004) and $CO_2$ and $H_2$ degassing (Carapezza et al., 2004), strongly suggesting that the shift in the style of activity is mainly controlled by changes in the volatile flux.

**Figure 5b.** Basalts and scoria from the Paleostromboli volcano (image by the author)

## Lunar Pyroclastic material

The explosive eruptions that formed the lunar dark mantle deposits have been likened to some types of terrestrial volcanic activity. Intermittently explosive or Vulcanian-style eruptions are likely to have produced the small pyroclastic deposits, with explosive decompression acting to remove a plug of lava within a conduit and to form an endogenic vent crater (Head and Wilson, 1979). The small pyroclastic deposits have been further subdivided into three compositional classes on the basis of their "1.0-micron" or mafic absorption bands in Earth-based spectra (e.g., Gaddis et al and references therein , 2003). Mafic bands of small pyroclastic deposits in the Group 1 class are centered near 0.93 to 0.95 microns, have depths of 4 to 5%, and are asymmetrical,. Their spectra resemble those of typical highlands and are

indicative of the presence of feldspar-bearing mafic assemblages which are dominated by orthopyroxene (e.g . small pyroclastic deposits are found on the floors of Atlas Crater). Mafic bands in spectra for Group 2 deposits are centered near 0.96 microns, have depths of ~7%, and are symmetrical in shape. Group 2 spectra are similar to those of mature mare deposits, and they are dominated by clinopyroxene (e.g . two small deposits east of Aristoteles Crater ). Small pyroclastic deposits in Group 2 appear to consist largely of fragmented plug rock material, with insignificant amounts of highland and juvenile materials (e.g., Gaddis et al and references therein , 2003). Group 3 mafic bands are centered near 1.0 micron, have depths of ~5 to 7%, are relatively broad and asymmetrical, and are probably multiple bands. Spectra of Group 3 deposits are dominated by olivine and orthopyroxene; examples of Group 3 small pyroclastic deposits are those of J. Herschel Crater (62°N, 42°W) and the well known Alphonsus Crater (Fig. 17).

On the other hand, in a Strombolian eruption explosive decompression occurs as the pressure is released and the magma and gas rise in an expanding column of erupting material. For the moon the particles will spread out over an area roughly six times larger on the Moon than they would for a similar eruption on Earth. Larger fragments will be deposited closest to the vent. A Strombolian eruption is consistent with the volatile coated spheres returned from the Apollo 17 landing site. Among the largest of the dark mantle deposits are Aristarchus plateau, Mare Humorum, South Mare Vaporum and Sulpicius Gallus deposits.

**Figure 6 :**

stratrigraphy of lava flows and scoria produced from Paleostromboli and Vancori volcano (image by the author) .

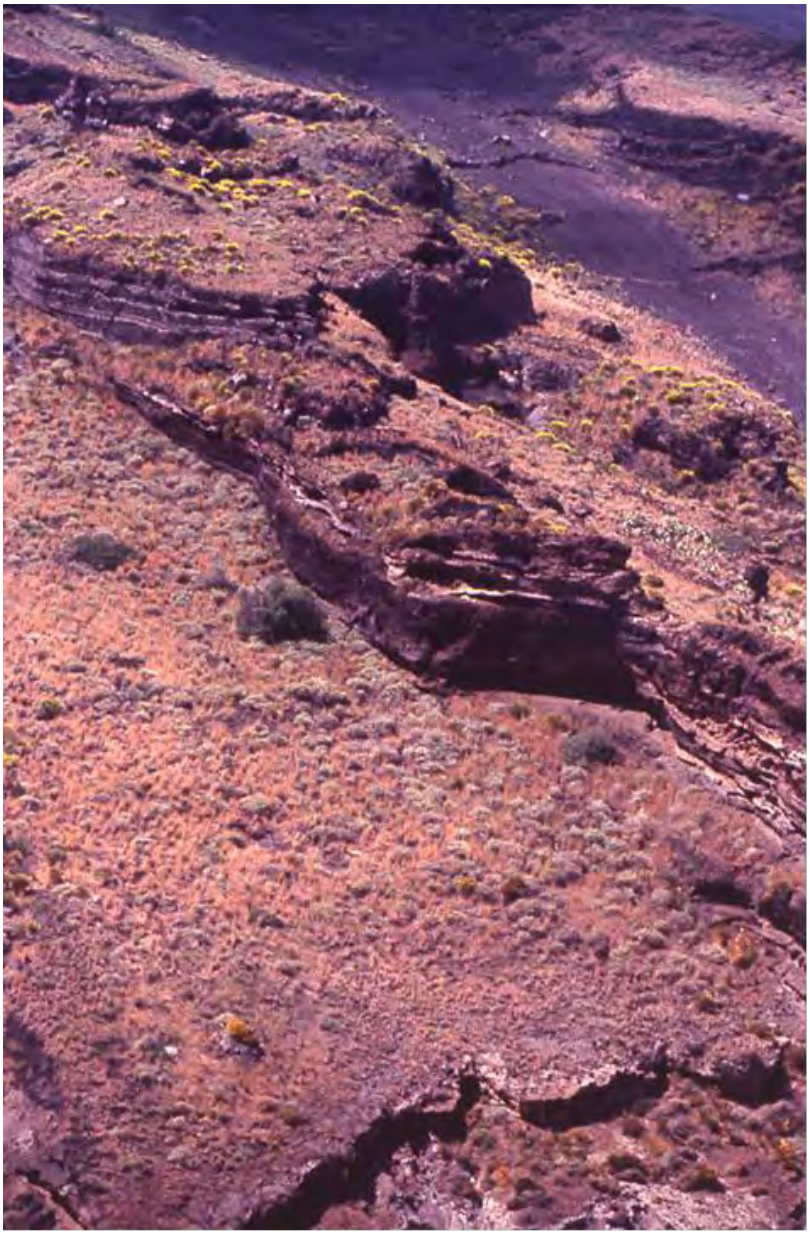

**Figure 7:**

the Vancori volcano has produced explosive eruptions. Ignimbrites, lapilli, solidified lava and pyroclastic deposits are apparent (image by the author).

**Figure 8:**

Volcanic products (scoria and lava flows) from Neostromboli volcano (image by the author)

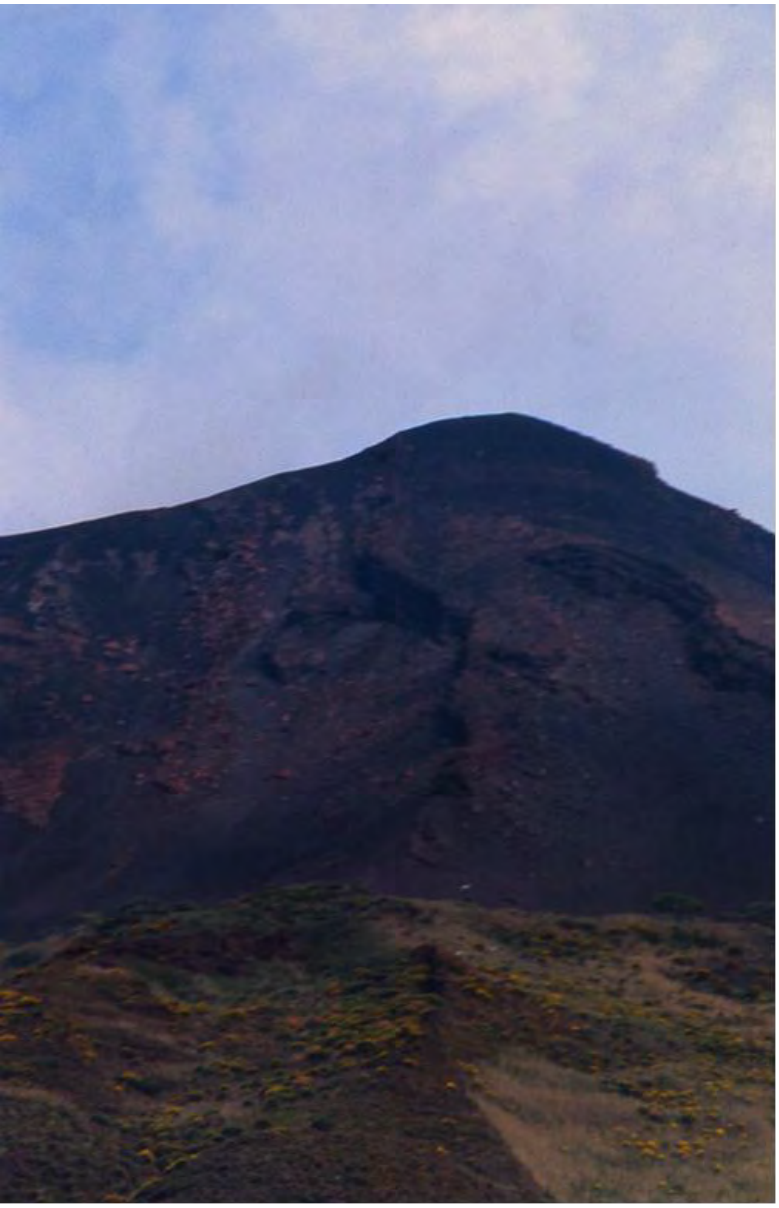

**Figure 9**:

the flank of the ancient Vancori volcano collapsed and was filled with volcanic products of Neostromboli. The surface is covered with

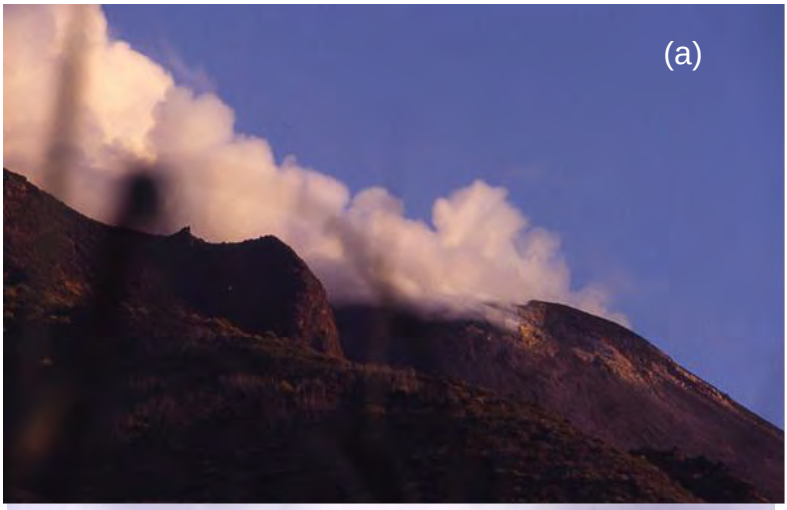



**Figure 10 a and 10 b** :

The crater 1 with small yellowish patches remains of Neostromboli volcano. In the two images the plumes produced by small Strombolian eruption are apparent (images by the author).

**Figure 11**

Andesite from Stromboli (private collection of the author)

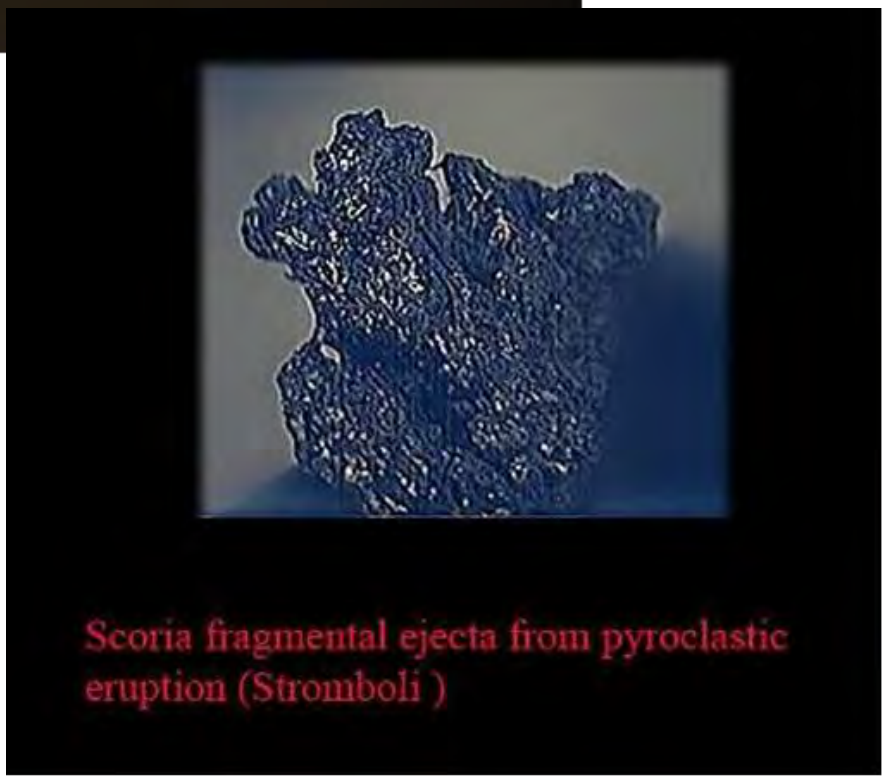


**Figure 12**

scoria from a Strombolian eruption (private collection of the author)

Figure 13:

different eruption material from Lipari. Obsidian (private collection of the author)


Figure 14 a.

The obsidian texture. The samples were collected in Lipari (private collection of the author)

Figure 14 b.

Pumice. The samples were collected in Lipari (private collection of the author)

Figure 15:

a strombolian eruption image from Crater 1. Image taken by the author from Punta Labronzo.

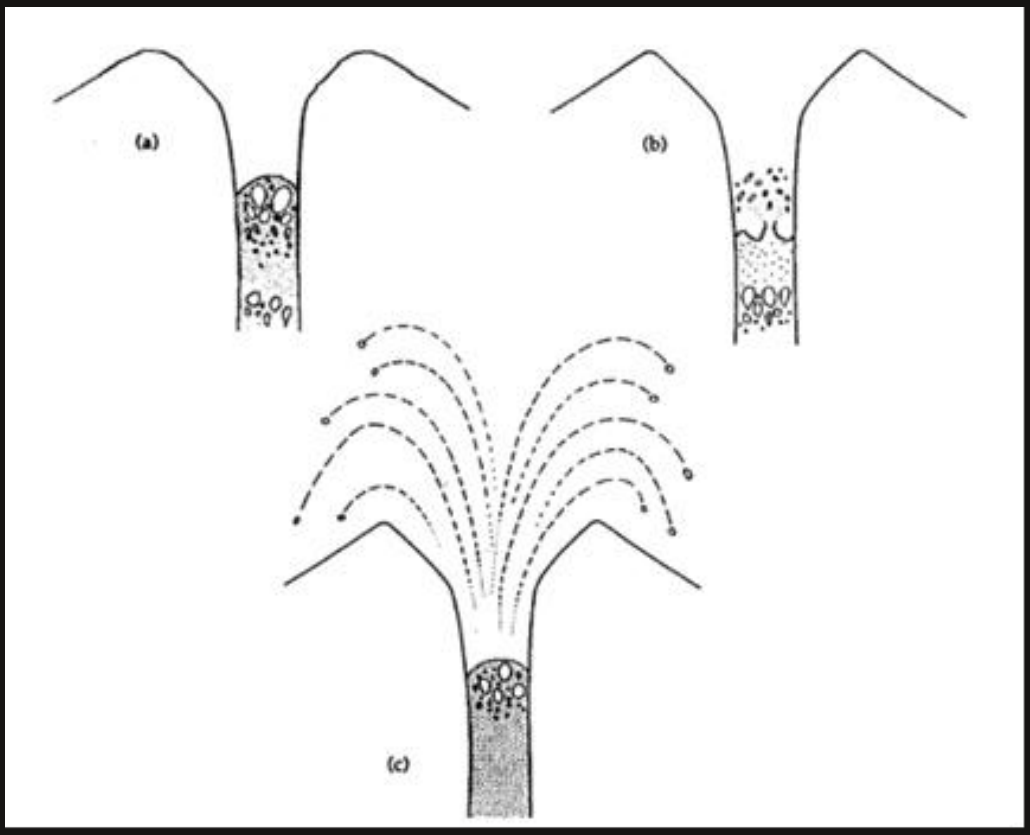


Figure 16

scheme of a Strombolian eruption

Selenology Today

References

[1] Aiuppa, A. & Federico, C., 2004. Anomalous magmatic degassing prior to the 5th April 2003 paroxysm on Stromboli. Geophysical Research Letters 31, L14607, doi: 10.1029/2004GL020458.

[2] Alean J. and Fulle M., 2008
http://www.swisseduc.ch/stromboli/volcano/photos/photo1005a-en.html

[3] Bertagnini, A., Metrich, N., Landi, P. & Rosi, M. (2003). Stromboli volcano (Aeolian Archipelago, Italy): an open window on the deep-feeding system of a steady state basaltic volcano. Journal of Geophysical Research 108(B7), 2336, doi: 10.1029/2002JB002146.

[4] Carapezza, M. L., Inguaggiato, S., Brusca, L. & Longo, M., 2004. Geochemical precursors of the activity of an open-conduit volcano: the Stromboli 2002–2003 eruptive events. Geophysical Research Letters 31, L07620, doi: 10.1029/2004GL019614.

[5] Francalanci, L., Manetti, P., Peccerillo, A., Keller, J., 1993. Magmatological evolution of the Stromboli volcano (Aeolian Arc, Italy): inferences from major and trace element and Sr isotopic composition of lavas and pyroclastic rocks. Acta Vulcanologica 3, 127-151.

[6] Gaddis, L. R., Staid, M. I., Tyburczy, J. A., Hawke B. R., Petro, N. E., 2003. Compositional analyses of lunar pyroclastic deposits, Icarus, vol. 161, no. 2, pp. 262-280, 2003.

[7] Gaddis L.R., C. Rosanova, B.R. Hawke, C. R. Coombs, M. Robinson, and J. Sable, 1998. Integrated multispectral and geophysical datasets: A global view of lunar pyroclastic deposits. New Views of the Moon, LPI, pp. 19-20 September, 1998. LPI, pp. 19-20 September, 1998.

[8] Head, J.W., III, Wilson, L., 1979. Alphonsus-type dark-halo craters: morphology, morphometry, and eruption conditions, in: Proc. Lunar Planet. Sci. Conf. 10th, pp. 2861–2897.

[9] Hornig-Kjarsgaard, I., Keller, J., Koberski, U., Stadlbauer, E., Francalanci, L. & Lenhart, R., 1993. Geology, stratigraphy and volcanological evolution of the island of Stromboli, Aeolian arc,
Italy. Acta Vulcanologica 3, 21–68.

[10] International Geoscience Programme http://www.geo.unimib.it/IGCP508/IGCP508_Areas_Stromboli.htm

[11] Pasquaré, G., Francalanci, L., Garduño, V.H., Tibaldi, A., 1993. Structure and geological evolution of the Stromboli volcano, Aeolian islands, Italy. Acta Vulcanologica, 3, 79-89.

[12] Tibaldi, A., Pasquaré, G., Francalanci, L., Garduño, V.H., 1994. Collapse type and recurrence at Stromboli volcano, associated volcanic activity, and sea level changes. Accademia dei Lincei, Atti dei Convegni Lincei, Roma, 112, 143-151.

[13] Weitz, C.A., Head, J.W., III, Pieters, C.M., 1998. Lunar regional dark mantle deposits: geologic, multispectral, and modeling studies. J. Geophys. Res. 103, 22725–22759.

[14] Wilson, M, Condliffe, E, Cortes, J. A, & Francalanci, L., 2006. The Occurrence of Forsterite and Highly oxidizing conditions in Basaltic Lavas from Stromboli Volcano, Italy. Journal of Petrology, 47, 1345- 1373

[15] Wood, C.A, 2008. A LUNAR PROCESS
http://the-moon.wikispaces.com/LPOD+June+16%2C+2008

Selenology Today

# Partial Solar Eclipse October 23, 2014

By Mike Wirths and Pamela Weston

A partial solar eclipse occurred this year. In the image you can make out the mountainous regions of the lunar south pole silhouetted against the solar disk. The huge sunspot AR 2192 is also detectable and it was imaged.

Partial solar eclipse Lunt 152mm solar scope (M. Wirths).

# Selenology Today

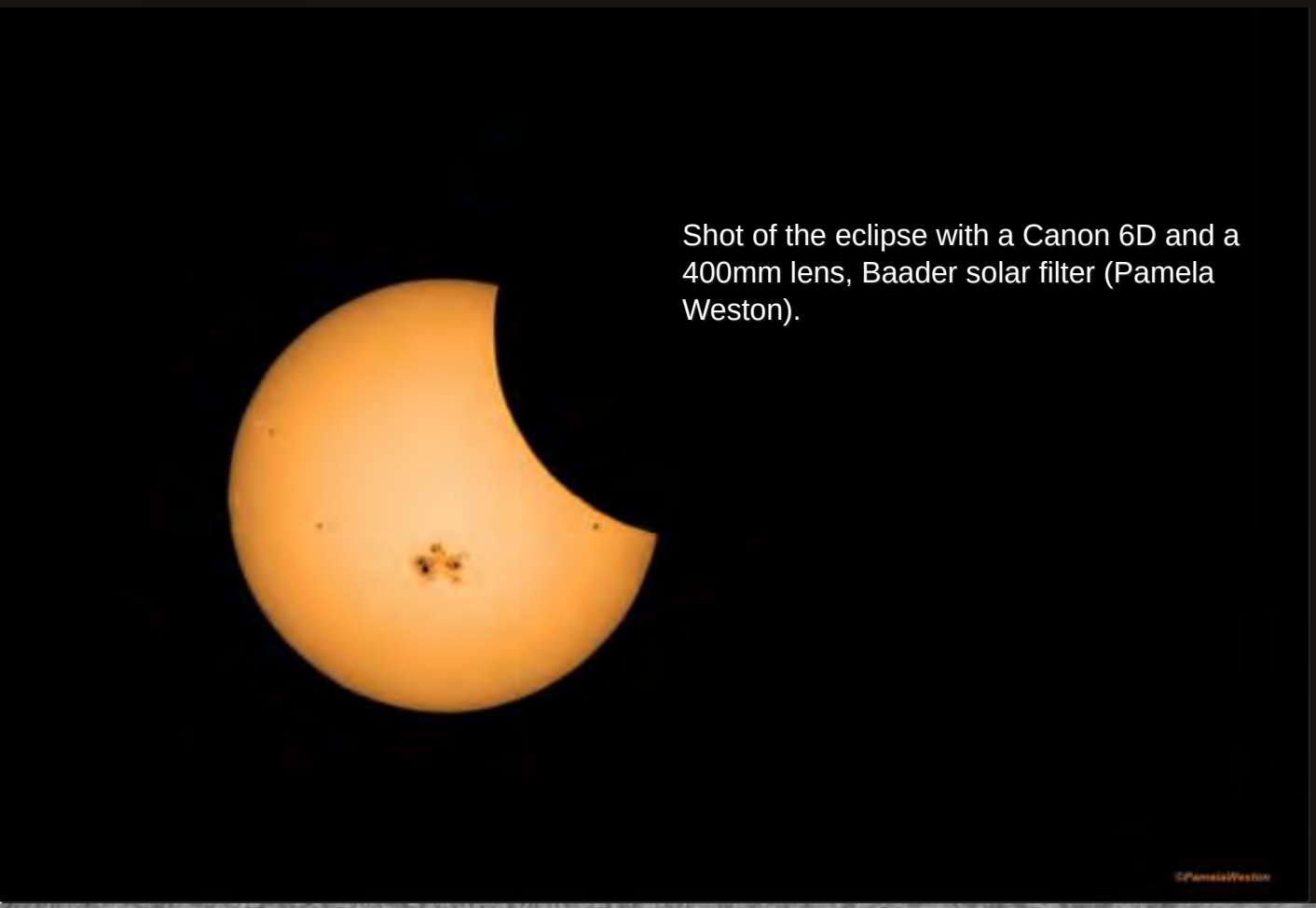

Shot of the eclipse with a Canon 6D and a 400mm lens, Baader solar filter (Pamela Weston).

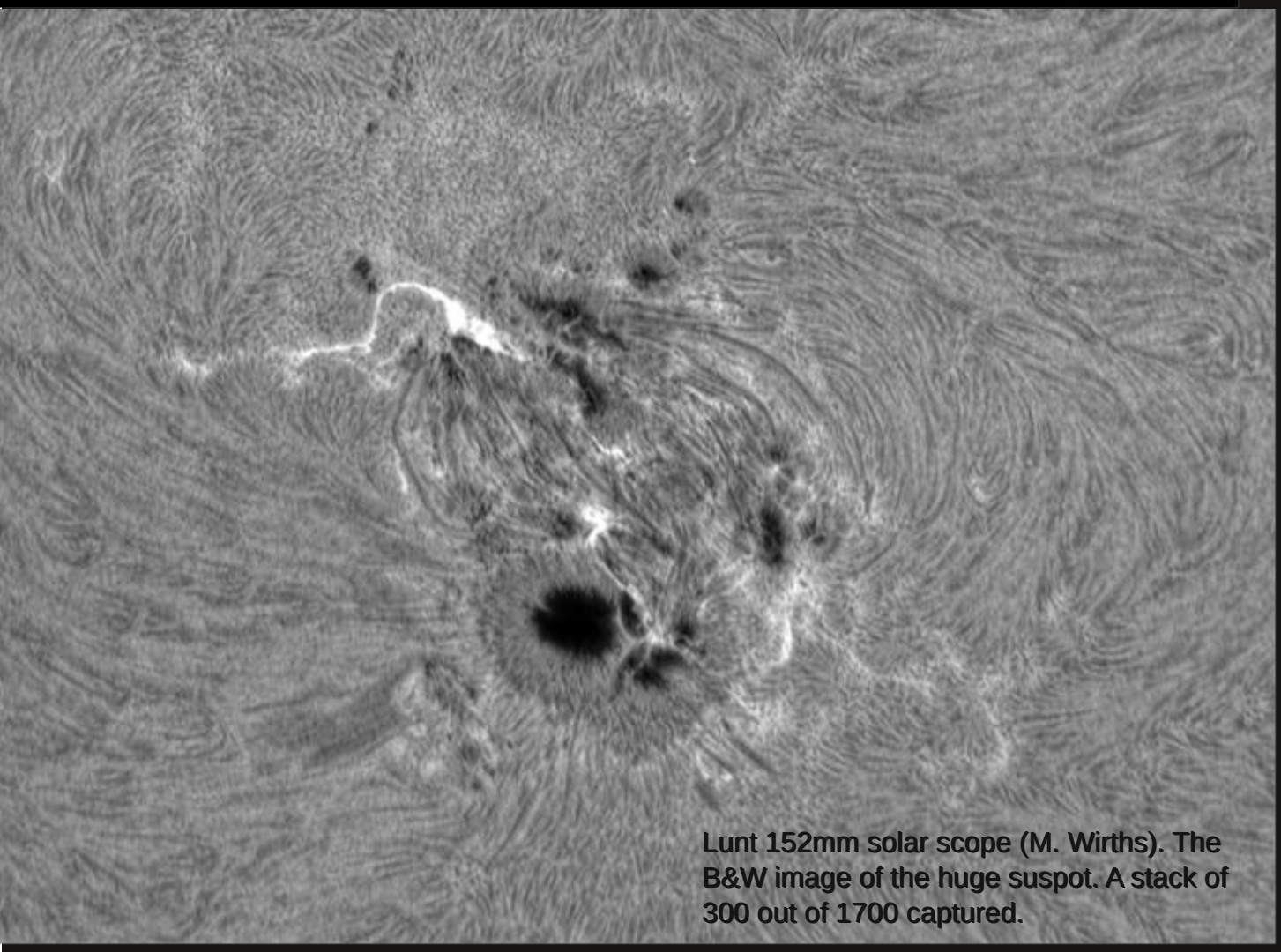

Lunt 152mm solar scope (M. Wirths). The B&W image of the huge suspot. A stack of 300 out of 1700 captured.

Selenology Today

# Lunar south pole with crater Neumayer at the point of maximum libration

By Rik Hill

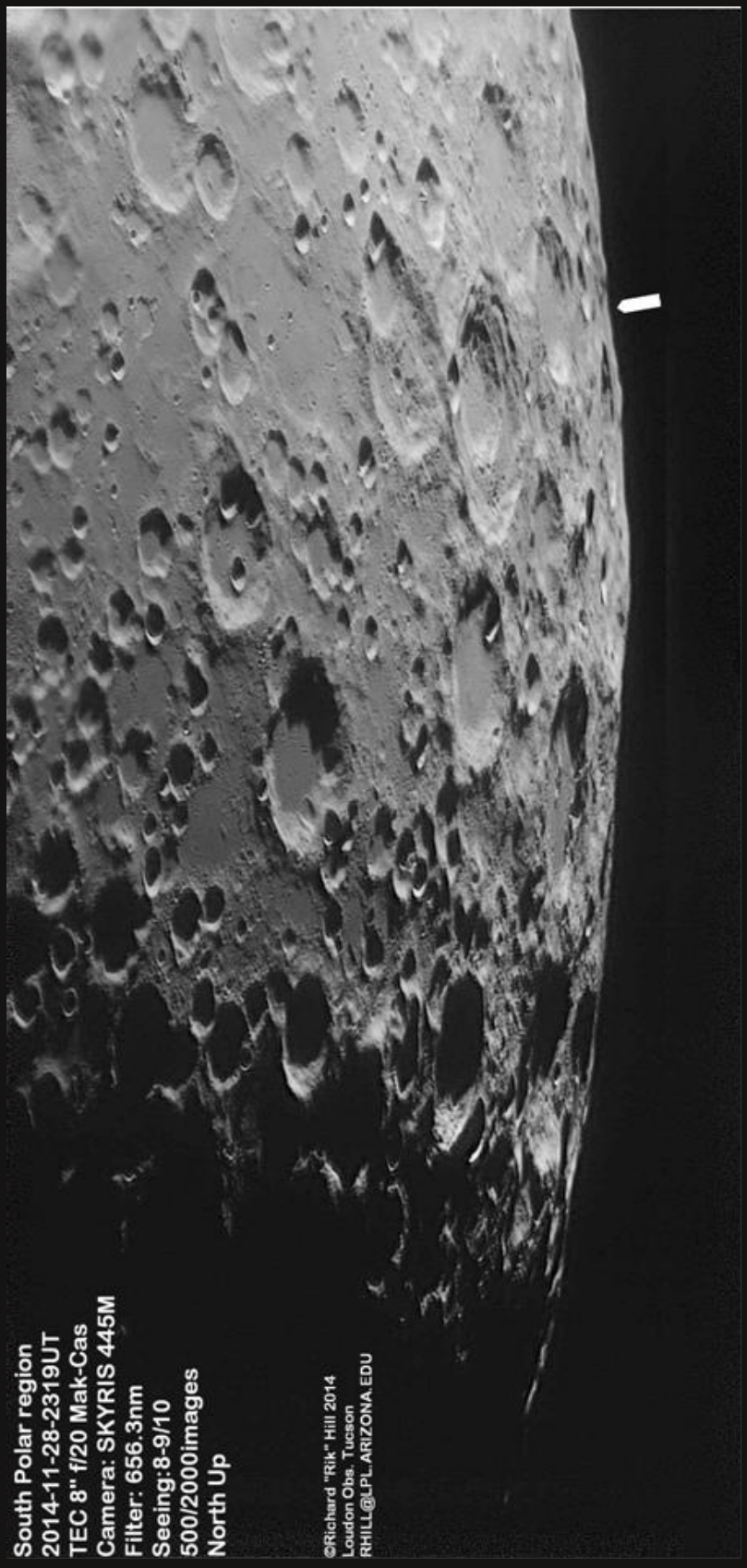


The small arrow marks the point of maximum libration giving the flat bottomed crater Neumayer, just above the arrow, good exposure. Above and to the right of that crater is the 99 km diameter crater Helmholtz and to the left of that is the crater in a crater Boussingault and Boussingault A. At 134 km diameter this is the largest crater in this image. Even further to the left is Boguslawsky. Going north from Boguslawsky is another flat bottomed crater, Manzinus and to its right is Mutus with the two smaller craters (17 & 24 km) in the bottom. Below Buguslawsky is the 117 km diameter, Demonax in one of the best presentations I have seen of it. Immediately to its left and half filled with shadow is Scott and right below Scott, almost all filled with shadow is Amundsen, as you might expect if you know your polar exploration history. A line through the center of Scott and Amundsen and extended one Amundsen diameter will take you to the exact pole, which is on the limb of this lighting and libration. Above Scott is Schomberger. This image is a montage of 2 images each made from 600 select frames from 3000 frame AVIs taken with the SKYRIS 445M camera. Stacking was done with AutoStakkert and final processing done with GIMP. The montage was put together with AutoStitch. Using LROC QuickMap I was able to identify craters to 1km diameter in the region of Mutus.

Selenology Today

# A small Meniscus Hollow field associated with extrusive volcanism in south eastern Mare Tranquillitatis

By Barry Fitz-Gerald Geologic Lunar Research (GLR) group


## Abstract

Lunar extrusive volcanism can take the form of localised (resulting in positive relief features) or regional (producing widespread low relief topography) pyrocastic activity, effusive dome formation or widespread basaltic flows together with a host of other associated structures such as sinuous rilles. A more enigmatic form that may owe their formation to volcanic activity are the structures known as Meniscus Hollows, the most well known example being 'Ina' in Lacus Felicitatis. A number of these structures have been previously reported from Mare Tranquillitatis, and this article describes the close association between what is interpreted to be a small effusive lobate flow of volcanic origin and a small field of Meniscus Hollow structures. A possible link between their spatial occurrence and mechanism of formation is discussed.


The imagery provided by the Lunar Reconnaissance Orbiter Camera has resulted in the discovery of numerous previously unknown features on the lunar surface. Many of these features are believed to be volcanic in origin, providing evidence of widespread activity over the course of lunar history. These features range from previously unrecognised pyroclastic deposits (Gustafson et.al 2012) effusive volcanic structures such as lunar domes (Lena, R and Lazzarotti 2014). Included in this list are the enigmatic 'Ina like' Meniscus Hollows which are interpreted as being the result of the release of residual volatile or radiogenic gasses, and probably form some of the youngest features on the lunar surface (Stooke, 2012).

The current article describes an unusual complex within the Lamont mare ridge structure of Mare Tranquillitatis, approximately 60kms to the south-east of the crater Arago (Fig.1). This complex consists of two different structures, one a suspected viscous flow like feature associated with a possible source vent, and another consisting of a field of Meniscus Hollow (MH) structures associated with what appears to be a submerged impact crater.

Both structures are associated with localised deposits of dark mantle material (DMD) as seen in the Clementine UVVIS Multispectral Mosaic images, adding support to the hypothesis that these structures are volcanic in nature.

The northernmost structure takes the form of a lozenge shaped, flow like feature, measuring approximately 8kms east-west and 5kms north-south (Fig.2). The upper surface of the feature is flat and table like, with a crater density similar to that of the surrounding mare. The margins of the feature exhibit a lobate form, with two prominent lobes to the north and smaller lobes around the remaining edges. Interestingly the two northern lobes partially overlap (Fig.3), with the western lobe superimposed on the eastern one, suggesting that the latter pre-dates the former (i.e the eastern lobe is younger).

The surrounding surface of mare lavas have a locally downwards slope towards the centre of the Lamont structure, with no indications of any protruding highland materials with which the structure could be related or form part of. The slope of the features margins is of the order of 25º, with the lower part forming what appears to be a debris or talus apron due to mass wastage. The eastern part of the structure is dominated by three craters, two of which appear to be impact craters in the region of 700m in diameter, the third appearing more sub-circular and subdued in nature and in the region of 900m in diameter (Fig.4). The possibility of this larger crater being a source vent will be discussed later.

Selenology Today

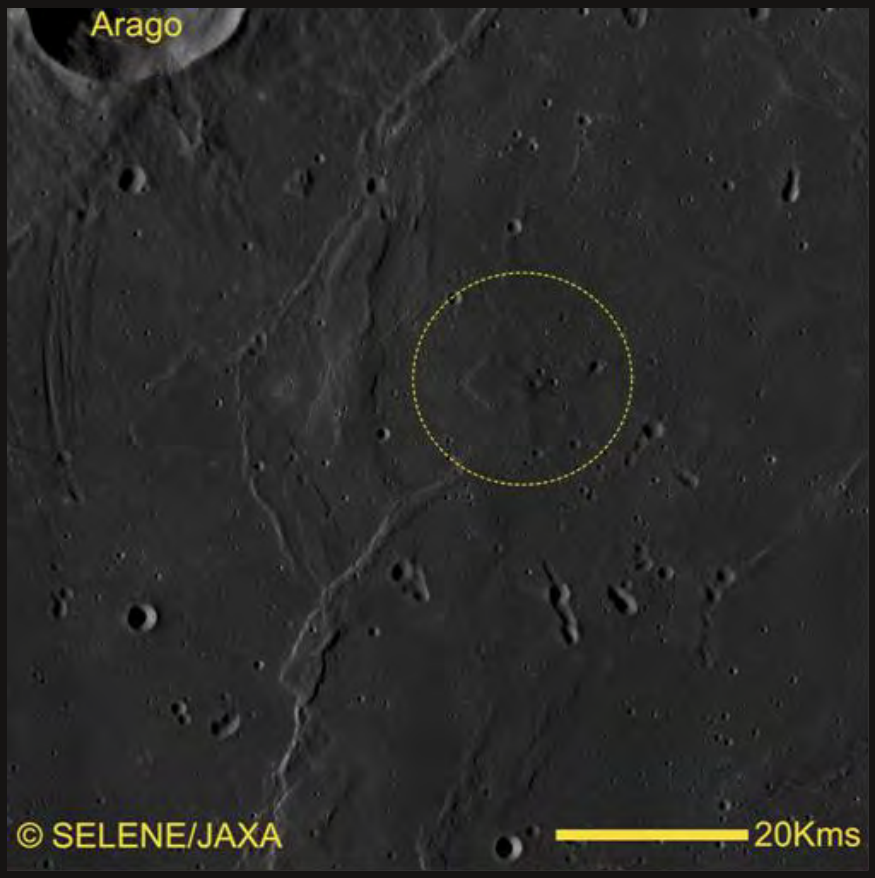


Fig.1

Location of the volcanic complex discussed in text. Note the mare ridges which form the western boundary of the Lamont structure.

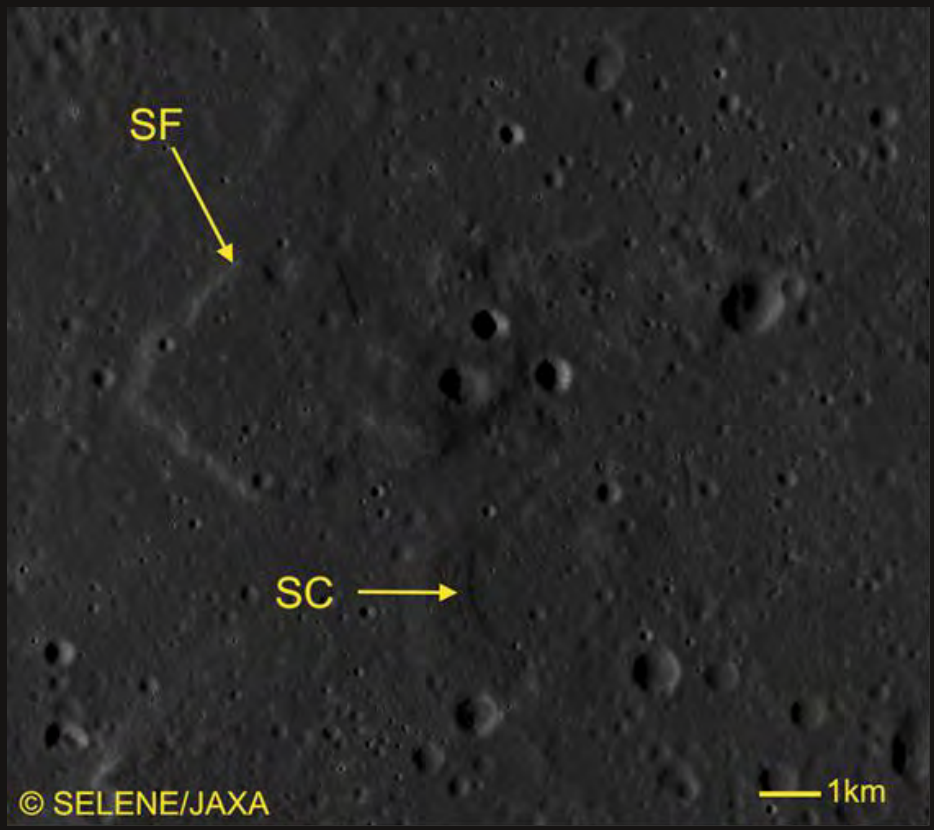


Fig.2

SELENE image of suspected flow like feature (SF) showing lobate margins, and submerged crater (SC) which appears to be the focus of localised Meniscus Hollow activity.

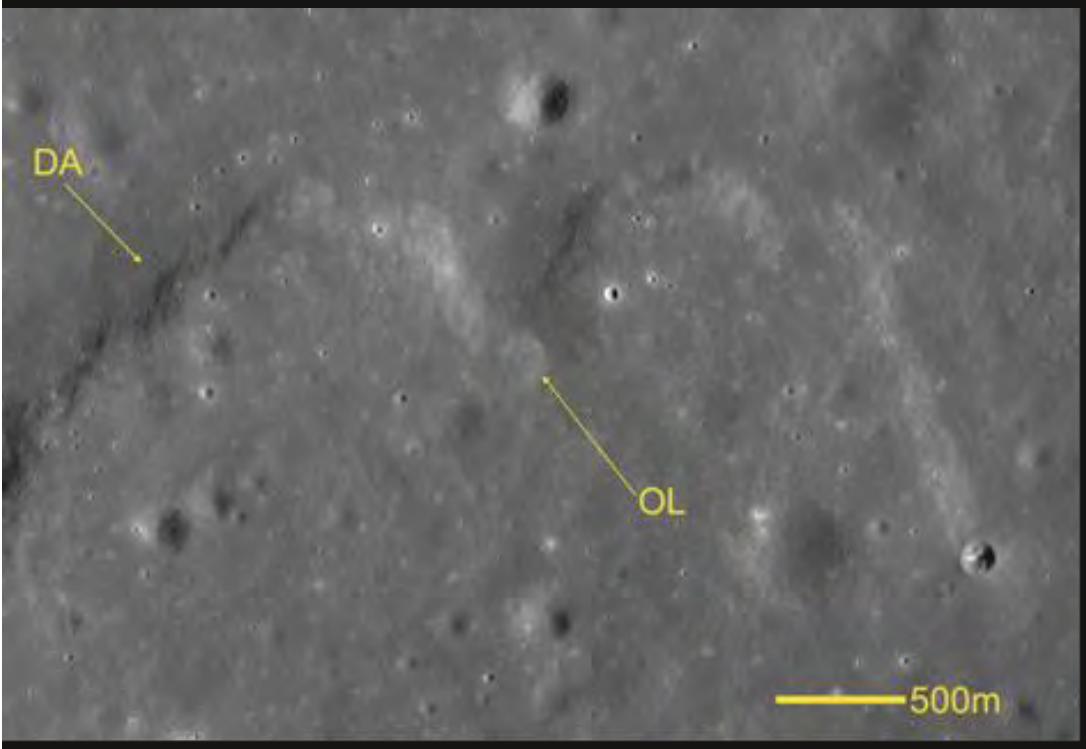


Fig.3

LRO Quickmap view of northern margin of flow the like feature. Note Debris Apron (DA) mantling lower slopes and the overlapping relationship between the western and eastern lobes (OL).

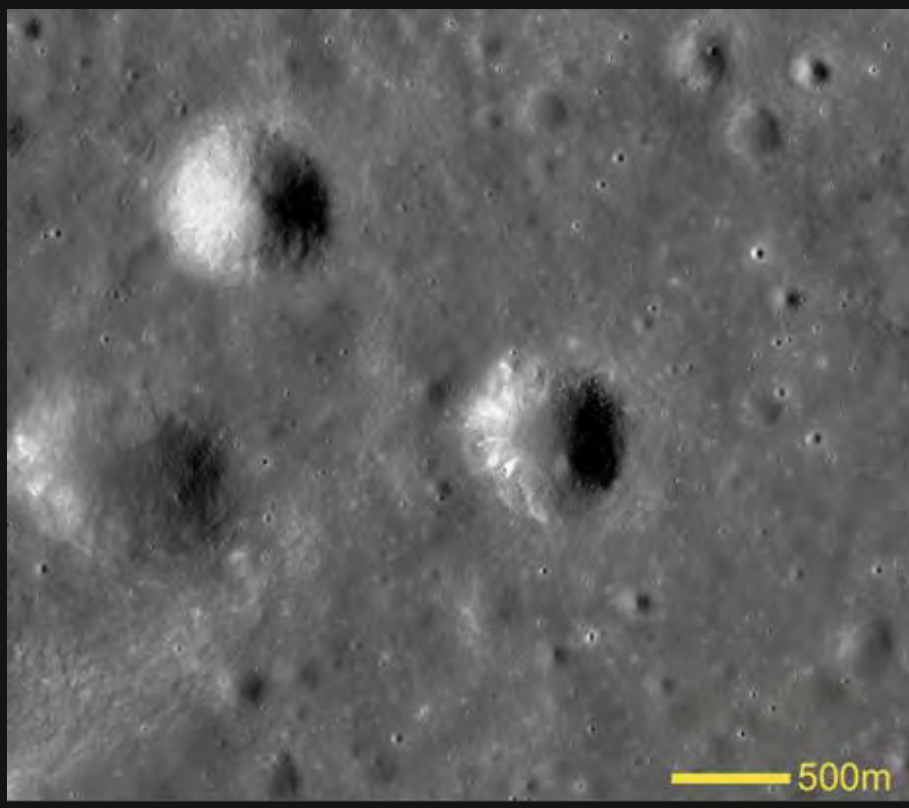


Fig.4

LRO Quickmap view of three craters at the eastern end of the flow feature under discussion. Note the more subdued nature of the crater lower left.

East of these three craters the structure takes on a more subdued and less well defined nature, but lobate edges are still visible especially along the southern margin. Approximately 2kms to the south of this trio of craters is the submerged circular structure noted above (Fig.5).

This is morphologically identical to the many widespread examples of submerged mare impact craters and suggests the flooding of a pre-existing impact crater by later low viscosity lava, followed by later subsidence of the lava levels, leaving the central part of the crater slightly depressed relative to the surrounding mare surface (Masursky et.al, 1978).

The structure appears slightly oval in shape, with an approximate diameter of some 3.5kms. The western rim is more elevated above the mare surface (by about 17m) than the eastern rim (1 to 2m) this may be a consequence of the general regional slope towards the east and the centre of the Lamont structure. The inner wall of the crater consists of a 200m wide slope with the subtle 'tree bark' texture indicative of mass wastage. Around the western section of the crater, and some 5m below the highest point, a narrow discontinuous moat or fissure is visible. This moat appears to be the focus of some of the numerous small MH structures that surround this crater (Fig.6). Similar structures have been observed in other mare flooded craters (Schultz, 1972) and may be interpreted as being a result of the subsidence of the mare infill. This would suggest a possible conduit via subsurface fractures to deeper levels within the structure.

These small MH structures range from small pits, to larger irregularly shaped depressions of the order of 100m in dimension. They appear to consist of areas where the superficial regolith is absent, revealing an underlying surface that is featureless at the resolution of the imagery. The floor of the larger hollows may have a sprinkling of loose boulders (Fig.7).

A larger MH structure can be seen to the north-north-west associated with the rim and inner walls and floor of a small crater. This appears to be a small impact crater some 350m in diameter, that has been heavily modified by MH activity. In this case, a high albedo

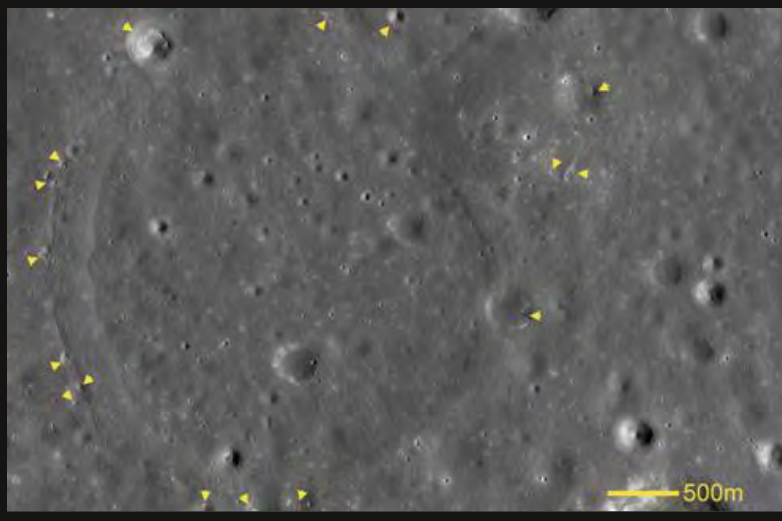


Fig.5

Image taken from LROC Observation M1108132323L of submerged circular structure identified in Fig.2. Note occurrence of Meniscus Hollow activity (yellow arrows) particularly associated with western margin of structure.

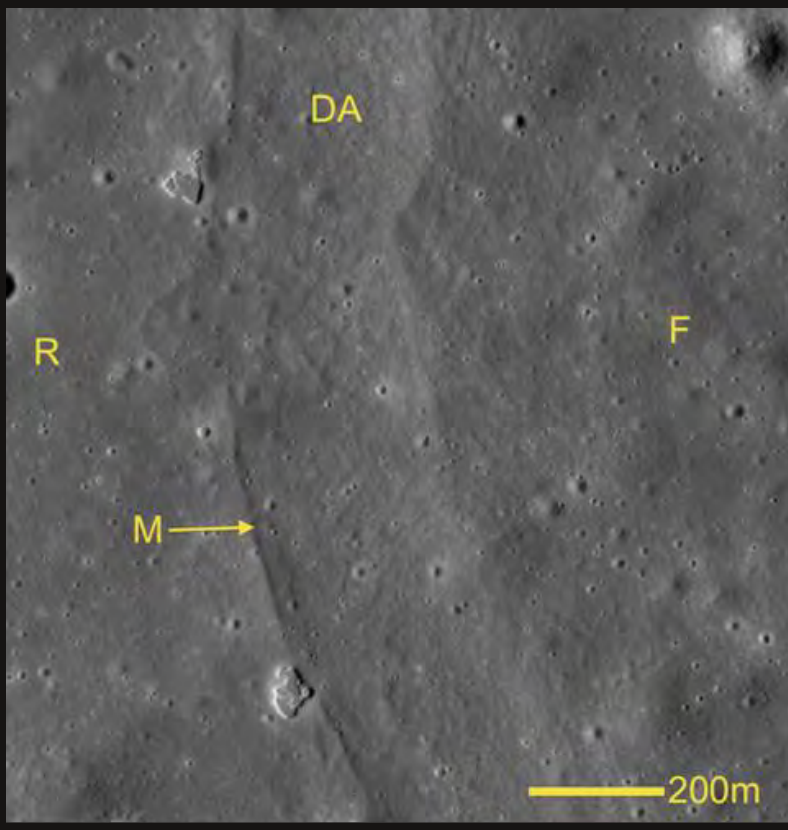


Fig.6

Image taken from LROC Observation M1108132323L of submerged crater showing western rim (R), moat (M), Debris Apron with tree bark texture (DA) and crater floor (F). Note Meniscus Hollows associated with moat.

featureless substrate appears to be exposed over the northern part of the crater with the higher slopes of the inner wall bearing the characteristic 'etched' appearance typical of small MH features.

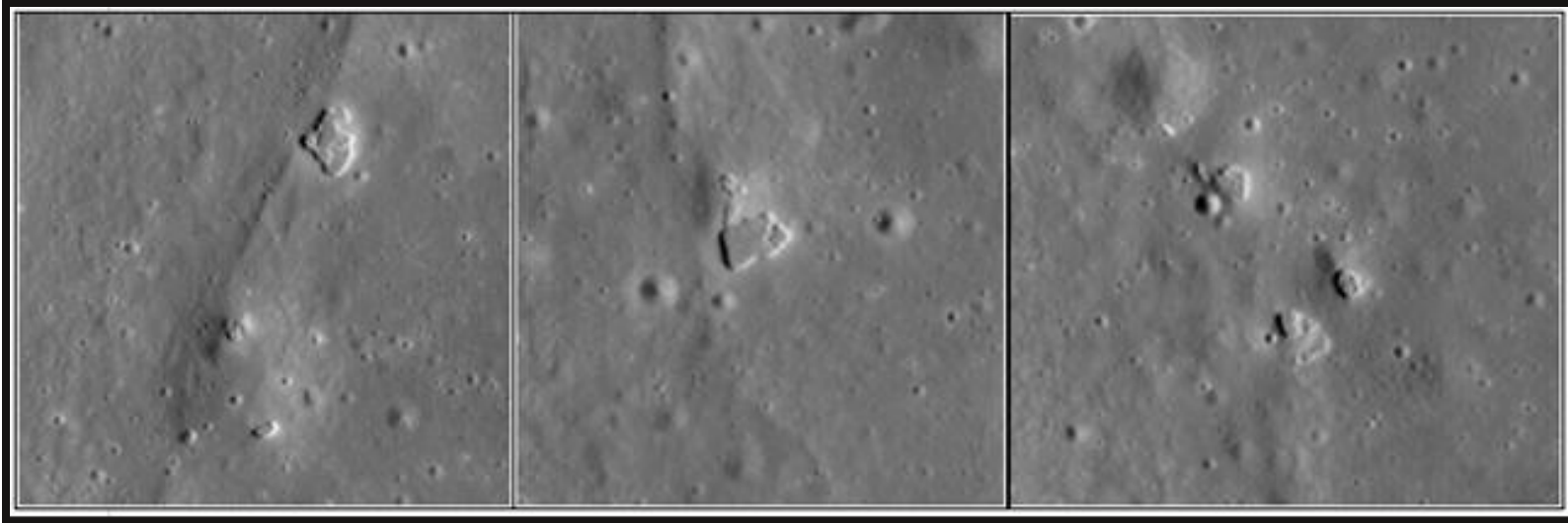

Fig.7

Details of Meniscus Hollow pits associated with the western section of the submerged crater (LROC Observation M1108132323L).

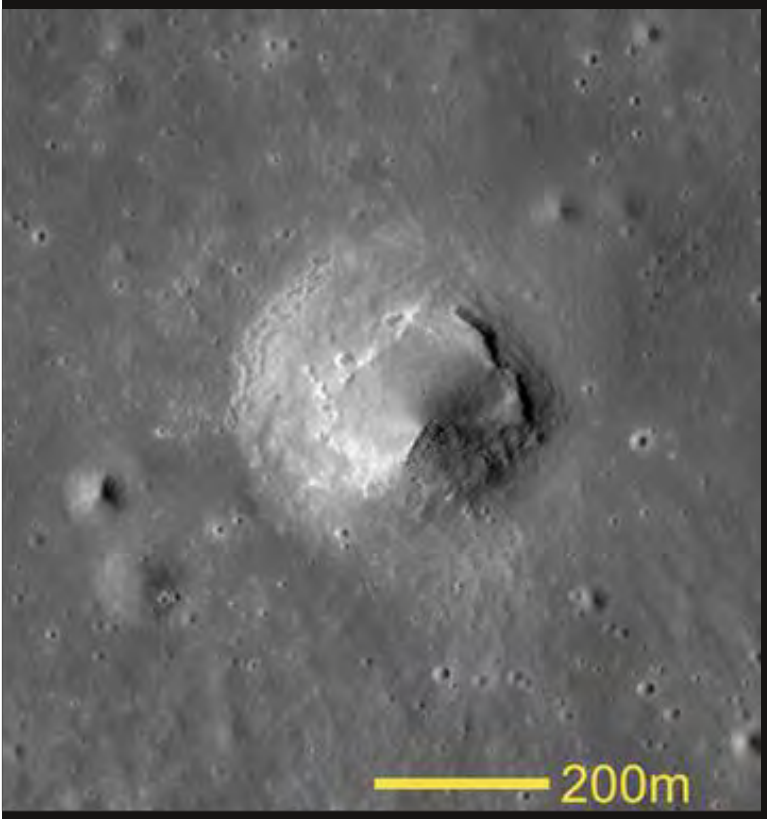


Fig.8

Detail of MH modified crater on NNW rim of submerged crater (LROC Observation M1108132323L).

A small talus cone of boulders can be seen on the crater floor, whilst the inner eastern wall exhibits what appears to be two cleft like structures running parallel to the crater rim and some 80-100m in length. These clefts may represent areas where material has been removed by some process – possibly related to the gas release implicated in MH formation generally. An interesting irregular MH structure can be seen located just to the east of the eastern rim of the submerged crater. This is approximately 200m in length, with irregular margins and a floor consisting of a smooth substrate, with in places, irregular low relief and possibly isolated boulders. This structure has a smooth featureless low albedo aureole surrounding it, extending out approximately 50-100m beyond the visible sharp rim of the depression (Fig.9).

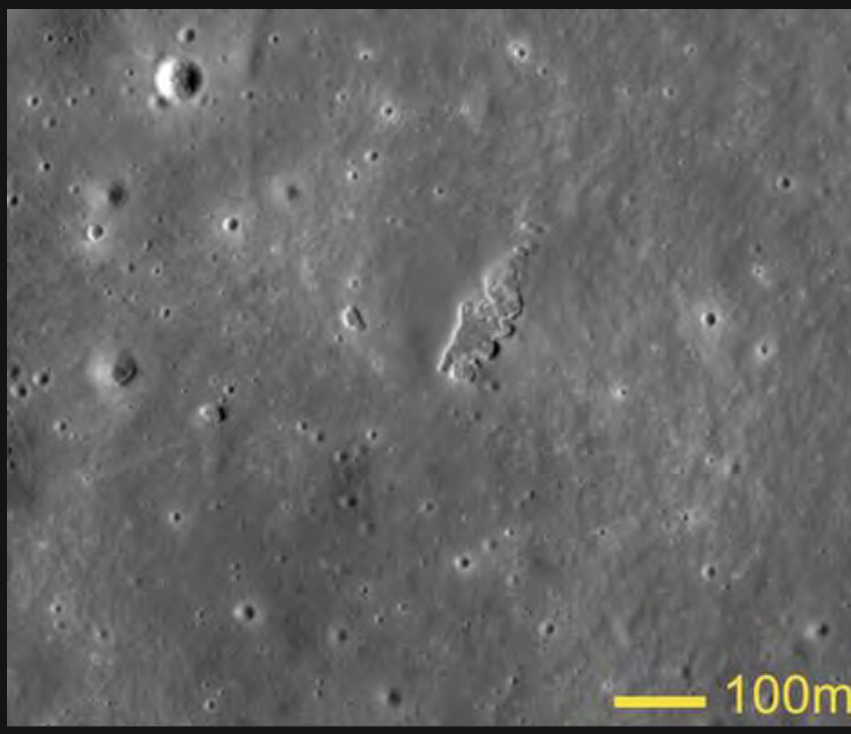


Fig.9

Detail of MH to the east of submerged crater. Note the smooth low albedo aureole.
(LROC Observation M1108132323L).

The remainder of the area surrounding the submerged crater contains additional small MH type structures, mostly on the scale of between 5 and 25m, some irregular and others with sharply defined edges. The floors (where visible) are similar to those already described with a smooth featureless surface with the suggestion of some superimposed boulders. The largest areas of MH appear to be associated with 2 impact craters both approximately 1km in diameter and lying within 1km of the submerged crater. The first of this pair lies to the south-east, and bears signs of extensive MH activity in the form of high albedo patches on the western inner wall, apparently associated with a concentric 'bench' visible around the inner circumference of the crater (Fig.10). The activity, as noted appears largely confined to the western half of the crater wall, where the 'upper surface' of the bench appears to be covered in a low albedo smooth material similar to the aureole noted in Fig.9.

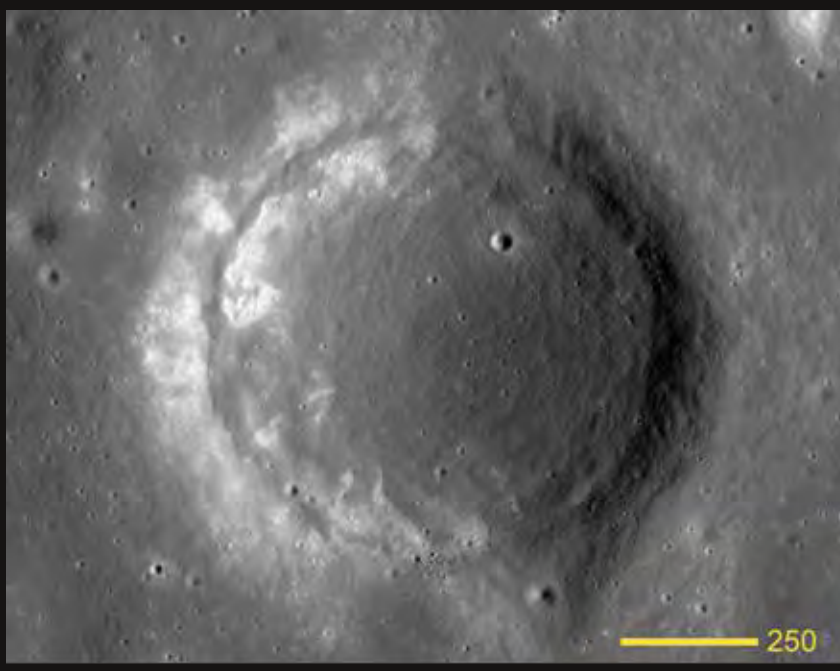


Fig.10

Small MH modified crater to the SE of submerged crater. Note the 'bench' located on the inner crater wall, and MH activity concentrated in the western half. (LROC Observation M1108132323L).

The second crater to the south-west is similarly modified by MH activity, but in this case most of the circumference of the inner crater inner wall

is affected, with large patches of high albedo material surrounded by smoother low albedo deposits. Some of the high albedo patches are clearly heavily boulder strewn. Vague indication of a 'bench' type structure on the slopes of the inner crater wall are visible, especially to the south, but the extensive modification and down slope movement may have obscured evidence of the feature elsewhere.

It might be hoped that the different units within this complex might exhibit unique multispectral signatures to assist in identifying their origin and composition. A glance at Fig.12 reveals that this is partially the case, with indications of low albedo, possibly mafic pyroclastic deposits in some areas, but little to distinguish the proposed high viscosity lobate flow from the surrounding mare.

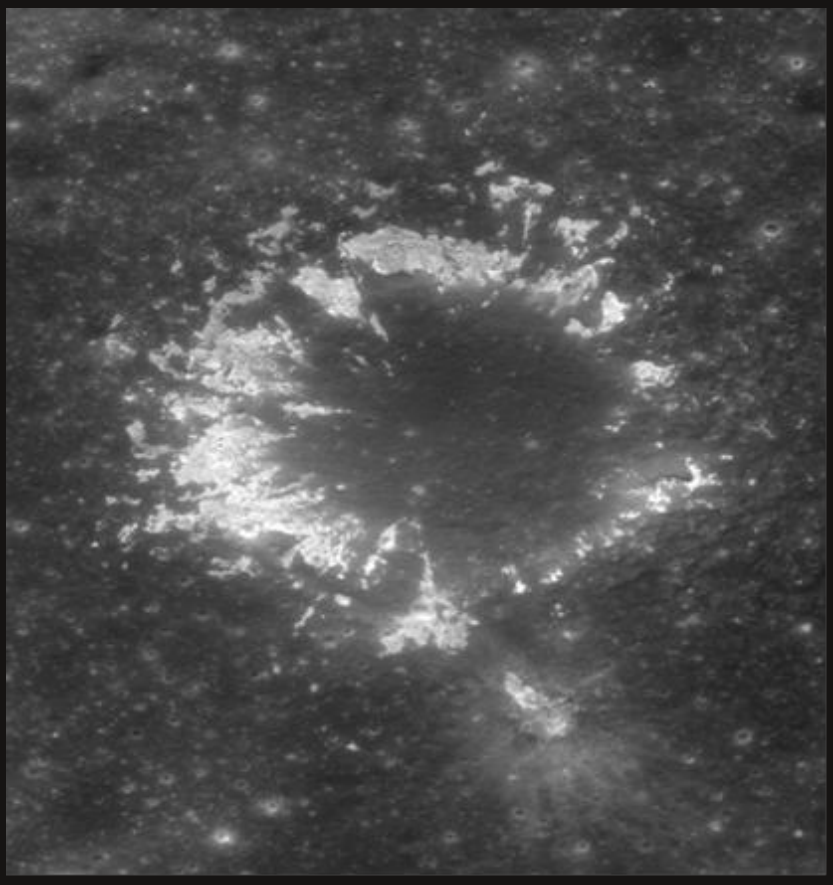

Fig.11

Small MH modified crater to the SW of submerged crater. Note MH activity around circumference of inner wall (LROC Observation M1131694020L oblique view looking west).

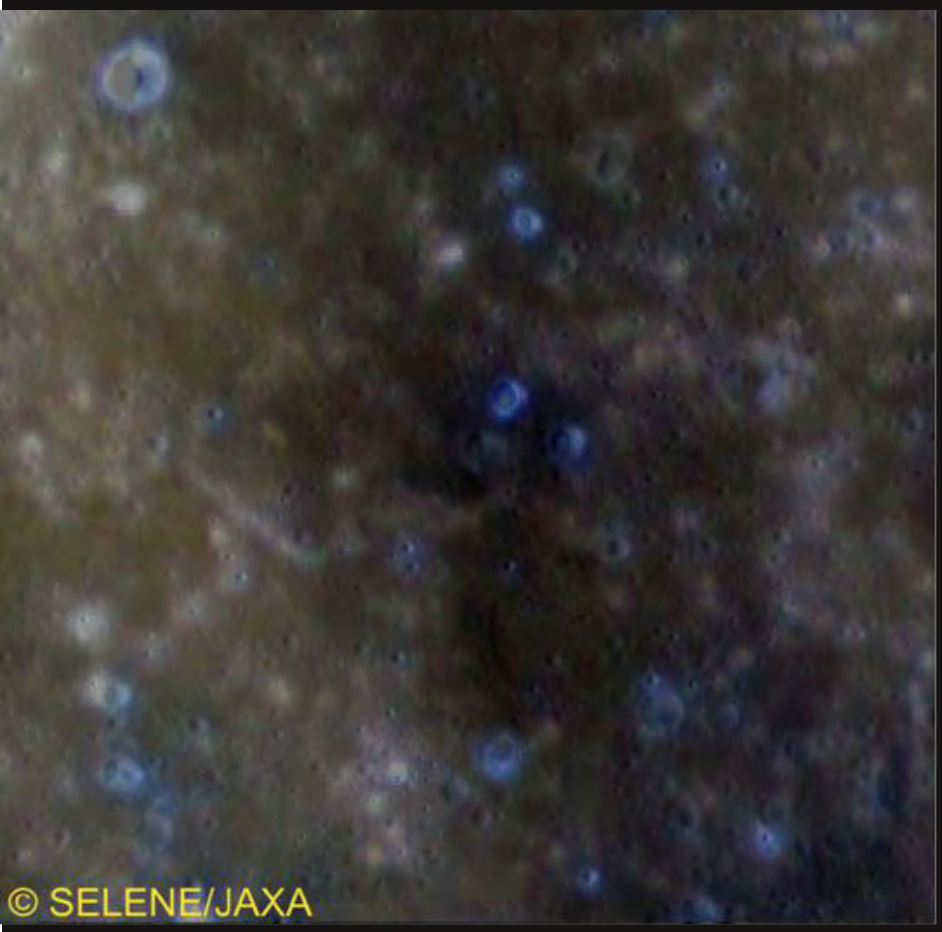


Fig.12

Composite consisting of SELENE image of area under discussion and superimposed Clementine UV-VIS Multispectral Mosaic (R=1000nm, G=900nm, B=415nm). Note dark possibly mafic material concentrated around craters identified in Fig.4, and western margin of submerged crater.

As can be seen, darker, possibly mafic pyroclastic material is evident in the area of the three craters noted in Fig.4, with a particularly dense concentration to the south of the more subdued of the three. This denser concentration corresponds to a spine of material that appears to be superimposed (together with a more tabular area of elevated material immediately to the north) on the suspected viscous flows, and may itself represent a late stage extrusion of even more viscous material (Fig.13).

A further dark, possibly pyroclastic signature is visible associated with the western rim of the submerged crater, but at the current resolution it is impossible to associate any of the MH structures with these darker areas.

## Discussion

The close proximity of the suspected viscous flow structure, possible source vent(s) and the MH activity surrounding the submerged crater are suggestive but not conclusive evidence of a common cause. The possible connection between volcanic areas and areas of MH activity such as to the west of Tobias Mayer has been commented on previously Stooke (2012), though it is fair to say that alternative mechanisms for the production of MH's (such as in the classical area Ina) have been proposed (Garry et.al, 2012 and Schultz et.al, 2006). The presence of the suspected viscous flow superimposed on the mare surface suggest that it's extrusion (if this is indeed the correct interpretation) occurred following the emplacement of the mare lavas and thus represents late stage volcanism. Similarly, the MH activity clearly post dates mare emplacement, the flooding of the submerged crater and subsequent lava withdrawal. Such late stage volcanism might be expected to produce a highly derived, acidic lava. Such effusive products might be expected to exhibit a different spectral signature to the surrounding mare but no such difference is visible, a potential counter argument to the present interpretation. Lawrence et al. (2013) however point out that there is no difference spectrally between the domes and cones of the Marius Hills and the surrounding mare, and suggest that a difference in mode of eruption rather than difference in composition is responsible for the observed variation in morphology. This situation may apply to the present case to some degree. The observed morphology consisting of lobate fronts, with evidence of lobes overlapping (suggestive of their formation being separated temporally) is again highly indicative of a series of viscous flow. The presence of the dark possible mafic pyroclastic material in the area of the subdued crater shown in Fig.4 adds further support to the volcanic interpretation offered here.

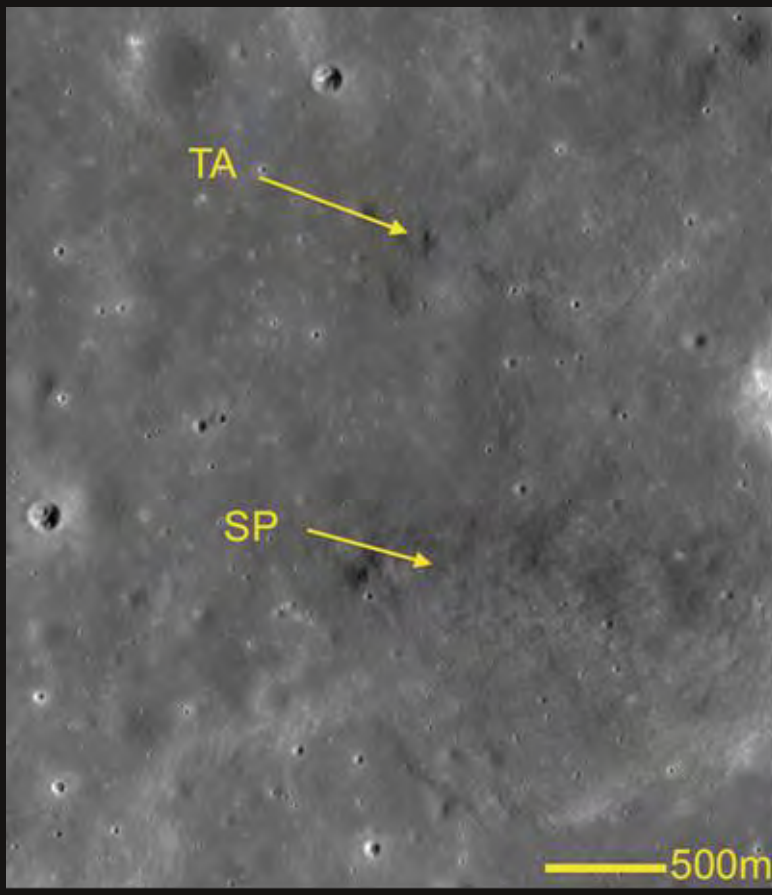


Fig.13

Spine of material (SP) corresponding in position to dark concentration of possibly mafic material as seen in the Clementine data. To the north a lower tabular structure (TA) of comparable morphology.

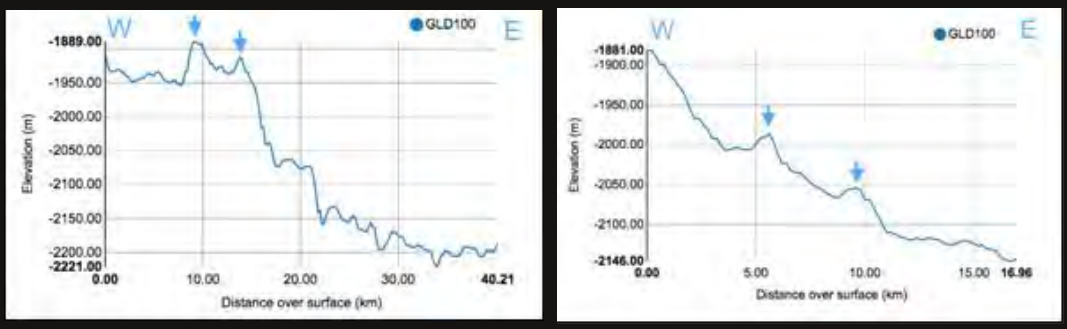


Fig.14

Quickmap GLD100 plot from west to east across the suspected viscous flow (left) and the suspected submerged crater (right). Note scales not identical.

Further information regarding the relative dating of the structures can be gleaned from the Quickmap GLD100 plots across both the suspected flow and the submerged crater. As can be seen from Fig.14, both are located on terrain with a regional dip towards the east, consistent with the down-warping of the central part of Lamont, a process that gave rise to the prominent circular wrinkle ridge system that defines the feature. In the case of the suspected viscous flow (Fig.14 left) formation must have pre-dated the down-warping as otherwise the flow would have occurred against the local topographic gradient (i.e. up-hill). Similarly the profile of the submerged crater (Fig.14 right) shows the floor sharing the same dip towards the east as the regional one, indicating that lava infilling pre-dated the down-warping, as otherwise a horizontal infilling would be observed. Both of these observations bracket the origin of these structures to after the final mare emplacement, but prior to the subsidence of the central part of the Lamont structure.

The MH's in the current example are a heterogeneous collection, with some having a well defined edges, others appearing quite irregular. Most have a well defined aureole of smoother, sometimes conspicuously darker material (such as the example seen in Fig.9), whilst some of the smaller examples lack any conspicuously darker margins. This MH activity would appear to be the most recent form of activity in this area, with the more conspicuous dark aureoles being devoid of any superimposed craters. This is consistent with the exceedingly recent dates proposed for similar structures such as Ina (Schultz et.al, 2006). Whilst heterogeneous in form, most of the MH's in the present example display a common trend in being located on either the inner crater wall of the submerged crater (and particularly with the 'moat' structure mentioned above) or the inner crater walls of a number of smaller, younger impact craters in the immediate surrounding area such as those in Fig's 8, 10 and 11. These smaller craters also poses an anomalous inner wall with the 'bench' type structure possibly being analogous to the 'moat' in the submerged crater.

These inner crater wall features may represent the surface expression of circumferential faults, fractures and fissures associated with the initial crater forming event. As such they may provide conduits for the escape for the residual volcanic or radiogenic gasses which are suggested as being responsible for the formation of MH's elsewhere by removal of the finer regolith component. Curiously no MH's are visible within the submerged crater, a possible consequence of the presence here of a thicker capping of mare lavas. The MH illustrated in Fig.9 is however the exception that demonstrates that not all of these features are associated with peripheral crater fracture systems, but can also be found on the nearby mare surface.

The presence of the dark, possibly pyroclastic material in the areas occupied by the MH's would

support the residual volcanic gas interpretation of formation as opposed to the release of radiogenically derived gas, though this is speculation and the coincidence of the two forms of gas release cannot be ruled out by this study.

Another example of a suspected viscous flow structure and MH activity can be seen approximately 19kms to the south of the crater Natasha and within the volcanic landscape surrounding Tobias Mayer. Here a small roughly rectangular elevated plateau, with talus rich lobate margins suggestive of viscous lava flow fronts, can be seen perched on top of a small massif which corresponds in position to a dark possibly pyroclastic deposit as seen in the Clementine data (Fig.15).

Whilst it is not intended to discuss this area in any great detail, it is worth commenting on the parallels between what can be seen here and the structures in the Lamont example. Both areas display the presence of a structure indicative of formation by a process involving viscous flow(s) of possible volcanic origin. Both areas share a mantling of dark possibly pyroclastic material, and both have associated MH type modification to what appear to be nearby impact craters. An examination of some of the other craters in the area shown in Fig.15 and 16 shows indications of MH activity in a zone within the inner crater walls as is seen in the Lamont area. This brief comparison serves to illustrate that this combination of features is not unique and may hint at similar geological activity in both areas. It would also suggest that a search for further areas of MH activity could be focussed on areas containing suspected late stage effusive volcanic activity and viscous flow structures.

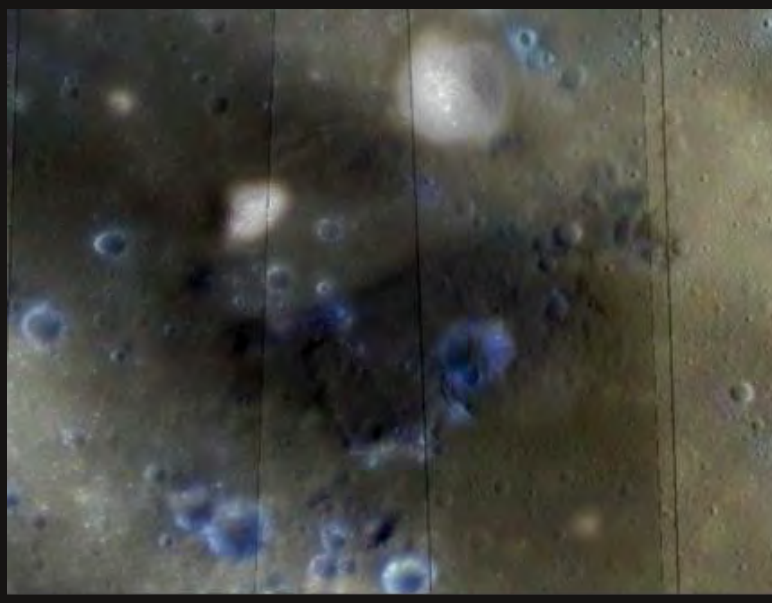

Fig.15

Composite image consisting of LRO Quickmap image of small massif and rectangular plateau south of Natasha superimposed Clementine UV-VIS Multispectral Mosaic (R=1000nm, G=900nm, B=415nm). Note dark possibly pyroclastic material corresponding in position to the massif.


Fig.16

LRO Quickmap image of the rectangular plateau discussed in text (left) – note lobate talus covered margins and inset box showing location of small MH modified crater shown in enlargement (right).

Selenology Today

## References

Garry, W. B.; Robinson, M. S.; Zimbelman, J. R.; Bleacher, J. E.; Hawke, B. R.; Crumpler, L. S.; Braden, S. E.; Sato, H., November 2012. The origin of Ina:Evidence for inflated lava flows on the Moon. Journal of Geophysical Research 117: E00H31.

Gustafson, J.O., Bell , J.F., Gaddis, L.R., Hawke, B.R., Giguere, T.A., 2012. Characterization of previously unidentified lunar pyroclastic deposits using lunar reconnaissance orbiter camera data. J. Geophys. Res. 117, E00H25

Lawrence, S., Stopar, J., Hawke, B., Greenhagen, B., Cahill, J., Bandfield, J., Jolliff, B., Denevi, B., Robinson, M., Glotch, T., 2013. LRO observations of morphology and surface roughness of volcanic cones and lobate lava flows in the Marius Hills. J Geophys Res-Planet. 118 (4):615-634.

Lena, R. and Lazzarotti, P, 2014. Domes in northern Mare Tranquillitatis: Morphometric analysis and mode of formation. Selenology Today, Issue 35.

Masursky, H., Colton, G. W., and El-Baz, F. eds. 1978. Apollo over the Moon: A view from Orbit. Washington, D.C.: NASA Scientific and Technical Information Office (Special Publication 362)

Stooke, P. J., 2012. Lunar Meniscus Hollows. 43rd Lunar and Planetary Science Conference, held March 19-23.

Schultz, P., 1972. Moon morphology. University of Texas Press, Austin, Texas-London, pp 340-341

Schultz, P. H. Staid, M. I. Pieters, C. M., November 2006. Lunar activity from recent gas release. Nature 444 (7116): 184–186

## Acknowledgements

LROC images and topographic charts reproduced by courtesy of the LROC Website at http://lroc.sese.asu.edu/index.html, School of Earth and Space Exploration, University of Arizona.

All multispectral images courtesy of the USGS PSD Imaging Node at http://www.mapaplanet.org/

Selene images courtesy of Japan Aerospace Exploration Agency (JAXA) at: http://l2db.selene.darts.isas.jaxa.jp

Selenology Today

# The Nectaris Multi-Ring Impact Basin: Formation, Modification, and Regional Geology

by Richard H. Handy

## Introduction

I must confess to being totally fascinated by the Nectaris Multi-Ring Impact Basin. Those dramatic set of nested concentric scarps, massifs and plateaus separated by lava and impact melt veneered moats surrounding a relatively small embayment of mare lavas. They are surprising relics from an impact event that occurred nearly 3.9 billion years ago. Surprising because most basins do not have obvious or strongly defined multi-ring scarps, despite the fact that they all originally possessed them. Presumably these are characteristics that have been either flooded by subsequent lava flows, eroded away by later impacts, or buried by ejecta blankets. The Orientale basin is a classic example of a multi ring impact basin with a relatively small area of maria due mainly to its youth, unfortunately for earthbound observers, its scarp rings and moats are seen in profile, close to the limb, depriving us of a plan view of the entire basin. The Nectaris basin, however is well placed for our observations, located near the middle of the south east quadrant in the northeast extension of the Southern Highlands. (See figure 1). This work examines the geological units, topography, petrography and formation of the Nectaris basin. A full list of books and articles published in the literature that were used to produce this work are compiled in the reference section.

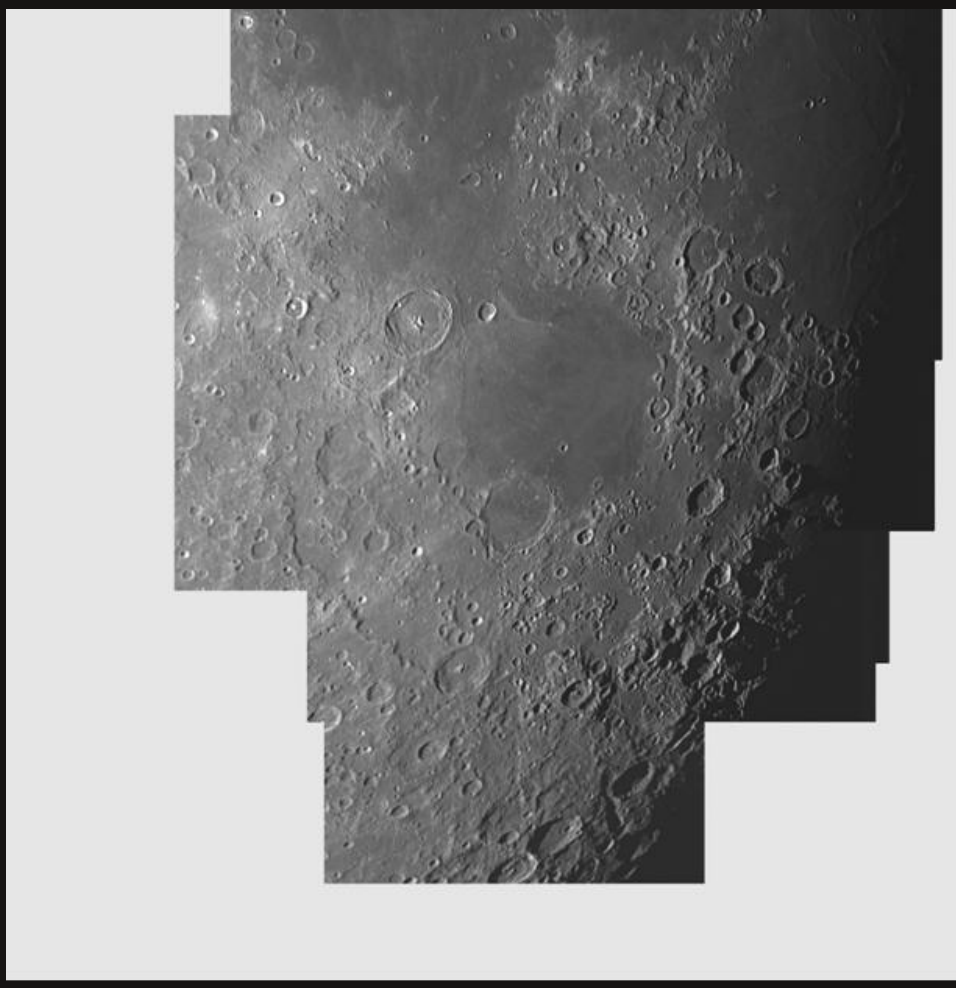

Figure 1

The Nectaris Multi-Ring Basin November 9, 2014. Mosaic images were acquired between approximately 9:45 and 10:20 UT using the author's Alter M815 Maksutov telescope and Lumenera Skynyx 2.0 1M video camera.

## The Geological Units of the Nectaris basin

Figure 2 is a color coded image representing the main Nectaris basin geological units based on a sketch from page 69 of "The Geology of Multi-Ring Impact Basins: The Moon and other Planets" by Paul D. Spudis, Cambridge Planetary Science Series, Cambridge University Press, 2005. In this colored image, deep blue is the Mare Material, yellow is the Crater Material, violet is the Smooth Plains, orange is the Descartes

Formation, Green is the Janssen Formation, red is the Hilly and Pitted Material, blue green is the Plateau Material, pink is the Terra Plains, black is the Massif Material and the gray of the uncolored surface represents the Undifferentiated Terra. Although a detailed examination of each of the main facies is beyond the scope of this article, their particular pattern suggests that a broad lens of material covers the zones to the west of the Altai Scarp with what appears to be anorthosite excavated from the Nectaris impact site. Apollo 16 confirmed these ideas when they retrieved samples from the Kant Plateau. The Censorius Highlands are also a rich source of high aluminum and mafic chemistries, indicating a deep excavation and redeposit as part of a broad ejecta blanket with similar origin to the Kant Plateau materials. The crater materials displays a pattern that suggests that the smaller 10 to 30 kilometer craters scattered around the basin are not random impacts. Their clustering in the zones outside the central mare indicates instead that these are predominately basin secondaries.
Presumably the secondaries that were closer to the basin center have been buried by later flows of mare lavas. Besides the fresh appearance of the scarp rings, the presence of platform massifs is also a hint that long term changes in the asthenosphere continued long after the basin initially formed. These massifs rafted to their isolated positions by riding the flows of a deeper intrusion of mare basalts. The system of rings around both the Fecunditatis and Tranquillitatis basins was probably responsible for the development of these isolated plateaus by allowing fractured crustal plates to extrude lava as they shifted about on the aesthenosphre. This style of lunar tectonics is regional in nature, not a global system of constantly moving lithic plates riding atop a continuous moving mantle such as the case for the Earth's Global Plate tectonics.

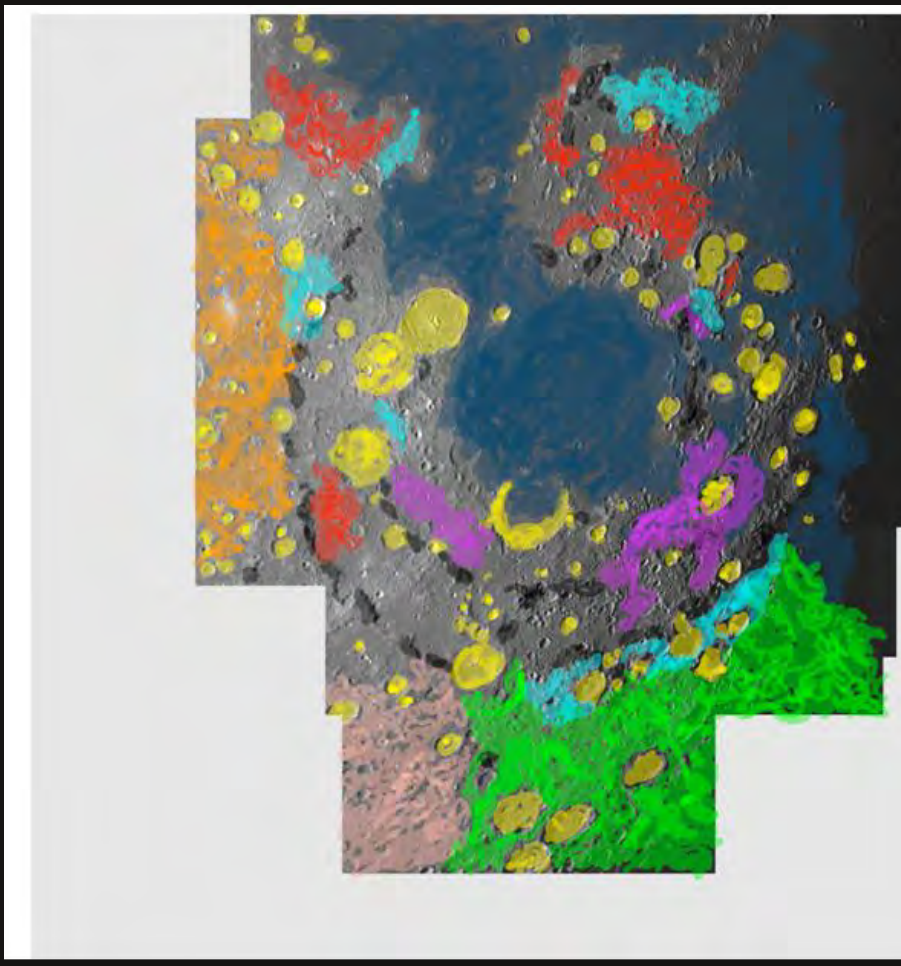

Figure 2

A color coded image based on a sketch by Paul D. Spudis in his classic volume "The Geology of Multi-Ring Impact Basins", Cambridge University Press, Copyright 2005 ref: pag. 69.

## Nectaris Basin Topography

Within the five basin rings currently accepted as artifacts of the Nectaris impact are a set of topographically distinct regions that are associated with both the impact event as well as those features related to the later phases of modification, including mare basalt infill of the nascent basin and the inner rings interior to the main topographic rim, rejuvenation of the scarp rings as well as very long term adjustments to the regional isostacy. Therefore, the terrain reflects all these elements, some being common to all major lunar basins and others being unique to the thermal and geological environment of the Nectaris impact. Elevation

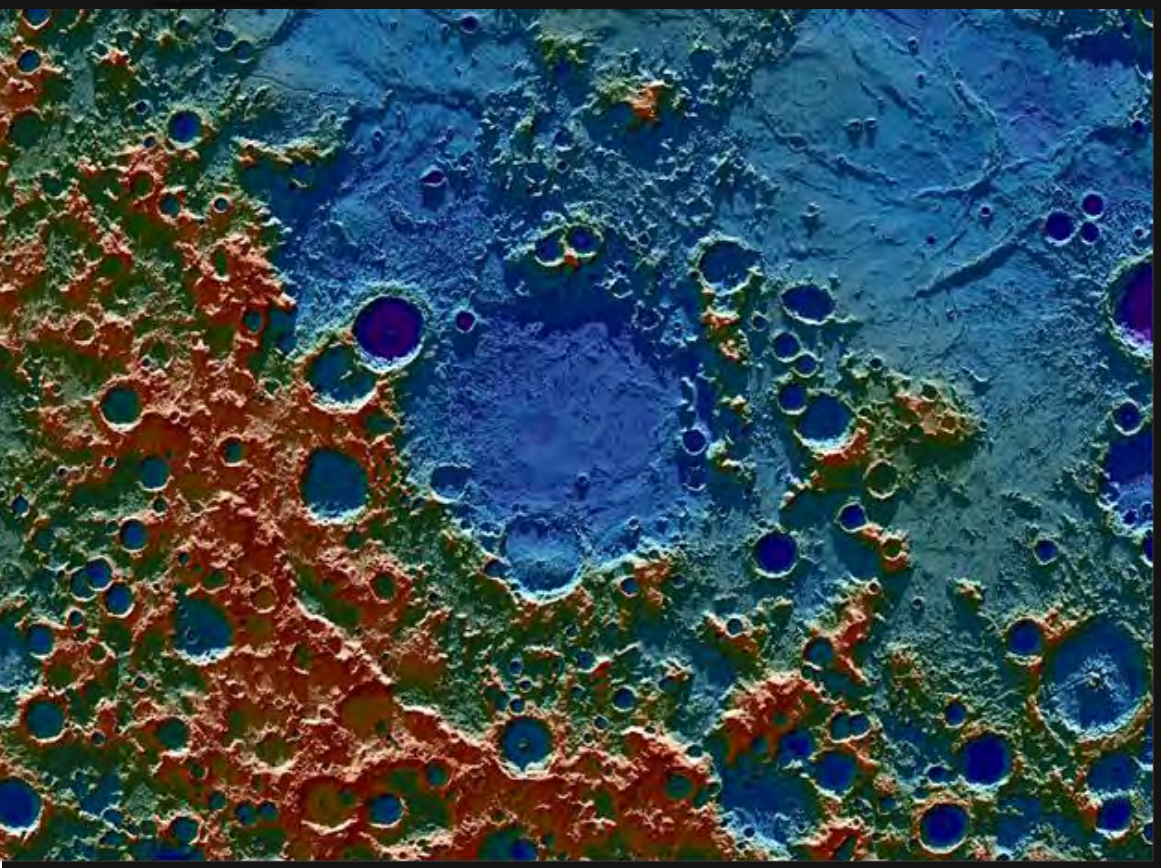

Figure 3

Lunar Reconnaissance Orbiter (LRO) image of the Nectaris Basin with colors representing the regional elevations derived from LOLA data sets. Red is the highest, orange and yellow are intermediate heights, greens are lower plains, blue are the mare areas and the basin center and some peripheral craters are violet, the deepest features. The light was recreated from an unnatural direction (from the north) using Jim Mosher's freeware software LTVT. Image courtesy of John Moore.

data from Lunar Reconnaissance Orbiter (LRO) LOLA (Lunar Orbiter Laser Altimeter) data show that the highest elevations (3.5 to 4.5 km above the mean lunar diameter) are immediately exterior to the Altai ring in a broad lens or fan that is especially prominent in the highlands to the west and south of the basin. To the northeast, an isolated plateau and hilly region, the Censorius Highlands, remains as an eroded and heavily cratered continuation of this giant basin ejecta blanket. The green colored terrain in this image is about one kilometer lower at 2.5 km, while the turquoise color is representative of the elevations that correspond to about 750 meters, those associated with the maria. Violet represents the deepest elevations, approximately 3 kilometers lower than the lunar mean diameter. It is clear to see that the north and eastern components of this blanket were either areas of paucity of the density of material in the ejecta curtain or were initially formed in situ and were later subsumed by lavas from Mare Fecunditatis and Mare Tranquillitatis. Both of these factors could have played out during the long evolution of the basin.

The annular inter scarp zones, what are referred to informally in this article as the "moats", descend in discreet steps of elevation (see Figure 4) from the main topographic rim at 4000 meters above the mean lunar diameter, followed by the first inner annulus shelf which is 1000 meters lower in elevation, the second inner shelf is another 1000 meters lower yet and the third annulus is 750 meters lower as one ventures inward from the main topographical rim. In this sense, inner basins rings and moats are the giant equivalent to the terraces of complex craters, which bear relation to the genetics of these features, i.e, mass wasting of the transient crater rim by the force of gravitation. Obviously, the extreme energy regime of basin producing impacts impose important morphological differences in the structures of these major classes of impact events seen on the surface of the Moon. Figure 3 is an image combination of LRO LOLA elevation data of the basin with simulated northern lighting applied using Lunar Terminator Visualization Tool (LTVT), freeware software developed by selenologist Jim Mosher. The image was created by Irish selenologist and author John Moore who kindly provided its use for this article.

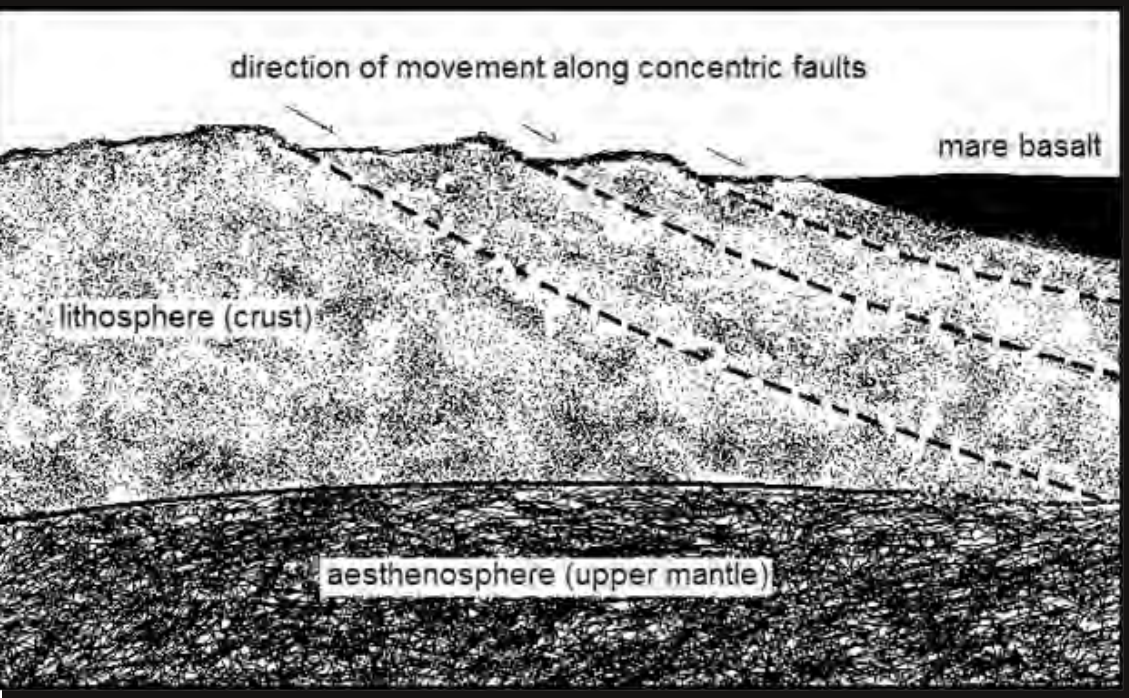


Figure 4

Schematic representation of a cross section through a basin from the main topographic rim to its center. The arrows indicate the direction of movement of large annular zones, the inter scarp zones informally referred to as the “moats” in this article. Sketch drawn by the author.

## The Petrology of the Nectaris Basin

Most of the data acquired to characterize the mineral constituents of the Nectaris basin were derived from orbital or ground based remote sensing. The Apollo missions, Lunar Prospector and then the Lunar Reconnaissance Orbiter have extended the opportunity to analyze Nectaris basin deposits. The Apollo16 mission sampled material directly from the Kant Plateau, offering a unique opportunity to compare mineral analysis based on remote sensing comparisons to laboratory results. The product of this synthesis allows a thorough mineral classification for the Nectaris facies.

Northeast of the basin center, the Censorius Highlands, in the area of the crater Capella, is a province characterized by its Very High Alumina (VHA) anorthositic deposits. Thorium deposits here are some of the highest in any isolated highlands area. Its prominent mafic component is thought to be related to the depth of crustal penetration by the Nectaris impactor. In contrast to Orientale, which lacks this signature, the thermal conditions in its target area must have cooled enough for the lithosphere to thicken. And due to the downward migration of the asthenosphere (also named as aesthenosphere) during the period of the Orientale impact, mafic components from the deepest excavation of the transient cavity should not be present in its distal deposits, as the mineral data indicates.

To the northwest, a similar province, the Kant Plateau, in the region around the crater Descartes, is also anorthositic in composition and similar to the Censorius Highlands, except that it has a higher proportion of alumina to silicon, in fact the highest ratio for any such deposit on the Moon. However, in stark contrast to the Censorius Highlands, the levels of thorium measured by remote sensing as well as by laboratory analysis of Apollo 16 samples indicate that this province has the lowest thorium levels, exceeding any region on the near side, and is comparable with the lowest percentages in the far side highlands with respect to this component. In both regions these results indicate that these materials were originally part of the upper anorthositic crust in the target zone, and along with a mixture with upper mantle components, which were deposited in their present location by the force of the Nectaris impact.

Interestingly, as one moves beyond the Kant Plateau further west past the Descartes Formation which is predominately composed of pure anorthosite, the levels of thorium and mafic components increase. Here the rock types are significantly different than the Nectaris components and the surface chemistries are thought to reflect subsequent pre-Imbrium volcanism and distal deposits and mixing of materials from the Imbrium impact as well as the

heterogeneous make up of the southern near side highlands. In general, the Nectaris facies are composed predominately of anorthositic and Low Potassium Fra Mauro (LKFM) components in a ratio of 3:1 respectively. A less significant component but one that must accounted for in the regional analysis, is the mare basalt contribution that increases as one approaches the basin center. Moreover, this mafic constitution, along with the KREEP (Potassium, Rare Earth Elements, and Phosphorus) component present in the highland areas suggest that mare basalts were present at the target location, presumably in pre-existing basalt deposits from Mare Tranquillitatis and Mare Fecunditatis. Because no ultramafic materials were identified in the spectral data for the distal units of the Nectaris facies, it is believed that this result points to an impact that did not excavate deep enough to penetrate the upper mantle, but rather was confined to the middle and lower lithosphere.

## The Formation of the Nectaris basin

Figure 5 is an image of the basin annotated to show the approximate location of the main topographic rim and two inner scarp rings. There are also two recognized rings outside the boundary of the Altai Scarp which are not shown in this image. Note the nested concentric pattern of the scarps. How did this distinctive structure form? Upon first impact of this 35 kilometer asteroid, all craters that had formed in the impact location were swept clean of the surface. The impactor was nearly totally vaporized in a blinding explosion as a huge spherical melt zone formed in the center of what would become a 500 kilometer by 35 kilometer deep transient crater. When the transient crater reached its greatest diameter, the melt zone rebounded into a giant column of melt that was ejected over a hundred kilometers upward, much in the same manner that a drop of water deforms the water surface into a peak as a reaction to the impact of the drop. At the moment of contact, when the asteroid delivered its full kinetic energy, the lunar crust literally rose and fell several kilometers as giant seismic ripples lifted and then dropped the lithosphere, fracturing, and down faulting huge annular zones, consequently exposing the scarps. An ejecta curtain, a giant cone of vaporized impactor and shock melted target material expanded outward from the transient crater rim. As the massive ejecta curtain swept through, it mixed with pulverized regolith, creating fluidized flow fronts, incredibly energetic tsunamis of flowing debris splaying out radially and nearly horizontal to the surface. They gouged long linear valleys and strange braided landforms and tear drop formations as they tore through crater walls, burying what they did not destroy. When the ejecta curtain impacted, the debris blanketed and inundated and covered both large and small craters in areas of the lunar surface exterior to the main topographic rim. A rain of secondary impacts followed, some taking long arcing trajectories before impacting several minutes later, hundreds of kilometers away into the distant surrounding terrain, gouging deep linear catenae radial to the impact center. Vallis Snellius and Vallis Rheita are prominent examples of Nectaris impact sculptures.

An intriguing aspect to the scarp ring spacing is that each succeeding ring diameter outward from the basin center measures about 1.4 times the diameter of the previous ring, the well known square root of 2 rule for basin rings. And while there are no simple answers for the existence of such a relation, it can be understood as primarily the result of the diminishing energy, expressed as a gradual reduction in the amplitude of the seismic shock waves as they propagate outward, dissipating their energy over a wider area of the crust.

Surprisingly, although the basin was formed in roughly two hours, the lavas that cover Mare Nectaris took hundreds of millions of years to emplace. Perhaps not as obvious, because they are not surficial, are the changes that occurred deep below the crust. Here concentric lenticular fracture zones in the mega regolith provided a path for hot magmas from the lithic/mantle interface below, feeding the expansion of mare basalt flows, which were extruded layer by layer for several hundred million years thereafter.

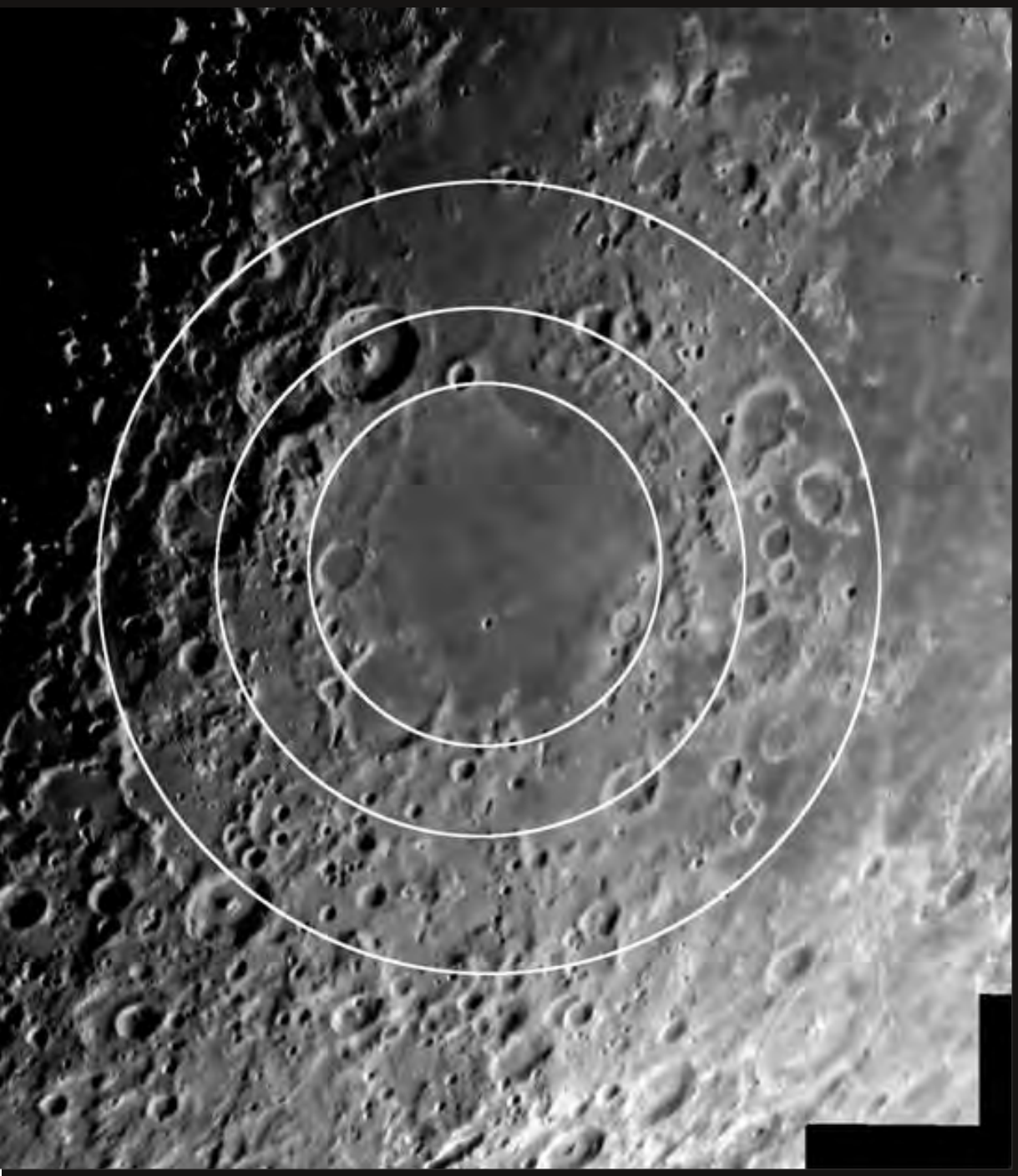

Figure 5

Approximate location of the Nectaris concentric scarp rings including the Altai ring and the rings interior to it. There are rings interior to the central ring shown here, but they have been almost entirely flooded and subsumed by mare lavas. Image by the author.

In concert with these processes in the lithosphere, were the changes happening in the lunar asthenosphere. The warmer and denser plastic upper mantle, initially pushed aside by the force of the Nectaris impact, would eventually flow inwards and upwards towards basin center where the annular crustal zones could be expected to be tugged in tectonic fashion. Extensional graben faults that would develop as the mass of building mare lavas later depressed and further fractured the crust provided sufficient venting of magmas to allow changes in aspects of basin morphology over long periods of lunar geologic history. These modifications, particularly in the areas adjacent to the scarps, probably occurred in episodic fashion long after the scarps initially formed, rejuvenating the appearance of the rings as regional isostasis was still being established in the evolving thermal environment of the early lunar asthenosphere.

The inter-scarp regions, stepped annular zones sometimes referred to as the moats, are destroyed, buried and broken, medium (about 50 km diameter) to small (10 km diameter) craters that are covered with a veneer of impact melt

and/or mare lavas. The moats interior to the main topographic rim are the most subject to obscuration by mare basalt lavas that have covered these zones predominately in the north from Mare Tranquillatatis and to the east from Mare Fecunditatis (see Figure 1). Here the jumbled texture of the inter-scarp zones are muted, and except for a few isolated areas, virtually covered by mare lavas. Yet to the south and west of the basin the moat zones are clearly exposed, displaying a layer of impact melt, the fresh appearance of its inner scarps belying its advanced age. There are surprises here, only the partial rims of some medium sized craters can be seen while almost the entire floor is submerged by ejecta deposits from the basin's formation. Other craters have only their basin facing ramparts remaining; their opposing walls and glacis have been scoured away by the force of the tremendous blast as the ejecta curtain swept through. This image indicates these inter-scarp zones and a few almost hidden craters partially submerged by ejecta.

## The Preservation of the Nectaris Scarp Rings

Why is the Nectaris multi-ring impact basin so well preserved? Nectaris is a large sized basin with a small mare area. If measured across its main topographic rim (the Altai Scarp) it is 860 km in diameter, but the mare is relatively small with a diameter of only 368 km and an area of 84,000 square kilometers, proportionately smaller than most near side basins. The Orientale basin displays an even greater paucity of mare basalts. Was the impactor smaller in diameter? Impactor size might be a major reason that basalt lavas did not completely inundate the rings interior to the main topographic rim, such as the Imbrium lavas have done to its inner rings. With a smaller impact, the crust/mantle faults would not be as deep or as widely dispersed in area, reducing the volume of lava erupted and consequently preserving the multiple scarps. Yet this seems unlikely because the main topographic rim of Nectaris is commensurate in diameter with a number of large basins. And given differences in morphology based on the range of kinetic energies and extreme angles of impact, impactors of similar mass produce similar sized crater/basin diameters.

Does the relative isolation of the Nectaris basin figure into its preservation? The Tranquillitatis basin to the north and the Fecunditatis basin to the east are the only basins close by whose lavas could have modified Nectaris. It does appear that they have flooded onto the northern and eastern regions of the Nectaris basin obscuring the rings there, however, they have not significantly destroyed the multi-ring scarps to the west and south of the mare. Could its location closer to the southern highlands have meant a thicker crust in the target region, slowing the degradation of the basin by impeding volcanism? This seems plausible, as it places Nectaris far from the vast plumbing of the Procellarum and Imbrium regions and a thicker crust would mean the depth of the transient cavity would not have penetrated as deeply.

Consequently the release of magma from chambers in the sub-lithospheric layer layers would have been minimal for this area of the Moon. There may well have been some kind of long term rejuvenation of the scarps that occurred much later, when mare lavas subsumed the fractured and broken craters in the moat zones, causing them to collapse, flatten and slide downslope towards the basin center as a result of the building mass of the dense mare basalts and the movements in the asthenosphere, further exposing and accenting their appearance. Whatever the details of the processes responsible for its preservation, we are all fortunate to witness the spectacular Nectaris multi ring impact basin which is not only ancient but remarkably well preserved. Within the confines of the main topographic rim are a magnificent collection of intermediate size complex craters, all much younger than the basin because they superpose it. (See Figure 6).

Chief among these are the classic trio, young Theophilus, mature Cyrillus, and ancient and battered Catharina. Several hundred thousand years after the basin was formed, Nectarian aged Catharina was created. Immediately thereafter it appears to have been repeatedly struck by smaller impactors, and a couple of hundred thousands years later, the impact that produced Cyrillus obliterated some of the smaller craters several kilometers to the northeast between the first and second scarp ring.

Theophilus, the Copernican age crowning jewel of this superb, partially overlapping group, was emplaced within the last billion years or so. Fracastorius, a large complex crater of Nectarian age, formed about the time of Catharina and is now nearly submerged by subsequent mare basalt flows that breached its eastern walls when the slope of the basin in its vicinity plastically deformed under the load of massive basalt deposits concentrated at basin center.. Tangent to the main topographic rim, Eratosthenian age Piccolomini (see Figure 7) shows its relatively young features especially when the terminator is close by. A puzzling aspect is the appearance of its southern walls. These terraces appear to reflect the Altai Scarp relief contours, as if the location of Piccolomini's impact next to the Altai Scarp helped to direct some of the energy of the event away from the scarp, preserving its general outline.

Figure 6

Mosaic image of the central mare and Nectaris basin scarp rings to the west of the mare. The prominent group of three large complex craters, Copernican aged Theophilus, Nectarian age Cyrillus and Catharina superpose two inner scarp rings. Image courtesy of Raffaello Lena, GLR group.

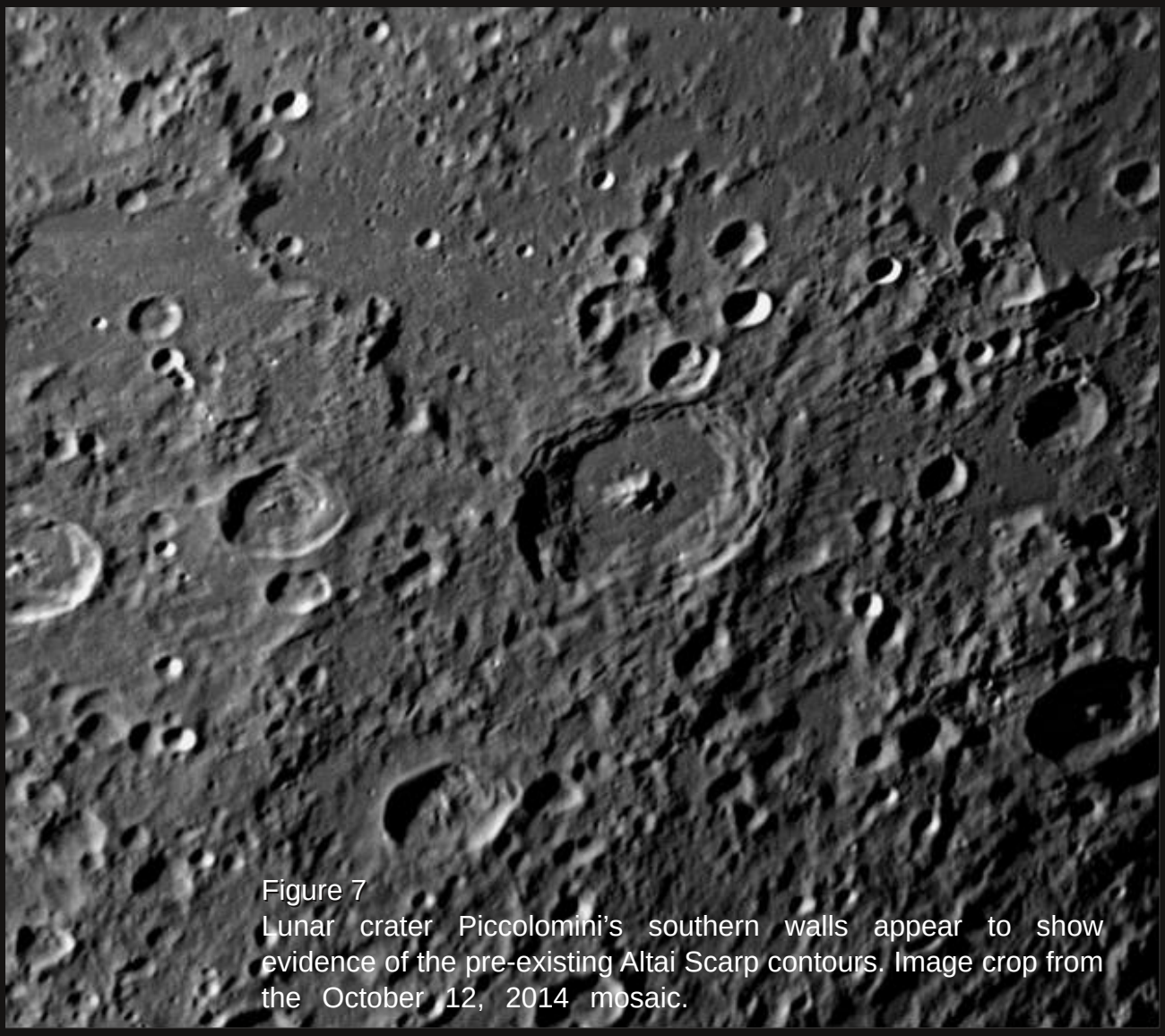

Figure 7
Lunar crater Piccolomini's southern walls appear to show evidence of the pre-existing Altai Scarp contours. Image crop from the October 12, 2014 mosaic.

Seeing the basin in various waxing and waning lighting can really help to discriminate some of its complex annular terrain and radial structure, Figures 8 and 9 are image mosaics of the basin region acquired with my Russian made 8" Alter 815M f/15 Maksutov telescope and Lumenera Skynyx 2.0-1M video camera on October 29, 2014 in waxing light, early lunar morning (see Figure 8), again in waxing light on November 9, 2014, early lunar morning (see Figure 9), and under waxing light, mid lunar morning on October 29, 2014 (see Figure 10), and finally in waxing, under mid lunar morning light (see Figure 11).

Figure 8

Mosaic of the Nectaris basin under waxing (early lunar morning) on October 29, 2014 at 03:30 to 04:45 UT. Image acquired and processed by the author.

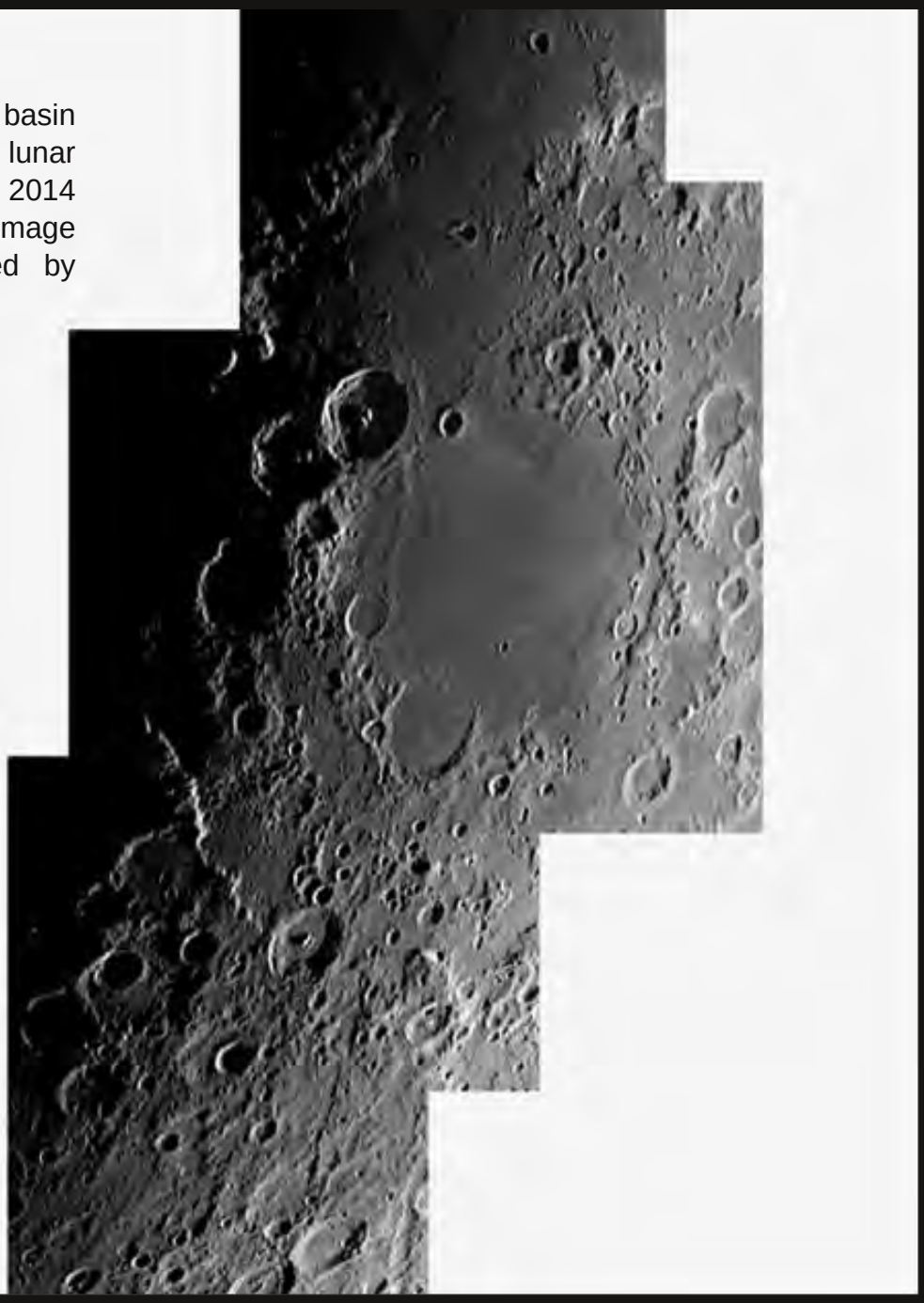

Figure 9

Mosaic of the Nectaris basin under waxing (mid lunar morning) on November 28, 2014 at 01:40 to 03:50 UT. Image acquired and processed by the author.

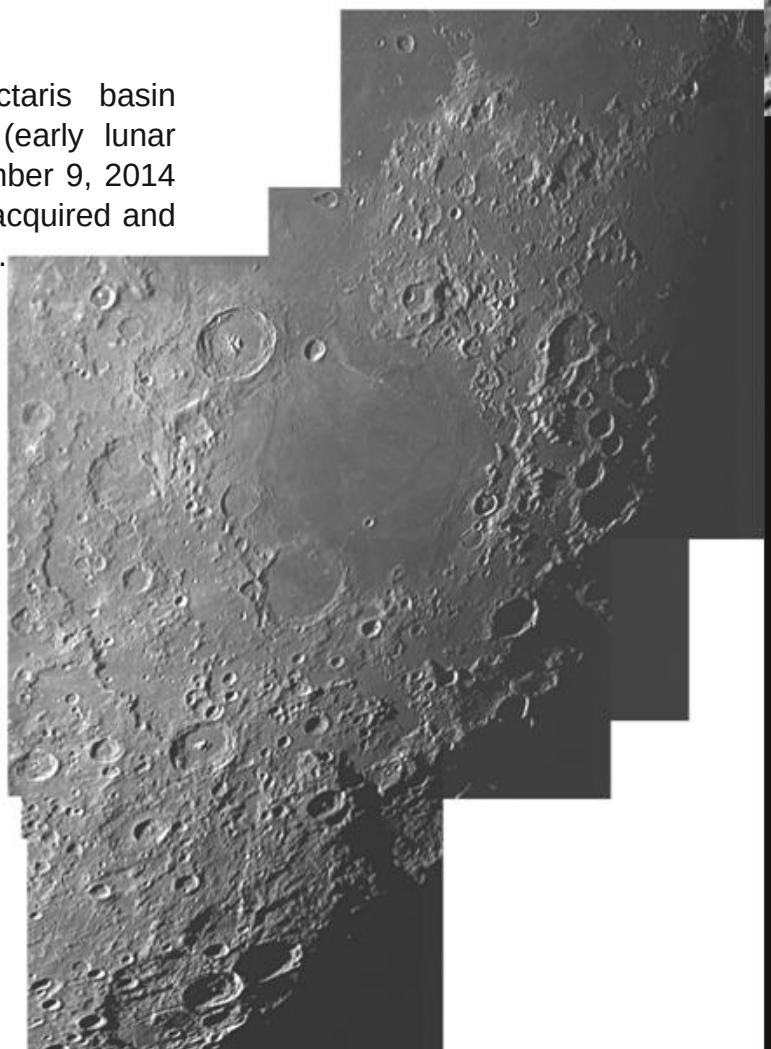

Figure 10

Mosaic of the Nectaris basin under waning light (early lunar afternoon) on November 9, 2014 at o5:30 UT. Image acquired and processed by author.

Figure 11

Mosaic of the Nectaris basin under waning light (late lunar afternoon) November 10, 2014 at 05:30 to 06:35 UT. Image acquired and processed by author.

## Acknowledgements

Finally, I would like to extend my gratitude to my friend Raffaello Lena of the GLR Group for both the use of his superb image mosaic and his consistent support and encouragement. Without his efforts, I would not have been able to pull this article together. Likewise, for the unusually lit LROC image merged with colored LOLA elevation data and the help and good cheer from my friend John Moore, author and selenographer and an author of several books on near side lunar craters, features and topography as well as an administrator and contributor for Charles A. Wood's MoonWiki. Thank you both.

There is one individual who is predominately responsible for my continued interest in lunar geology. His website aroused my mind and extended my understanding, as he still does today, despite the fact that his site is no longer being currently published (it is online in archival form). That man is Charles A. Wood. To you sir, I owe a debt of gratitude I will never be able to repay. However, I suspect this is true for the thousands of folks who visit his “Lunar Photo of the Day” (LPOD) website every day and who are fortunate enough to have acquired his classic tome “The Modern Moon: A Personal View”, the commentaries that accompany “The Kaguya Lunar Atlas” that he co-authored with Motomaru Shirao, or those commentaries

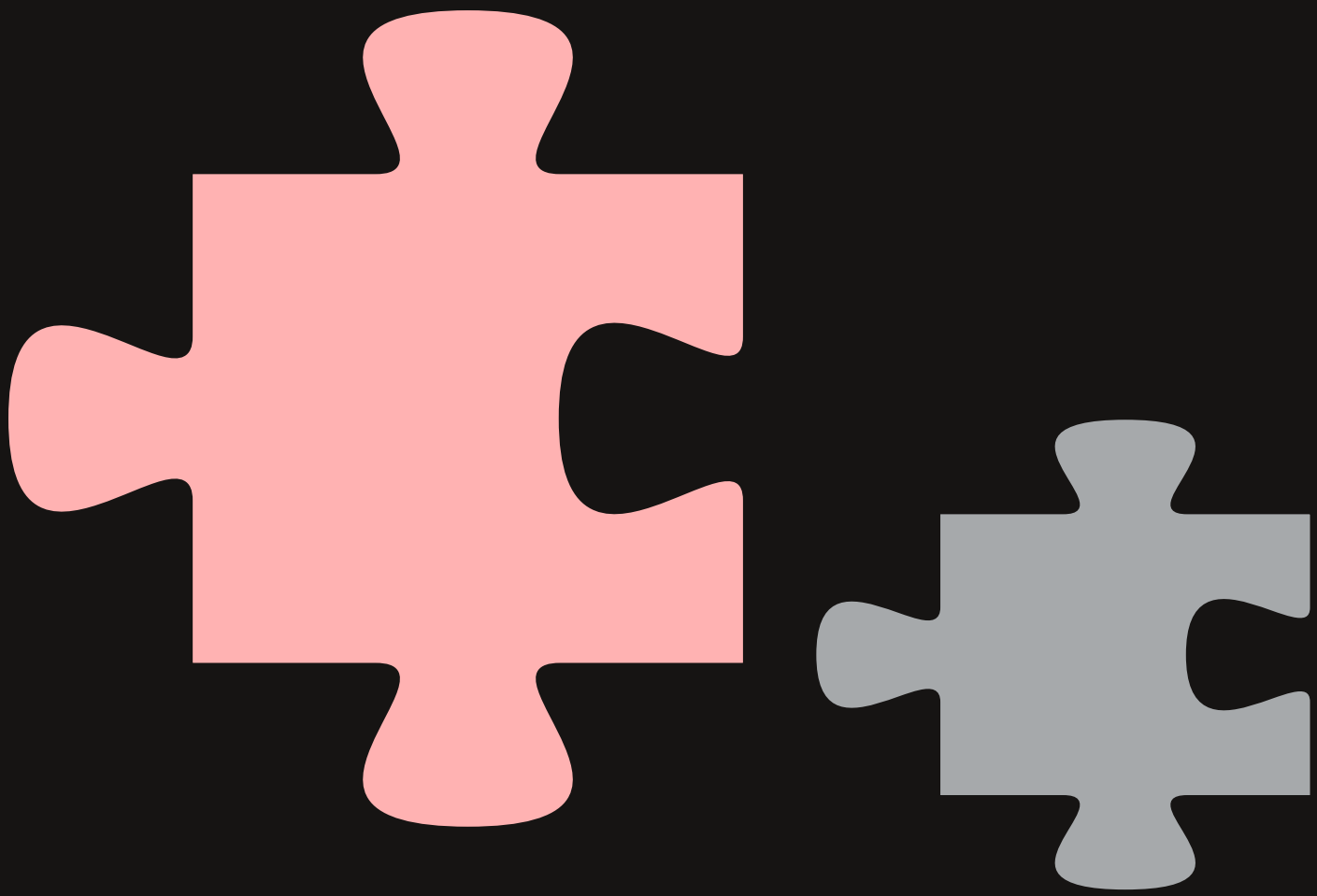

Selenology Today

## References


1. "The Geology of Multi-Ring Impact Basins: The Moon and Other Planets" by Paul D. Spudis, Cambridge University Press, paperback edition, Copyright 2005.

2. "The Geologic History of The Moon" by Don E. Wilhelms with sections by John F. McCauley and Newell J. Trask, U.S. Geological Survey Professional Paper Paper 1348. United States Printing Office, Washington : 1987.

3. "Traces of Catastrophe: A Handbook of Shock-Metamorphic Effects in Terrestrial Meteorite Impact Structures" by Bevan M. French, Lunar and Planetary Institute Contribution No. 954, Copyright 1998 by LPI.

4. "The Clementine Atlas of the Moon" by Ben Bussey and Paul Spudis, Cambridge University Press, Copyright 2004.

5. "The Modern Moon: A Personal View" by Charles A. Wood, Sky Publishing Corp., Copyright 2003.

6. "A Geologic Time Scale 1989" W. Brian Harland, Richard L. Armstrong, Allen V. Cox Lorraine E. Craig, Alan G. Smith, David G. Smith, Cambridge University Press, Copyright 1990.

7. "The Face of the Moon" by Ralph B. Baldwin, University of Chicago Press, copyright 1949.

8. "Geological Map of the Nectaris Basin and its Deposits" by M.C. Smith and Paul D. Spudis, Department of earth and Planetary Sciences, University of Tennessee, Lunar and Planetary Institute, 44th Lunar and Planetary Science Conference (2013).

9. "Lunar Sourcebook: A User's Guide to the Moon" edited by Grant H. Heiken, David Vaniman, and Bevan M. French ©1991, Cambridge University Press - Digital version of the classic 1991 publication, a one-volume reference encyclopedia of scientific and technical information about the Moon.

10. "Stratigraphy and Composition of Nectaris Basin Deposits" by Paul D. Spudis and M.C Smith, Lunar and Planetary Institute, Department of Earth and Planetary Sciences, University of Tennessee, 44th Lunar and Planetary Science Conference (2013).

11. "On the Age of the Nectaris Basin" by R. L. Korotev, J. J. Gillis, L. A. Haskin, and B. L. Jolliff, Department of Earth and Planetary Sciences, Washington University, Saint Louis MO, Workshop on Moon Beyond 2002

12. "Nectaris Basin Ejecta From Clementine Data" by D. Ben. J. Bussey, Paul D. Spudis, B. Ray Hawke, Paul G. Lucey, and Dave Blewett, Lunar and Planetary Institute, Houston TX , University of Hawaii, Honolulu HI, 60th Annual Meteoritical Society Meeting.

13. "What is the Age of the Nectaris Basin? New Re-Os Constraints for a Pre-4.0 Ga Bombardment History of the Moon" by M. Fischer-Gödde and H. Becker, Institut für Geologische Wissenschaften, FR Geochemie, Freie Universität Berlin, Germany, Institut für Planetologie, Westfälische Wilhelms- Universität Münster, Germany, 42nd Lunar and Planetary Science Conference (2011)

14. "Composition of the impact melt sheets of the Orientale and Nectaris impact basins" by Paul D. Spudis, Lunar and Planetary Institute, Houston TX, EPSC Abstracts Vol. 8, EPSC2013-758, 2013 European Planetary Science Congress Copyright 2013 Author(s).

15. "Remote Sensing Studies of Geologic Units in the Eastern Nectaris Region of the Moon" by B. R. Hawke, C. R. Coombs, L. R. Gaddis, P. G. Lucey, C. A. Peterson, M. S. Robinson, G. A. Smith and P. D. Spudis. Planetary Geosciences, HIGP, Univ. of Hawaii, Honolulu, HI, College

Selenology Today